Response to Reviewers

We would like to thank the reviewers for their valuable comments. We proceeded to a revision of our manuscript according to the comments of the Reviewers. We have confronted all points raised by the Reviewers and hope that now our manuscript will be satisfactory to both the Reviewers and the Editor.

In the following we present a detailed report, containing all answers / actions taken and references to the manuscript changes. Each one of our replies is given in blue-colored fonts, following the corresponding Reviewer's comment (in `black colored fonts`). In the replies text, **bold fonts** indicate inserted / changed text. We also provide a "track-changes" version of the revised manuscript at the end of the report, so that the Reviewers and the Editor can easily identify the changes made on the originally submitted manuscript.

Before we proceed to the detailed answers to Reviewers' comments, we would like to note that we took also into account the short comment published by F. Vallianatos, by including the following sentence just before the proposed position for Fig. 10:

"**…Note that a very recent analysis on the foreshock seismic activity before EQ1, in terms of a combination of multiresolution wavelets and NT analysis, which was performed on concentric areas of 50 km and 30 km radii around the epicenter of EQ1, also found that NT analysis criticality requirements are met a few days before EQ1 (at approximately 20 January) (Vallianatos et al., 2015).**"

We also included the corresponding paper of Vallianatos et al. in our references list, while we updated the bibliographic reference data for (Skeberis et al., 2015) and (Vamvakaris et al., 2013) [which became (Vamvakaris et al., 2016)]

T. Chelidze (Referee)

"The standard approach to earthquake (EQ) prediction (both pro-active and retrospective) is to investigate, whether the physical quantity accepted as a precursor (here signatures of critical, as well as tricritical, dynamics) is statistically significant, namely, it should be estimated how often the anomaly considered as a precursor is observed in seismically quiet periods (false alarms), really preceded EQ (hits) and was absent before strong EQ (misses). As it is very difficult to meet all these criteria it would be sufficient at this stage to estimate probability of false alarms, i.e. to show that critical dynamics features are absent in quiet periods."

Reply:

Our up to now research efforts, through the application of the method of critical dynamics (MCF) and, lately, of the natural time (NT) method on MHz fracture-induced electromagnetic emissions (EME), has led us to the conclusion that a few days (approximately during the last week) before a strong, on-land or near coast-line, earthquake (EQ) takes place, critical characteristics are identified in the recorded MHz time-series (usually referred to as "critical window", CW). Note that these kind of EQs (M>6, with an epicenter on land or near coast-line) are not often in the area of Greece, where our measurement network is deployed. Prior to all such EQ events MHz EME have been recorded, however not all of them could be analyzed either due to short data lengths or due to low amplitude (the recorded radiation is not always clearly emerging from the EM background) (see remark in page 016104-4 of Karamanos et al., 2006). The above mentioned conclusion has been verified for a number of such EQ events which have taken during the last years and for which data of adequate length and amplitude, so that reliable time-series analysis was possible, were available (e.g., Contoyiannis et al., 2010, Potirakis et al., 2015; Contoyiannis et al., 2015, the present article about the Cephalonia EQs). The naturally arising question is whether after each time that criticality characteristics are identified in the MHz time-series a strong EQ event definitely follows. Before replying to this question we have to remind that in the frame of our proposed four-stage model, the appearance of a valid MHz anomaly (CW) is not a "necessary and sufficient" condition for a main EQ event to happen (e.g., Eftaxias et al., 2013, and references therein; Eftaxias and Potirakis, 2013, and references therein; Contoyiannis et al., 2015, and references therein; Donner et al., 2015). Indeed, there has been a very small number of cases for which critical MHz EME signals were recorded but no strong EQ took place after that. However, for these cases, a significant increase of seismicity (with events of M approximately <5) followed the identified MHz critical signal without an EQ event with (M>6) to happen. According to our proposed model, this means that the organization in the studied area reaches a critical condition during which the long-range correlation of fracture events expands over the wider activated area. During this phase the family of asperities sustaining the fault are sieged by the developed stresses, however in the specific cases the process did not developed to the direction of fracturing the asperities themselves. We emphasize that we have never found a critical MHz signal during a time period of seismic quiescence. In conclusion, according to our view, there is no meaning of studying the probability of false alarms for the MHz EME, since it is a candidate electromagnetic precursor of which appearance is not a "necessary and sufficient" condition for a main EQ event to happen.

"One of the first papers devoted to criticality as a precursory sign are: T.Chelidze. Percolation and fracture. Physics of the Earth and Planetary Interiors. 1982, 28, 93- 101. T.Chelidze, Yu. M. Kolesnikov. Percolation Modell des Bruchprozesses. Gerlands Beitr. Geophysik. Leipzig. 1982, 91, 35 - 44. more recents are: T.Chelidze, Yu. Kolesnikov, T.Matcharashvili. Seismological criticality concept and percolation model of fracture // Geophysical Journal International. 2006,164,125-136. J. Wanliss, V. Muñoz, D. Pastén, B. Toledo, and J. A. Valdivia. Critical behavior in earthquake energy dissipation. Nonlin. Processes Geophys. Discuss., 2, 619–645, 2015 John B. Rundle, James R. Holliday, William R. Graves, Donald L. Turcotte, Kristy F. Tiampo, and William Klein. Probabilities for large events in driven threshold systems. PHYSICAL REVIEW E 86, 021106 (2012) Inclusion of some of these papers into references seems to be desirable."

Reply:

The reviewer is right, the suggested papers have been added to the references list of the revised version of our article. Specifically, we added one sentence as the first sentence of Section 2. In the first version of our manuscript it was: "Critical phenomena have been proposed as the likely model to study the origins of EQ related EM fluctuations,…" and now it reads: "**Criticality has early been suggested as an EQ precursory sign (Chelidze, 1982; Chelidze and Kolesnikov, 1982; Chelidze et al., 2006; Rundle et al., 2012; Wanliss et al., 2015)**. Critical phenomena have been proposed as the likely **framework** to study the origins of EQ related EM fluctuations,…"

"Authors' belief that the natural time approach extracts maximum possible information from a given time series seems to be a bit exaggerated: for example I am not sure that NTM permits proper analysis of scaling in waiting times' distribution between events in a given time series as in NTM the time scale is homogenized."

Reply:

The Reviewer is right about the exaggeration. We rephrased the specific part to be more accurate. The specific part of the text was originally "…and has been shown to extract the maximum information possible from a given time series (Abe et al., 2005)", it has been changed to "…and has been shown **to be optimal for enhancing the signals in the time-frequency space** (Abe et al., 2005)."

Concerning the part of the Reviewer's comment about waiting times distribution, we have to note that in natural time analysis, as published by the proponents: "*For a time series comprised of N events, we define the natural time for the occurrence of the kth event by χk=k/N (1), which means that we ignore the time intervals between consecutive events, but preserve their order.*" (Sarlis et al., PNAS (2013) vol.110 pp.13734–13738). In other words, natural time analysis does not consider at all the waiting times' distribution.

R. V. Donner (Referee)

"The manuscript is based on pre-seismic MHz electromagnetic recordings as well as seismicity data prior to two recent earthquakes at Cephalonia Island (Greece). The systematic existence of distinct electromagnetic signatures prior to at least a certain not yet fully specified class of earthquakes is still a subject of ongoing debates, even though a lot of observational evidence has been provided during the last years. Accepting the latter findings, it is valuable to study the dynamical properties of such emissions and, more precisely, their temporal changes prior to earthquakes in order to contribute to a better understanding of the underlying processes in the solid ground. It is important to note that the present work is far from claiming that relevant dynamical signatures suggested as earthquake precursors can be systematically applied as early warning signals of upcoming events - rather, they should be used as a posteriori diagnostics. In order to avoid possible confusion raised by the utilization of the term "percursor" in the title of the paper, I would recommend to make this point even more explicit in the introduction of the manuscript."

Reply:

As the Reviewer has noticed, we have already pointed out our view that this article, as well as all our previous studies, aims not at EQ prognosis but at a better understanding of the processes preceding a strong EQ. In this direction, we have included the following text in the first version of our manuscript:

"*…However, the understanding of the physical processes involved in the preparation of an EQ and their relation to various available observables is an open scientific issue. Much effort still remains to be paid before one can claim clear understanding of EQ preparation processes and associated possible precursors.*
As it has been repeatedly pointed out in previous works (e.g., Eftaxias et al., 2013; Eftaxias and Potirakis, 2013, and references therein), our view is that such observations and the associated analyses offer valuable information for the comprehension of the Earth system processes that take place prior to the occurrence of a significant EQ. As it is known, a large number of other precursory phenomena are also observed, both by ground and satellite stations, prior to significant EQs. Only a combined evaluation of our observations with other well documented precursory phenomena could possibly render our observations useful for a reliable short-term forecast solution."

However, we have also added text in the first paragraph of the introduction of the revised version of our manuscript in order to make this point even more explicit. The specific part of the text was originally "…The possible relation of the field observed fracture-induced electromagnetic emissions (EME) in the frequency bands of MHz and kHz, associated with shallow EQs with magnitude 6 or larger that occurred in land or near coast, has been examined in a series of publications (e.g., Eftaxias et al., 2001, 2004, 2008, 2013; Kapiris et al., 2004; Karamanos et al., 2006; Papadimitriou et al., 2008; Contoyiannis et al., 2005, 2013, 2015; Eftaxias and Potirakis, 2013; Potirakis et al., 2011, 2012a, 2012b, 2012c, 2013, 2015; Minadakis et al., 2012a, 2012b), while a four-stage model…", it has been changed to "…The possible relation of the field observed fracture-induced electromagnetic emissions (EME) in the frequency bands of MHz and kHz, associated with shallow EQs with magnitude 6 or larger that occurred in land or near coast, has been examined in a series of publications **in order to contribute to a better understanding of the underlying processes** (e.g., Eftaxias et al., 2001, 2004, 2008, 2013; Kapiris et al., 2004; Karamanos et al., 2006; Papadimitriou et al., 2008; Contoyiannis et al., 2005, 2013, 2015; Eftaxias and Potirakis, 2013; Potirakis et al., 2011, 2012a, 2012b, 2012c, 2013, 2015; Minadakis et al., 2012a, 2012b), while a four-stage model…"

"Scientific comments:"

"1. In all applications of MCF, I wonder about the fitting procedure and model selection. Equation (3) presents a statistical model to be fitted to data that does not provide direct access to proper parameter estimates by simple regression in log-log space. Instead, proper parameter estimates for p2 and p3 would require a "clean" maximum likelihood approach. What is the authors take on this? In particular, one could formulate the identification of critical windows as a model selection problem of comparing the statistical models with p3=0 and p3>0 by means of suitable penalized-likelihood criteria or similar approaches. I don't find any details on the parameter estimation in the manuscript, but think that since the distinction between the latter cases is an important part of the present analysis, the best and most robust statistical methodology should be applied at this point."

Reply:

We agree that not enough information is given about the fitting process and this could lead to puzzling the reader. In order to avoid such a situation, we have appropriately revised our manuscript. We note that the model of Eq. (3) is adopted following the reasoning described in the already cited reference (Contoyiannis and Diakonos, 2007). In the revised manuscript we shortly explain why we selected this model rather than just providing a citation to the specific paper. Specifically, we added the following text, shortly after Eq. (3):

"**Note that the choice of the function $\rho(l)$ of Eq. (3), which combines both power-law and exponential decay, to model the distribution of waiting times was deliberately made in order to include both these fundamentally different behaviors, i.e., the critical dynamics (Contoyiannis et al., 2002) and the complete absence of specific dynamics (stochastic processes) (Contoyiannis et al., 2004b), respectively. Of course, the specific function also models intermediate behaviors (Contoyiannis and Diakonos, 2007).**

In applying the MCF the corresponding factors of $\rho(l)$ appear to be competitive: any increase of the p_2 exponent value corresponds to a p_3 exponent value reduction and vice versa. However, this is expected because, for example, any increase of the value of p_3 exponent signifies the departure from critical dynamics and thus the reduction of p_2 exponent value. What is interesting to us is to apply MCF analysis to observe this competition in the case of pre-earthquake EME time-series and see whether the obtained exponent values are consistent with those of MCF analyzes performed on other time-series with large statistics which are considered as references for the application of our method. This competition can be observed even within the critical windows as shown in Figs. 2 (d) and 3 (d)."

Concerning the fitting of the distribution of laminar lengths (waiting times) to the function $\rho(l)$ of Eq. (3), this is directly performed using the Levenberg-Marquardt algorithm, while the fitting criterion is the chi-square minimization. The fitting is not done in log-log space (as for example one does in order to calculate the DFA a-exponent). In order to clarify this issue, the following text has been added in the second paragraph of Section 3 (just before the proposed position for Fig. 2). The specific part of the text was originally "Fig. 2c portrays the obtained laminar distribution for the end point $\phi_l = 655mV$, that is the distribution of waiting times, referred to as laminar lengths l, between the fixed-point ϕ_o and the end point ϕ_l, as well as the fitted function $f(l) \propto l^{-p_2} e^{-p_3 l}$ with the corresponding exponents $p_2 = 1.35$, $p_3 = 0.000$ with $R^2 = 0.999$.", now it has been enhanced as: "Fig. 2c portrays the obtained **distribution of laminar lengths** for the end point $\phi_l = 655mV$, that is the distribution of waiting times, referred to as laminar lengths l, between the fixed-point ϕ_o and the end point ϕ_l, as well as the fitted function $f(l) \propto l^{-p_2} e^{-p_3 l}$ with the corresponding exponents $p_2 = 1.35$, $p_3 = 0.000$ with $R^2 = 0.999$. **Note that the distribution of laminar lengths is directly fitted to the specific model using the Levenberg-Marquardt algorithm, while the fitting criterion is the chi-square minimization. The fitting is not done in log-log space; the axes of Fig. 2c are logarithmic for the easier depiction of the distribution of laminar lengths.**"

"2. For a self-sustained description of the NT method in Sect. 2.2, some minor points should be added to this section: (i) What exactly is Phi (p. 1597, l. 12)? I don't find a corresponding explanation. (ii) Please provide an explicit definition (with equation?) of <D>. (iii) The "theoretical estimation"(?) of the normalized power spectrum (p. 1598, l.10) is not fully clear. Please provide a few more details. (iv) The introduction of a magnitude threshold to NT (p. 1598, l.14) comes very ad hoc; some brief motivation/explanation/background would be desirable."

Reply:

Clarifications on all the raised points have been made:

(i) The text at the specific point was: "..., $\varpi = 2\pi\varphi$, with φ the natural frequency,...", A clarification has been added to the manuscript and the specific point now reads: "..., $\varpi = 2\pi\varphi$, with φ **standing for the frequency in natural time, termed "natural frequency"**, and $p_k = Q_k / \sum_{n=1}^{N} Q_n$ corresponds to the k^{th} event's normalized energy. **Note that, the term "natural frequency" should not be confused with the rate at which a system oscillates when it is not driven by an external force; it defines an analysis domain dual to the natural time domain, in the framework of Fourier–Stieltjes transform (Varotsos et al., 2011b).**"

(ii) & (iii) The initial text was: "The "average" distance $\langle D \rangle$ between the curves of normalized power spectra $\Pi(\varphi)$ of the evolving seismicity and the theoretical estimation of $\Pi(\varphi)$ for $\kappa_1 = 0.070$ should be smaller than 10^{-2};...";it has been improved and now it reads: "The "average" distance $\langle D \rangle$ between the curves of normalized power spectra $\Pi(\varpi)$ of the evolving seismicity and the theoretical estimation of $\Pi(\varpi)$, $\boldsymbol{\Pi_{critical}(\varpi) = (18/5\varpi^2) - (6\cos\varpi/5\varpi^2) - (12\sin\varpi/5\varpi^3)}$**,** $\boldsymbol{\Pi_{critical}(\varpi) \approx 1 - \kappa_1 \varpi^2}$**,** for $\kappa_1 = 0.070$ should be smaller than 10^{-2}**, i.e.,** $\boldsymbol{\langle D \rangle = \langle |\Pi(\varpi) - \Pi_{critical}(\varpi)| \rangle < 10^{-2}}$;..."

(iv) The following text has been added at the end of Section 2, to explain the use of magnitude threshold:

"**Note that in the case of NT analysis of foreshock seismicity, the introduction of magnitude threshold,** M_{thres}**, excludes some of the weaker EQ events (with magnitude below this**

threshold) from the NT analysis. On one hand, this is necessary in order to exclude events for which the recorded magnitude is not considered reliable; depending on the installed seismographic network characteristics, a specific magnitude threshold is usually defined to assure data completeness. On the other hand, the use of various magnitude thresholds, M_{thres}, offers a means of more accurate determination of the time when criticality is reached. In some cases, it happens that more than one time-points may satisfy the rest of NT critical state conditions, however the time of the true coincidence is finally selected by the last condition that "true coincidence should not vary upon changing (within reasonable limits) either the magnitude threshold, M_{thres}, or the area, used in the calculation.""

"3. In Sect. 3, the authors study "stationary" time series segments. How has the stationarity been tested? Just by visual inspection or in a strict mathematical sense?"

Reply:

We thank the Reviewer for the opportunity to clarify this point. Stationarity is always tested in a strict mathematical sense before the application of the MCF analysis. A cumulative stationarity test, which to our opinion is a proper and adequate stationarity test for the stationarity requirements of the MCF method, is always performed. Such examples, of executing the specific cumulative stationarity test on time-series excerpts before applying the MCF method, can be found in (Contoyiannis et al., 2004a, 2005, 2010; Contoyiannis and Eftaxias, 2008; Potirakis et al., 2015). In order to clarify this point we have added the following sentence at the end of Section 2.1: "**Note that in order for a time-series to be possible to be analyzed by the MCF, it should at least present cumulative stationarity. Therefore, a cumulative stationarity test is always performed before applying the MCF method; examples can be found in already published articles (e.g., Contoyiannis et al., 2004a, 2005, 2010; Contoyiannis and Eftaxias, 2008; Potirakis et al., 2015).**"

"4. One very interesting fact is the observation of VLF anomalies for the same earthquakes as studied in the present work (Skeberis et al., 2015). I would be curious to learn about the authors' opinion on whether (and how) this kind of signal could be integrated with their four-stage model. Which stage could be accompanied by such seismic-ionospheric disturbances, and under which general conditions?"

Reply:

The VLF anomalies belong to the class of precursors that are rooted in anomalous propagation of EM signals over epicentral regions due to a pre-seismic Lithosphere-Atmosphere-Ionosphere (LAI) coupling (Liu et al., 2000; Ouzounov and Freund, 2004; Uyeda et al., 2009). During quiet periods, there is a standard diurnal variation of the EM data (periodic variation where the main period is ~24h). The records refer to the Earth's ionosphere waveguide propagation of natural EM emissions. Any change in the lower ionosphere due to an induced pre-seismic LAI-coupling may result in significant changes in the signal propagation and consequently in the signal received at a station. Therefore, the emergence of an ionospheric EM anomaly is recognized as a strong perturbation of the characteristic bay-like morphology in the chain of daily data.

According to our view, the observation of VLF anomalies, seems to be associated with the EQ preparation phase happening during the first stage of our proposed four stage model, i.e., during the phase that the critical MHz EME are observed. We focus on the fact that ionospheric precursors appear a few days before the earthquake occurrence and disappear before the earthquake occurrence exactly as it happens in the case of the preseismic MHz EME. Pulinets et al. (2003) have provided a strong evidence for occurrence of ionospheric precursors before the main shock: ionospheric precursors within 5 days before the main seismic shock have been registered in 73% of the cases for earthquakes with magnitude 5, and in 100% of the cases for earthquakes with magnitude 6.

The generation of a preseismic ionospheric anomaly is rooted in physical and chemical transformations that occur in the preparation (activation) zone of an impending earthquake. Its observation implies that the preparation zone is extended up to the surface of the Earth in an extensive spatial region. We recall that we refer to the surface earthquakes which occur on land with magnitude 6 or larger. For such events the aforementioned requirement is valid during the first stage of our proposed four-stage model. Indeed, the conception of the earthquake "preparation zone" was developed by different authors (Pulinets and Boyarchuk, 2004 and references there in). In general, this is an area, where local deformations connected with the source of the future earthquake are observed. According to the dilatation theory (Scholz et al., 1973; Myachkin et al, 1975), formation of the cracks happens within the preparation zone and will be accompanied by physical and chemical changes (Rikitake, 1976; Mogi, 1985; Sobolev 1993; Pulinets and Boyarchuk, 2004). According to Dobrovolsky's formula, the earthquake preparation zone radius is of the order of 380 km for magnitude 6. Kossobokov et al. (2000) obtained the value of the preparation zone through a new formula that leads to estimations that is in agreement with that performed by Dobrovolsky's formula. The theory of criticality has been also accepted as an approach concerning the scale of earthquake preparation (or activation in other publications) zone. This approach leads to the same scale parameters as the dilatation (Kossobokov et al., 2000). An approach in terms of criticality leads to the conclusion that for an earthquake with magnitude 6 the foreshock activity is extended up to a critical radius of ~ 120 km (Bowman et al., 1998). Please note that the specific mechanism of Levy flight that the MHz EM precursor follows (Contoyiannis, and Eftaxias, 2008) "has no characteristic scale". This means that the microcracking process is expected to extend to very long distances, up to the limits of the system. In our case this means that microcracking propagates up to the surface of the Earth.

The disappearance of both MHz and ionospheric anomalies before the earthquake occurrence is also in agreement with the proposed four-stage model. The appearance of "symmetry breaking" at the tail of the first stage reveals the transition from the phase of non-directional, almost symmetrical, cracking distribution in an extensive area to a directional localized cracking zone; the completion of the "symmetry breaking" implies that the rupture process has already been obstructed along the backbone of strong asperities distributed across the surfaces of the main fault. The ''siege" of asperities has started. The strong localization of fracture process leads to the corresponding localization of the induced physical and chemical transformations which justifies the disappearance of both MHz and ionospheric anomalies before the earthquake occurrence.

Finally, we should also note that the beyond VLF anomalies, the observed prseismic ULF anomalies are also associated with the EQ preparation phase corresponding to the first stage of our proposed four-stage model (Hayakawa et al., 2015a,b; Contoyiannis et al., 2016).

"Technical comments:"

"1. The third and second last paragraphs of the Introduction provide a very (probably unusually) detailed summary of the findings of the present paper, which would better fit to the conclusions section. In the introduction, much less details should be given."

Reply:

The specific part of the Introduction has been significantly shortened (from 16 lines to 6 lines), while parts of it have been moved to the Discussion – Conclusions section. The specific part now reads: "Moreover, we analyzed the foreshock seismic activity using the NT method; the obtained results indicate that seismicity also presented critical characteristics before each one of the two important events. This result implies that the observed EM anomaly and the associated foreshock seismic activity might be considered as "two sides of the same coin". Last but not least, one day before the occurrence of EQ2, and five days after the corresponding critical EME signal, tricritical characteristics were revealed in the EME recorded by the Cephalonia station.
The remainder of this manuscript is organized as follows: …"

"2. p.1593, l.5: Terming "critical phenomena" as a "model" might be a wording that one could discuss about. Some minor rephrasing of the corresponding sentence would help avoiding possible misunderstandings."

Reply:

We have rephrased this point. In the first version of our manuscript it was: "Critical phenomena have been proposed as the likely model to study the origins of EQ related EM fluctuations,…" and now it reads: "Critical phenomena have been proposed as the likely **framework** to study the origins of EQ related EM fluctuations,…"

"3. p.1593, l.13: What exactly is meant by "multiply" here?""

Reply:

We have rephrased this point. In the first version of our manuscript it was: "…which, then, progressively grow and multiply, leading to cooperative effects." and now it reads: "…which, then, progressively grow and **proliferate**, leading to cooperative effects."

"4. p.1593, l.16: The terms short vs. long range correlations are typically related to a distinction between exponential and algebraic (power-law) decay of correlations with increasing distance. Is this what is meant here, or do the authors simply refer to increasing spatial correlation lengths?"

Reply:

Yes, we refer to the distinction between exponential and power-law decay of correlations with increasing distance, which actually corresponds to the critical phase.

“5. p.1595, ll.17-18: "forming the distribution" sounds a bit strange.”

Reply:
We have rephrased this point. In the first version of our manuscript it was: “…can be estimated by forming the distribution of laminar lengths and fitting it to a function $\rho(l)$…”, and now it reads: “…can be estimated by **fitting the distribution of waiting times (laminar lengths)** to a function $\rho(l)$…”

“6. The term "laminar distribution" (p. 1599, l. 13, as well as several figure captions) is short but rather imprecise. I recommend using a longer but precise term here.”

Reply:
We have substituted the term “laminar distribution” with the term “**distribution of laminar lengths**” throughout the manuscript. For example, a part of the text that initially was “Fig. 2c portrays the obtained laminar distribution for the…”, it is now “Fig. 2c portrays the obtained **distribution of laminar lengths** for the…”

“7. The fourth paragraph of Sect. 3 is an almost literal repetition of the second one with just numbers changed. Just concentration on the differences between the two signals would allow shortening the results on the second one (Fig. 3) considerably. In the same spirit, it is not necessary to have almost identical figure captions in all figures using the MCF. Just give all details once and then refer to the caption of the first of these figures, emphasizing only the differences.”

Reply:
The fourth paragraph has been considerably shortened (from 13 lines to 4 lines) by revising it in the direction pointed out by the Reviewer, and now reads: “The **application of the** MCF analysis on the specific time series (cf. Fig. 3), revealed that the criticality conditions, $p_2 > 1$ and $p_3 \approx 0$, are satisfied for a wide range of end points ϕ_l**, for this signal too. In other words, this signal has also embedded the power-law decay feature that indicates intermittent dynamics, rendering it a CW.**”.
The figure captions of Figs. 3, 4, 5 and 7 have been shortened as advised by the Reviewer. For example, the caption of Fig. 5, in its revised version now reads: “**Figure 5.** (a) The 18,000 samples long critical window of the MHz EME that was recorded before the Cephalonia $M_w = 5.9$ EQ at the Zante station**; (b), (c), and (d) are similar to the corresponding parts of Fig. 2. In Fig. 5c, the distribution of laminar lengths corresponds to the end point** $\phi_l = 400mV$ ”

"8. Some sentences in the conclusions are literal repetitions from the introduction (e.g., the disclaimer regarding the four-stage conceptual model). I strongly recommend avoiding such self-repetitions. Content-wise recapitulation of results is okay, but just copy and paste sentences should be avoided."

Reply:

The Discussion - Conclusions as well as the Introduction have been revised so as to limit the self-repetitions. For instance, the phrase: "Note that the specific four-stage model is a suggestion that seems to be verified by the up to now available MHz-kHz observation data and corresponding time-series analyzes, while a rebuttal has not yet appeared in the literature." that has been used as an example by the Reviewer has been deleted from the Introduction. Please also refer to our reply to technical comment 1.

"9. In Fig. 1, it is really hard to see the different symbols in front of the green background. Just using the land contours without filling would present a much better visualization option. The same also applies to Figs. 8, 9 and 11."

Reply:

We have improved Figs. 1, 8, 9 and 11 by removing the green filling from the land parts of the maps. The revised Figures are:

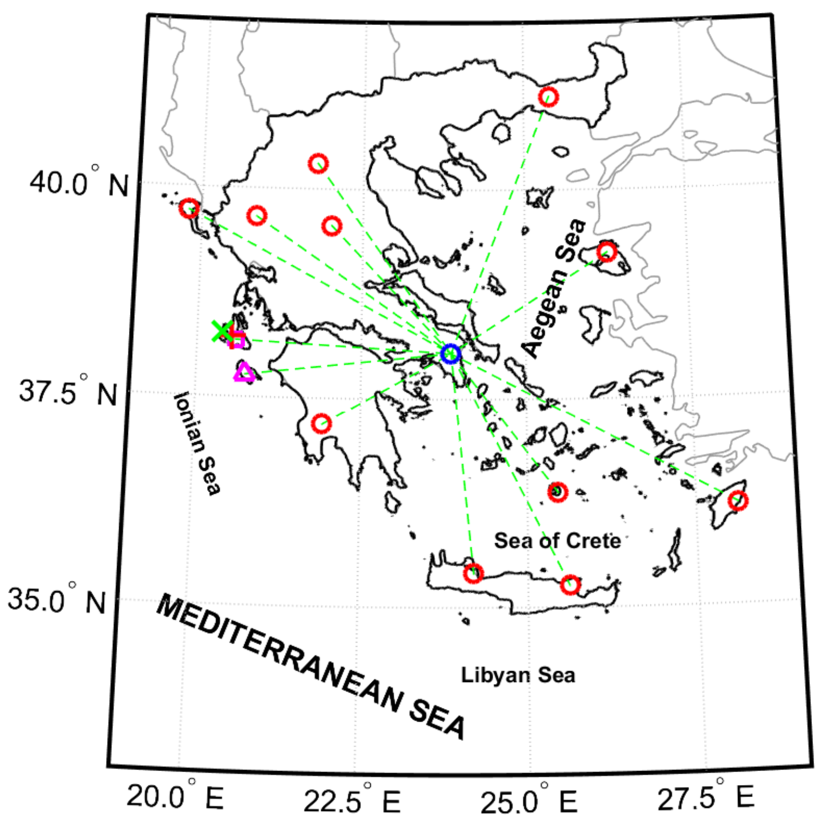

Fig. 1:

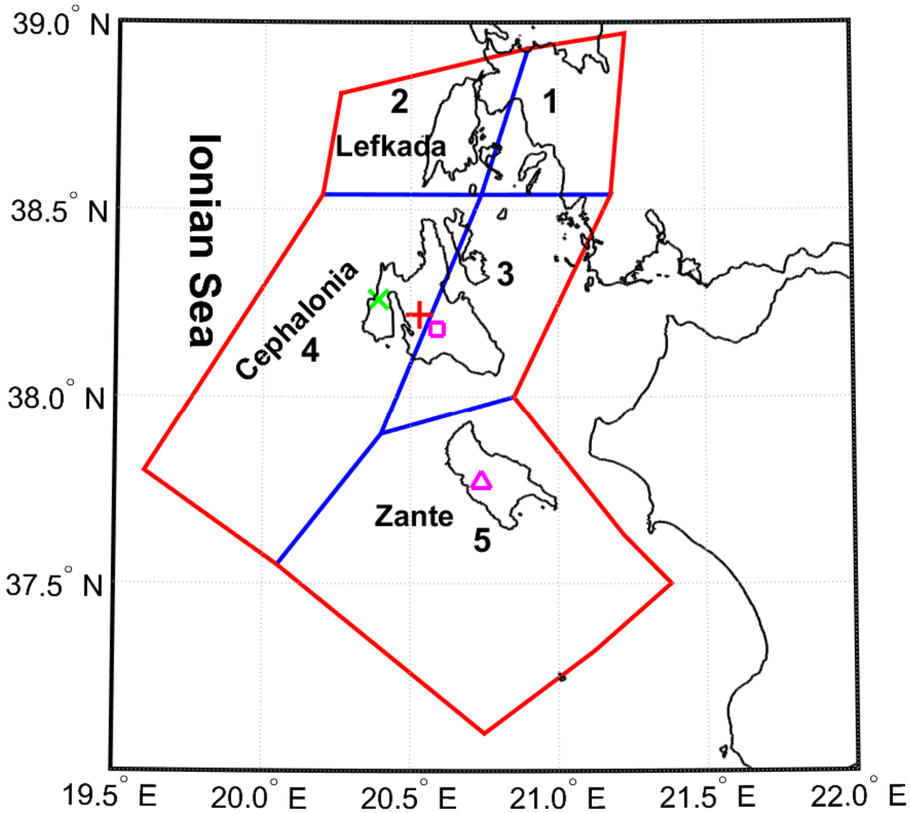
39.0° N
38.5° N
38.0° N
37.5° N
19.5° E
20.0° E
20.5° E
21.0° E
21.5° E
22.0° E
Ionian Sea
Lefkada
Cephalonia
Zante
1
2
3
4
5

Fig. 8:

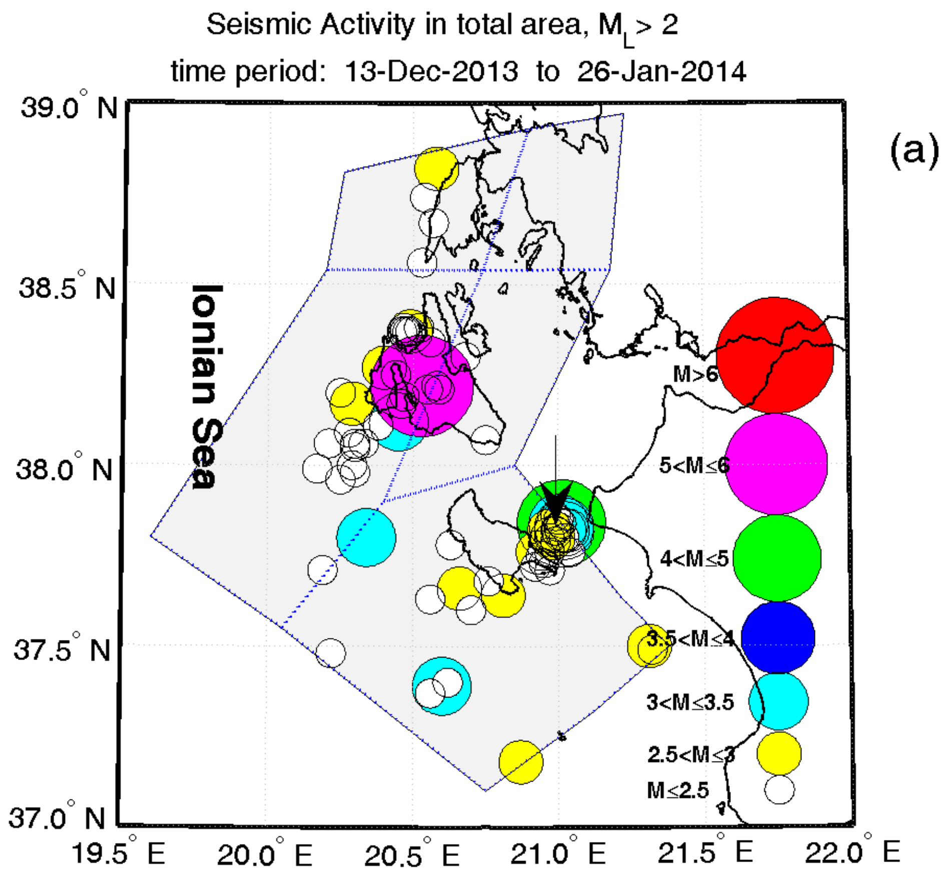
Seismic Activity in total area, M_L > 2
time period: 13-Dec-2013 to 26-Jan-2014
(a)
39.0° N
38.5° N
38.0° N
37.5° N
37.0° N
19.5° E
20.0° E
20.5° E
21.0° E
21.5° E
22.0° E
Ionian Sea
M>6
5<M≤6
4<M≤5
3.5<M≤4
3<M≤3.5
2.5<M≤3
M≤2.5

Fig. 9a:

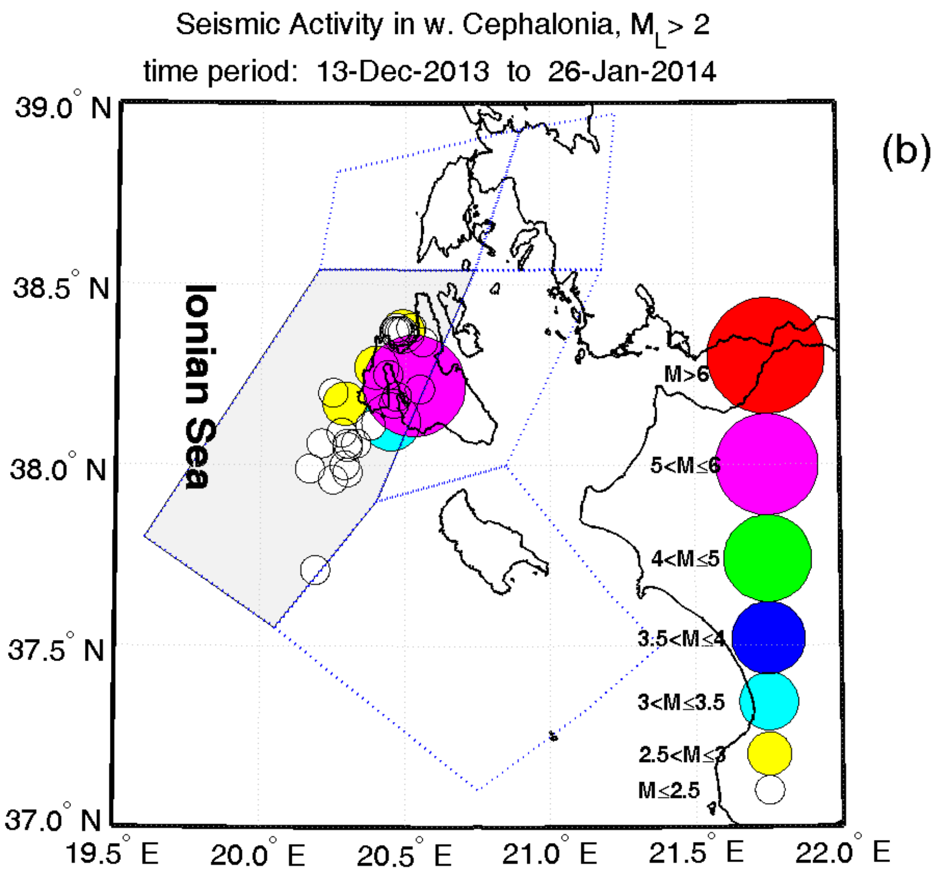
Seismic Activity in w. Cephalonia, M_L > 2
time period: 13-Dec-2013 to 26-Jan-2014
(b)
Ionian Sea
39.0° N
38.5° N
38.0° N
37.5° N
37.0° N
19.5° E
20.0° E
20.5° E
21.0° E
21.5° E
22.0° E
M>6
5<M≤6
4<M≤5
3.5<M≤4
3<M≤3.5
2.5<M≤3
M≤2.5

Fig. 9b:

Fig. 11b:

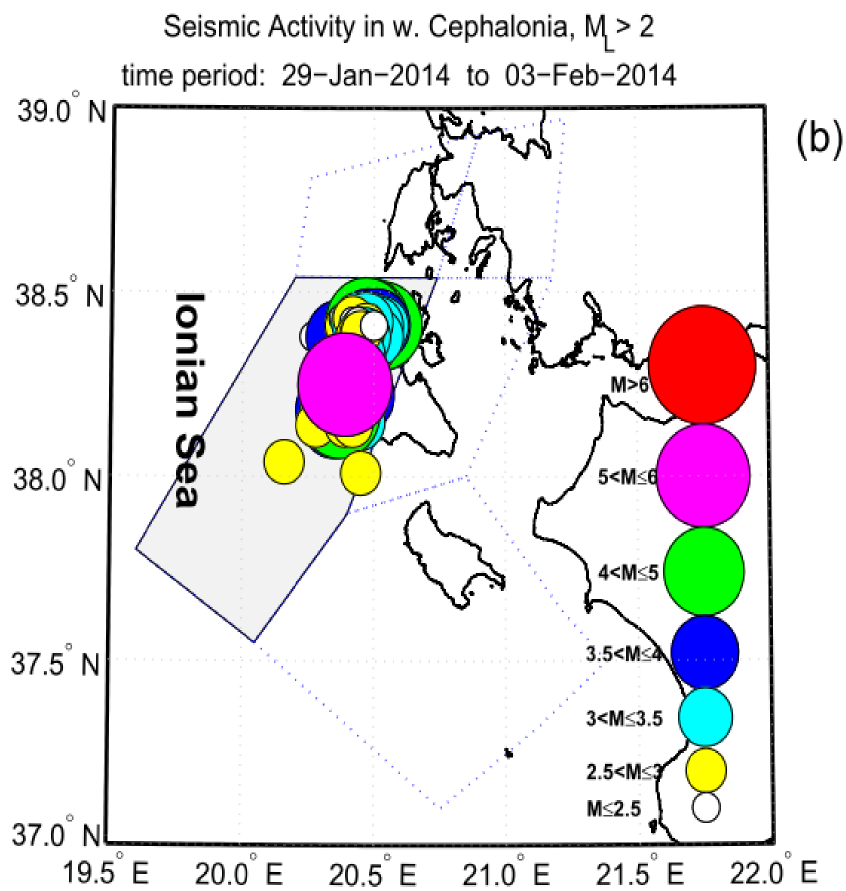

REFERENCES (cited in this Response, not included in the manuscript)

Bowman, D.D., G., Ouillon, C. G., Sammis, A. Sornette, and D. Sornette, An observational test of the critical earthquake concept, J. Geophys. Research, 103, 24359-24372, 1998.

Contoyiannis, Y., S.M. Potirakis, K. Eftaxias, M. Hayakawa, A. Schekotov, Intermittent criticality revealed in ULF magnetic fields prior to the 11 March 2011 Tohoku earthquake (Mw=9), Physica A, 2016, doi:10.1016/j.physa.2016.01.065

Hayakawa, M., A. Schekotov, S. Potirakis, K. Eftaxias, Criticality features in ULF magnetic fields prior to the 2011 Tohoku earthquake", Proc. Jpn. Acad., Ser. B, vol. 91, no. 1, pp. 25-30, 2015a, doi: 10.2183/pjab.91.25.

Hayakawa, M., A. Schekotov, S.M. Potirakis, K. Eftaxias, Q. Li, and T. Asano, An Integrated Study of ULF Magnetic Field Variations in Association with the 2008 Sichuan Earthquake, on the Basis of Statistical and Critical Analyses", Open J. Earthq. Res., 4, 85-93, 2015. doi: 10.4236/ojer.2015.43008.

Kossobokov, V. G., Keilis-Borok, V I., Turcotte, D. L., and Malamud, B. D., Implications of a statistical physics approach for earthquake hazard assessment and forecasting, Pure Appl. Geophys., 157, 2323-2349, 2000.

Liu, J., Chen, Y., Pulinets, S., Tsai, Y., and Chuo, Y.: Seismo-ionospheric signatures prior to M>6 Taiwan earthquakes, Geophys. Res. Letters, 27, 3113-3116, 2000.

Mogi, K., Earthquake Prediction, Academic Press, Harcourt Brace Jovanovich, Publishers, Tokyo-Orlando-San Diego-New York-London-Toronto-Mondreal-Sydney, 355pp, 1985.

Myachkin, V. I., Brace, W. F., Sobolev, G. A., Dieterich, J. H., Two models of earthquakes forerunners, Pure Appl. Geophys., 113, 1-2, 169-183, 1975.

Ouzounov, O., and Freund, F: Mid-infrared emission prior to strong earthquakes analyzed by remote sensing data, Adv. in Space Res., 33, 268-273, 2004.

Pulinets, S., and K. Boyarchuk, Ionospheric precursors of earthquakes, Springer, 2004.

Pulinets, S.A., A.D. Legen'ka, T.V. Gaivoronskaya, and V.Kh. Depuev, Main phenomenological features of ionospheric precursors of strong earthquakes, Journal of Atmospheric and Solar-Terrestrial Physics, 65, 1337– 1347, 2003.

Rikitake, T., Earthquake Prediction, Elsevier, Amsterdam, 357pp, 1976.

Sarlis et al., Minimum of the order parameter fluctuations of seismicity before major earthquakes in Japan, PNAS (2013) vol.110 pp.13734–13738.

Scholz, C. H., Sykes, L. R., Aggarwal Y. P., 1973. Earthquake prediction: a physical basis Science, 181, 803–810.

Sobolev, G. A. Fundamentals of earthquake prediction, M, "Nauka", 1993, p. 314.

Uyeda, S., Nagao, T., and Kamogawa, M.: Short-term earthquake prediction: Current status of seismo-electromagnetics, Tectonophysics, 470(3-4), 205-213, 2009.

In the following, a “track-changes” version of our revised manuscript is appended

Recent seismic activity at Cephalonia island (Greece): A study through candidate electromagnetic precursors in terms of nonlinear dynamics.

S. M. Potirakis [1], Y. Contoyiannis [2], N. S. Melis [3], J. Kopanas [4], G. Antonopoulos [4], G. Balasis [5], C. Kontoes [5], C. Nomicos [6], K. Eftaxias [2]

[1] {Department of Electronics Engineering, Piraeus University of Applied Sciences (TEI of Piraeus), 250 Thivon and P. Ralli, Aigalao, Athens, GR-12244, Greece, spoti@teipir.gr }.

[2] {Department of Physics, Section of Solid State Physics, University of Athens, Panepistimiopolis, GR-15784, Zografos, Athens, Greece,(Y. C: yconto@yahoo.gr ; K. E.: ceftax@phys.uoa.gr)}

[3] {Institute of Geodynamics, National Observatory of Athens, Lofos Nimfon, Thissio, Athens, GR-11810, Greece, nmelis@noa.gr}

[4] {Department of Environmental Technologists, Technological Education Institute (TEI) of the Ionian islands, Zakynthos, GR-29100, Greece, (J. K.: jkopan@otenet.gr ; G. A.: sv8rx@teiion.gr)}

[5] {Institute for Astronomy, Astrophysics, Space Applications and Remote Sensing, National Observatory of Athens, Metaxa and Vasileos Pavlou, Penteli, Athens, GR-15236, Greece, (G. B.:gbalasis@noa.gr ; C. K.: kontoes@noa.gr)}

[6] {Department of Electronics Engineering, Technological Education Institute (TEI) of Athens, Ag. Spyridonos, Aigaleo, Athens, GR-12210, Greece, cnomicos@teiath.gr}

Correspondence to: G. Balasis (*gbalasis@noa.gr*)

Abstract

The preparation process of two recent earthquakes (EQs) occurred in Cephalonia (Kefalonia) island, Greece, [(38.22° N, 20.53° E), 26 January 2014, $M_w = 6.0$, depth = 21 km], and [(38.25° N, 20.39° E), 3 February 2014, $M_w = 5.9$, depth = 10 km], respectively, is studied in terms of the critical dynamics revealed in observables of the involved non-linear processes. Specifically, we show, by means of the method of critical fluctuations (MCF), that signatures of critical, as well as tricritical, dynamics were embedded in the fracture-induced electromagnetic emissions (EME) recorded by two stations in locations near the epicenters of these two EQs. It is worth noting that both, the MHz EME recorded by the telemetric stations on the island of Cephalonia and the neighboring island of Zante (Zakynthos), reached simultaneously critical condition a few days before the occurrence of each earthquake. The critical characteristics embedded in the EME signals were further verified using the natural time (NT) method. Moreover, we show, in terms of the NT method, that the foreshock seismic activity also presented critical characteristics before each one of these events. Importantly, the revealed critical process seems to be focused on the area corresponding to the west Cephalonia zone, following the seismotectonic and hazard zoning of the Ionian Islands area near Cephalonia.

Keywords: Fracture-induced electromagnetic emissions; Earthquake dynamics; Criticality - Tricriticality; Method of Critical Fluctuations; Natural Time Analysis; Seismotectonic Zone Partitioning.

1. Introduction

The possible connection of the electromagnetic (EM) activity that is observed prior to significant earthquakes (EQs) with the corresponding EQ preparation processes, often referred to as seismo-electromagnetics, has been intensively investigated during the last years. Several possible EQ precursors have been suggested in the literature (Uyeda et al., 2009a; Cicerone et al., 2009; Hayakawa, 2013a, 2013b; Varotsos 2005; Varotsos et al., 2011b). The possible relation of the field observed fracture-induced electromagnetic emissions (EME) in the frequency bands of MHz and kHz, associated with shallow EQs with magnitude 6 or larger that occurred in land or near coast, has been examined in a series of publications in order to contribute to a better understanding of the underlying processes (e.g., Eftaxias et al., 2001, 2004, 2008, 2013; Kapiris et al., 2004; Karamanos et al., 2006; Papadimitriou et al., 2008; Contoyiannis et al., 2005, 2013, 2015; Eftaxias and Potirakis, 2013; Potirakis et al., 2011, 2012a, 2012b, 2012c, 2013, 2015; Minadakis et al., 2012a, 2012b), while a four-stage model for the preparation of an EQ by means of its observable EM activity has been recently put forward (Eftaxias and Potirakis, 2013, and references therein; Contoyiannis et al., 2015, and references therein). ~~Note that the specific four-stage model is a suggestion that seems to be supported by the up to now available MHz-kHz observation data and corresponding time-series analyzes, while a rebuttal has not yet appeared in the literature.~~ In summary, the proposed four stages of the last part of EQ preparation process and the associated, appropriately identified, EM observables, specifically EM time series excerpts for which specific features have been identified using appropriate time series analysis methods, appear in the following order (Donner et al., 2015, and references therein): 1st stage: valid MHz anomaly; 2nd stage: kHz anomaly exhibiting tri-critical characteristics; 3rd stage: strong avalanche-like kHz anomaly; 4th stage: electromagnetic quiescence. It is noted that, according to the aforementioned four-stage model, the pre-EQ MHz EM~~ emission~~E is considered to be emitted during the fracture of the part of the Earth's crust that is characterized by high heterogeneity. During this phase the fracture is non-directional and spans over a large area that surrounds the family of large high-strength entities distributed along the fault sustaining the system. Note that for an EQ of magnitude ~6 the corresponding fracture process extends to a radius of ~120km (Bowman et al., 1998).

Two strong shallow EQs occurred recently in western Greece (see Fig. 1). On 26 January 2014 (13:55:43 UT) an $M_w = 6.0$ EQ, hereafter also referred to as "EQ1", occurred on the island of Cephalonia (Kefalonia), with epicenter at (38.22^o N, 20.53^o E) and depth of ~16km. The second significant EQ, $M_w = 5.9$, hereafter also referred to as "EQ2", occurred on the same island on 3 February 2014 (03:08:45 UT), with epicenter at (38.25^o N, 20.40^o E) and depth of ~11km. Various studies of the two earthquakes have already been published indicating their seismotectonic importance (Karastathis et al., 2014; Valkaniotis et al., 2014; Papadopoulos et al., 2014; Ganas et al., 2015; Sakkas and Lagios, 2015; Merryman Boncori et al., 2015) as they were located on two different active faults that belong to the same seismic source zone.

Two pairs of MHz EM signals were recorded, with a sampling rate of 1 sample/s, prior to each one of the above mentioned significant shallow EQs; one pair of simultaneous signals was recorded by two different stations prior to each one of them. On 24 January 2014, two days before the $M_w = 6.0$ Cephalonia EQ (EQ1), two telemetric stations of our EM signal monitoring network (see Fig. 1), the station of Cephalonia, located on the same island (38.18^o N, 20.59^o E), and the station of Zante (Zakynthos), located on a neighboring island belonging to the same (Ionian) island complex (37.77^o N, 20.74^o E), simultaneously recorded the first pair of aforementioned signals. The same picture was repeated for the second significant Cephalonia EQ, $M_w = 5.9$ (EQ2). Specifically, both the Cephalonia and the Zante stations simultaneously recorded the second pair of aforementioned signals on 28 January 2014, six days prior to the specific EQ. Note that it has been repeatedly made clear that all the pre-EQ EME signals, which have been observed by our monitoring network, have been recorded only prior to strong shallow EQs, that have taken place on land (or near the coast-line); this fact, in combination to the recently proposed fractal geo-antenna model (Eftaxias et al., 2004; Eftaxias and Potirakis, 2013), explains why they succeed to be transmitted on air. This model gives a good reason for the increased possibility of detection of such EM radiation, since a fractal geo-antenna emits significantly increased power, compared to the power that would be radiated by the same source, if a dipole antenna model was considered. It should also be noted that, none of the recordings of the other monitoring stations of our network (except from the ones of Cephalonia and Zante) presented critical characteristics before these two specific EQs.

<Figure 1 should be placed around here>

The analysis of the specific EM time series, using the method of critical fluctuations (MCF) (Contoyiannis and Diakonos, 2000; Contoyiannis et al., 2002, 2013), revealed critical features, implying that the possibly related underlying geophysical process was at critical state before the occurrence of each one of the EQs of interest. The critical characteristics embedded in the specific time series were further verified by means of the natural time (NT) method (Varotsos et al., 2011a, 2011b, Potirakis et al., 2013, 2015). The presence of the "critical point" during which any two active parts of the system are highly correlated, theoretically even at arbitrarily long distances, in other words when "everything depends on everything else", is consistent with the view that the EQ preparation process during the period that the MHz EME are emitted is a spatially extensive process. Note that this process corresponds to the first stage of the aforementioned four-stage model.

Moreover, we analyzed the foreshock seismic activity using the NT method; the obtained results indicate that seismicity also presented critical characteristics before each one of the two important events. This result implies that the observed EM anomaly and the associated foreshock seismic activity might be considered as "two sides of the same coin". ~~Importantly, the revealed critical process seems to be focused on an area corresponding to the west Cephalonia zone, one of the parts according to the seismotectonic and hazard zone partitioning of the wider area of the Ionian Islands.~~

Last but not least, one day before the occurrence of EQ2, and five days after the corresponding critical EME signal, tricritical characteristics were revealed in the EME recorded by the Cephalonia station. ~~This finding is also quite important, indicating that the tricritical behavior attributed to the second stage of the aforementioned four-stage model can be identified either in kHz or in MHz EME, leading thus to a revision of the specific four-stage model.~~ ~~Unfortunately, the Zante station was out of order for several hours during the specific day, including the time window during which the tricritical features were identified in the Cephalonia recordings. As a result, we could not cross check whether tricritical signals simultaneously also reached Zante.~~

The remainder of this manuscript is organized as follows: A brief introduction to the MCF and the NT analysis methods is provided in Section 2. The analysis of the EME recordings according to these two methods is presented in Section 3. Section 4 presents the results obtained by the analysis of the foreshock seismic activity using the NT method, while Section 5 concludes the manuscript by summarizing and discussing the findings.

2. Critical Dynamics Analysis Methods

Criticality has early been suggested as an EQ precursory sign (Chelidze, 1982; Chelidze and Kolesnikov, 1982; Chelidze et al., 2006; Rundle et al., 2012; Wanliss et al., 2015). Critical phenomena have been proposed as the likely ~~model~~ framework to study the origins of EQ related EM fluctuations, suggesting that the theory of phase transitions and critical phenomena may be useful in gaining insight to the mechanism of their complex dynamics (Bowman et al., 1998; Contoyiannis et al., 2004a, 2005, 2015; Varotsos et al., 2011a, 2011b). One possible reason for the appropriateness of this model may be the way in which correlations spread thought a disordered medium/ system comprised of subunits. From a qualitative / intuitive perspective, according to the specific approach, initially single isolated activated parts emerge in the system which, then, progressively grow and ~~multiply~~proliferate, leading to cooperative effects. Local interactions evolve to long-range correlations, eventually extending along the entire system. A key point in the study of dynamical systems that develop critical phenomena is the identification of the “critical epoch” during which the “short-range” correlations evolve into “long-range” ones. Therefore, the theory of phase transitions and critical phenomena seem to be appropriate for the study of dynamical complex systems in which local interactions evolve to long-range correlations, such as the disordered Earth’s crust during the preparation of an EQ. Note that for an EQ of magnitude ~6 the corresponding fracture process extends to a radius of ~120km (Bowman et al., 1998).

It is worth noting that key characteristics of a critical point in a phase transition of the second order are the existence of highly correlated fluctuations and scale invariance in the statistical properties. By means of experiments on systems presenting this kind of criticality as well as by appropriately designed numerical experiments, it has been confirmed that right at the “critical point” the subunits are highly correlated even at arbitrarily large “distance”. At the critical state self-similar structures appear both in time and space. This fact is quantitatively manifested by power law expressions describing the distributions of spatial or temporal quantities associated with the aforementioned self-similar structures (Stanley, 1987, 1999).

The time series analysis methods employed in this paper for the evaluation of the MHz EME recordings and the seismicity around the Cephalonia island in terms of critical dynamics are briefly presented in the following. Specifically, the method of critical fluctuations (MCF) is described in Sub-Section 2.1, while the natural time (NT) method is described in Sub-Section 2.2.

2.1 Method of critical fluctuations (MCF)

In the direction of comprehending the dynamics of a system undergoing a continuous phase transition at critical state, the method of critical fluctuations (MCF) has been proposed for the analysis of critical fluctuations in the systems' observables (Contoyiannis and Diakonos, 2000; Contoyiannis et al., 2002). The dynamics of various dynamical systems have been successfully analyzed by MCF; these include thermal (e.g., 3D Ising) (Contoyiannis et al., 2002), geophysical (Contoyiannis and Eftaxias 2008; Contoyiannis et al., 2004a, 2010, 2015), biological (electro-cardiac signals) (Contoyiannis et al., 2004b; Contoyiannis et al., 2013) and economic systems (Ozun et al., 2014).

It has been shown (Contoyiannis and Diakonos, 2000) that the dynamics of the order parameter fluctuations ϕ at the critical state for a second-order phase transition can be theoretically formulated by the non-linear intermittent map:

$$\phi_{n+1} = \phi_n + u\phi_n^{\ z}, \quad (1)$$

where ϕ_n is the scaled order parameter value at the time interval n; u denotes an effective positive coupling parameter describing the non-linear self-interaction of the order parameter; z stands for a characteristic exponent associated with the isothermal exponent δ for critical systems at thermal equilibrium ($z = \delta + 1$). The marginal fixed-point of the above map is the zero point, as expected from critical phenomena theory.

However, it has been shown that in order to quantitatively study a real (or numerical) dynamical system one has to add an unavoidable "noise" term, ε_n, to Eq. (1), which is produced by all stochastic processes (Contoyiannis and Diakonos, 2007). Note that, from the intermittency mathematical framework point of view, the "noise" term denotes ergodicity in the available phase space. In this respect, the map of Eq. (1), for positive values of the order parameter, becomes:

$$\phi_{n+1} = \left| \ \phi_n + u\phi_n^{\ z} + \varepsilon_n \ \right|. \quad (2)$$

Based on the map of Eq. (2), MCF has been introduced as a method capable of identifying whether a system is in critical state of intermittent type by analyzing time-series corresponding to an observable of the specific system. In a few words, MCF is based on the property of maps of intermittent-type, like the ones of Eqs. (1) and (2), that the distribution of properly defined laminar lengths (waiting times) l follow a power-law $P(l) \sim l^{-p_l}$ (Schuster, 1998), where the exponent p_l is $p_l = 1 + \frac{1}{\delta}$ (Contoyiannis et al., 2002). However, the distribution of waiting times for a real data time series which is not characterized by critical dynamics follows an exponential decay, rather than a power-law one (Contoyiannis et al., 2004a), due to stochastic noise and finite size effects. Therefore, the dynamics of a real time series can be estimated by ~~forming the distribution of laminar lengths and~~ fitting the distribution of waiting times (laminar lengths) ~~it~~ to a function $\rho(l)$ combining both power-law and exponential decay (Contoyiannis and Diakonos, 2007):

$$\rho(l) \sim l^{-p_2} e^{-l p_3} . \tag{3}$$

The values of the two exponents p_2 and p_3, which result after fitting laminar lengths distribution in a log-log scale diagram, reveal the underlying dynamics. Exact critical state calls for $p_3 = 0$; in such a case it is $p_2 = p_l > 1$. As a result, in order for a real system to be considered to be at critical state, *both criticality conditions* $p_2 > 1$ *and* $p_3 \approx 0$ *have to be satisfied*.

Note that the choice of the function $\rho(l)$ of Eq. (3), which combines both power-law and exponential decay, to model the distribution of waiting times was deliberately made in order to include both these fundamentally different behaviors, i.e., the critical dynamics (Contoyiannis et al., 2002) and the complete absence of specific dynamics (stochastic processes) (Contoyiannis et al., 2004b), respectively. Of course, the specific function also models intermediate behaviors (Contoyiannis and Diakonos, 2007).

In applying the MCF the corresponding factors of $\rho(l)$ appear to be competitive: any increase of the p_2 exponent value corresponds to a p_3 exponent value reduction and vice versa. However, this is expected because, for example, any increase of the value of p_3 exponent signifies the departure from critical dynamics and thus the reduction of p_2 exponent value. What is interesting to us is to apply MCF analysis to observe this competition in the case of pre-earthquake EME time-series and see whether the obtained exponent values are consistent with those of MCF analyzes performed on other time-series with large statistics which are considered as references for the application of our method. This competition can be observed even within the critical windows as shown in Figs. 2d and 3d.

Moreover, a special dynamics case is the one known as "tricritical crossover dynamics". In statistical physics, a tricritical point is a point in the phase diagram of a system at which the two basic kinds of phase transition, that is the first order transition and the second order transition, meet (Huang, 1987). A characteristic property of the area around this point is the co-existence of three phases, specifically, the high symmetry phase, the low symmetry phase, and an intermediate "mixing state". A passage through this area, around the tricritical point, from the second order phase transition to the first order phase transition through the intermediate mixing state constitutes a tricritical crossover (Huang, 1987).

The specific dynamics is proved to be expressed by the map (Contoyiannis et al., 2015):

$$m_{n+1} = \left| m_n - u m_n^{-z} + \varepsilon_n \right|, \tag{4}$$

where m stands for the order parameter. This map differs from the critical map of Eq. (2) in the sigh of the parameter u and exponent z. Note that for reasons of unified formulation we use for these parameters the same notation as in the critical map of Eq. (2). At the level of MCF analysis this dynamics is expressed by the estimated values for the two characteristic exponents p_2, p_3 values, that satisfy *the tricriticality condition* $p_2 < 1, p_3 \approx 0$. These values have been characterized in (Contoyiannis and Diakonos, 2007) as a signature of tricritical behavior.

Note that in order for a time-series to be possible to be analyzed by the MCF, it should at least present cumulative stationarity. Therefore, a cumulative stationarity test is always performed before applying the MCF method; examples can be found in already published articles (e.g., Contoyiannis et al., 2004a, 2005, 2010; Contoyiannis and Eftaxias, 2008; Potirakis et al., 2015). More details on the application of MCF can be found in several published articles (e.g., Contoyiannis et al. 2002, 2013, 2015), as well as in Section 3 where its application on the MHz EM variations is presented.

2.2 Natural time method (NT)

The natural time method was originally proposed for the analysis for a point process like DC or ultra-low frequency (≤1 Hz) SES (Varotsos et al., 2002; Varotsos, 2005), and has been shown to be optimal for enhancing the signals in the time-frequency space to extract the maximum information possible from a given time series (Abe et al., 2005). The transformation of a time-series of "events" from the conventional time domain to natural time domain is performed by ignoring the time-stamp of each event and retaining only their normalized order (index) of occurrence. Explicitly, in a time series of N successive events, the natural time, χ_k, of the k^{th} event is the index of occurrence of this event normalized, by dividing by the total number of the considered events, $\chi_k = k/N$. On the other hand, the "energy", Q_k, of each, k^{th}, event is preserved. We note that the quantity Q_k represents different physical quantities for various time series: for EQ time series it has been assigned to a seismic energy released (e.g., seismic moment) (Varotsos et al., 2005; Uyeda et al., 2009b), and for SES signals that are of dichotomous nature it corresponds to SES pulse duration (Varotsos, 2005), while for MHz electromagnetic emission signals that are of non-dichotomous nature, it has been attributed to the energy of fracto-electromagnetic emission events as defined in Potirakis et al. (2013). The transformed time series (χ_k, Q_k) is then studied through the normalized power spectrum $\Pi(\varpi) = \left|\sum_{k=1}^{N} p_k \exp(j\varpi\chi_k)\right|^2$, where ϖ is the natural angular frequency, $\varpi = 2\pi\varphi$, with φ standing for the frequency in natural time, termed the "natural frequency", and $p_k = Q_k \big/ \sum_{n=1}^{N} Q_n$ corresponds to the k^{th} event's normalized energy. Note that, the term "natural frequency" should not be confused with the rate at which a system oscillates when it is not driven by an external force; it defines an analysis domain dual to the natural time domain, in the framework of Fourier–Stieltjes transform (Varotsos et al., 2011b).

The study of $\Pi(\varpi)$ at ϖ close to zero reveals the dynamic evolution of the time series under analysis. This is because all the moments of the distribution of p_k can be estimated from $\Pi(\varpi)$ at $\varpi \to 0$ (Varotsos et al., 2011a). Aiming to that, by the Taylor expansion

$\Pi(\varpi)=1-\kappa_1\varpi^2+\kappa_2\varpi^4+\ldots$, the quantity κ_1 is defined, where $\kappa_1=\sum_{k=1}^{N}p_k\chi_k^2-\left(\sum_{k=1}^{N}p_k\chi_k\right)^2$, i.e., the variance of χ_k weighted for p_k characterizing the dispersion of the most significant events within the "rescaled" interval $(0,1]$. Moreover, the entropy in natural time, S_{nt}, is defined (Varotsos et al., 2006) as $S_{nt}=\sum_{k=1}^{N}p_k\chi_k\ln\chi_k-\left(\sum_{k=1}^{N}p_k\chi_k\right)\ln\left(\sum_{k=1}^{N}p_k\chi_k\right)$ and corresponds (Varotsos et al., 2006, 2011b) to the value at $q=1$ of the derivative of the fluctuation function $F(q)=\langle\chi^q\rangle-\langle\chi\rangle^q$ with respect to q (while κ_1 corresponds to $F(q)$ for $q=2$). It is a dynamic entropy depending on the sequential order of events (Varotsos et al., 2006). The entropy, S_{nt-}, obtained upon considering (Varotsos et al., 2006) the time reversal T, i.e., $Tp_m=p_{N-m+1}$, is also considered.

A system is considered to approach criticality when the parameter κ_1 converges to the value $\kappa_1=0.070$ and at the same time both the entropy in natural time and the entropy under time reversal satisfy the condition $S_{nt},S_{nt-}<S_u=(\ln 2/2)-1/4$ (Sarlis et al., 2011), where S_u stands for the entropy of a "uniform" distribution in natural time (Varotsos et al., 2006).

In the special case of natural time analysis of foreshock seismicity (Varotsos et al., 2001, 2005,2006; Sarlis et al., 2008), the seismicity is considered to be in a true critical state, a "true coincidence" is achieved, when three additional conditions are satisfied: (i) The "average" distance $\langle D\rangle$ between the curves of normalized power spectra $\Pi(\varpi)$ of the evolving seismicity and the theoretical estimation of $\Pi(\varpi)$, $\Pi_{critical}(\varpi)=\left(18/5\varpi^2\right)-\left(6\cos\varpi/5\varpi^2\right)-\left(12\sin\varpi/5\varpi^3\right)$, $\Pi_{critical}(\varpi)\approx 1-\kappa_1\varpi^2$, for $\kappa_1=0.070$ should be smaller than 10^{-2}, i.e., $\langle D\rangle=\left\langle\left|\Pi(\varpi)-\Pi_{critical}(\varpi)\right|\right\rangle<10^{-2}$; (ii) the parameter κ_1 should approach the value $\kappa_1=0.070$ "by descending from above" (Varotsos et al., 2001); (iii) Since the underlying process is expected to be self-similar, the time of the true coincidence should not vary upon changing (within reasonable limits) either the magnitude threshold, M_{thres}, or the area, used in the calculation.

It should be finally clarified that in the case of seismicity analysis, the temporal evolution of the parameters κ_1, S_{nt}, S_{nt-}, and $\langle D \rangle$ is studied as new events that exceed the magnitude threshold M_{thres} are progressively included in the analysis. Specifically, as soon as one more event is included, first the time series (χ_k, Q_k) is rescaled in the natural time domain, since each time the k^{th} event corresponds to a natural time $\chi_k = k/N$, where N is the progressively increasing (by each new event inclusion) total number of the considered successive events; then all the parameters involved in the natural time analysis are calculated for this new time series; this process continues until the time of occurrence of the main event.

More details on the application of NT on MHz EME as well as on foreshock seismicity can be found in already published articles (Potirakis et al. 2013, 2015), as well as in Sections 3 and 4, where its application on the MHz EM variations and foreshock seismicity is presented, respectively.

Note that in the case of NT analysis of foreshock seismicity, the introduction of magnitude threshold, M_{thres}, excludes some of the weaker EQ events (with magnitude below this threshold) from the NT analysis. On one hand, this is necessary in order to exclude events for which the recorded magnitude is not considered reliable; depending on the installed seismographic network characteristics, a specific magnitude threshold is usually defined to assure data completeness. On the other hand, the use of various magnitude thresholds, M_{thres}, offers a means of more accurate determination of the time when criticality is reached. In some cases, it happens that more than one time-points may satisfy the rest of NT critical state conditions, however the time of the true coincidence is finally selected by the last condition that "true coincidence should not vary upon changing (within reasonable limits) either the magnitude threshold, M_{thres}, or the area, used in the calculation."

3. Electromagnetic Emissions Analysis Results

Part of the MHz recordings of the Cephalonia station associated with the $M_w = 6.0$ EQ (EQ1) is shown in Fig. 2a. This was recorded in day of year 24, that is ~2 days before the occurrence of EQ1. This stationary time series excerpt, having a total length of 2.8 h (10,000 samples) starting at 24 Jan. 2014 (12:46:40 UT), was analyzed by the MCF method and was identified to be a "critical window" (CW). CWs are time intervals of the MHz EME signals presenting features analogous to the critical point of a second order phase transition (Contoyiannis et al., 2005).

The main steps of the MCF analysis (e.g., Contoyiannis et al., 2013, 2015) on the specific time series are shown in Fig. 2b- Fig. 2d. First, a distribution of the amplitude values of the analyzed signal was obtained from which, using the method of turning points (Pingel et al., 1999), a fixed-point, that is the start of laminar regions, ϕ_o of about 700 mV was determined. Fig. 2c portrays the obtained laminar distributiondistribution of laminar lengths for the end point $\phi_l = 655mV$, that is the distribution of waiting times, referred to as laminar lengths l, between the fixed-point ϕ_o and the end point ϕ_l, as well as the fitted function $f(l) \propto l^{-p_2} e^{-p_3 l}$ with the corresponding exponents $p_2 = 1.35$, $p_3 = 0.000$ with $R^2 = 0.999$. Note that the distribution of laminar lengths is directly fitted to the specific model using the Levenberg-Marquardt algorithm, while the fitting criterion is the chi-square minimization. The fitting is not done in log-log space; the axes of Fig. 2c are logarithmic for the easier depiction of the distribution of laminar lengths. Finally, Fig. 2d shows the obtained plot of the p_2, p_3 exponents vs. ϕ_l. From Fig. 2d it is apparent that the criticality conditions, $p_2 > 1$ and $p_3 \approx 0$, are satisfied for a wide range of end points ϕ_l, revealing the power-law decay feature of the time series that proves that the system is characterized by intermittent dynamics; in other words, the MHz time series excerpt of Fig. 2a is indeed a CW.

<Figure 2 should be placed around here>

Part of the MHz recordings of the Zante station associated with EQ1 is shown in Fig. 3a. This was also recorded in day of year 24, that is ~2 days before the occurrence of Cephalonia EQ1. This stationary time series excerpt, having a total length of 2.8 h (10,000 samples) starting at 24 Jan. 2014 (12:46:40 UT), was also analyzed by the MCF method and was identified to be a "critical window" (CW).

The main stepsapplication of the MCF analysis (e.g., Contoyiannis et al., 2013, 2015) on the specific time series (cf. Fig. 3), revealed that the criticality conditions, $p_2 > 1$ and $p_3 \approx 0$, are satisfied for a wide range of end points ϕ_l, for this signal too. In other words, this signal has also embedded the power-law decay feature that indicates intermittent dynamics, rendering it a CW. are shown in Fig. 3b- Fig. 3d. First, a distribution of the amplitude values of the analyzed signal was obtained from which, using the method of turning points (Pingel et al., 1999), a fixed-point, that is the start of laminar regions, ϕ_o of about 600 mV was determined. Fig. 3c portrays the obtained laminar distribution for the end point $\phi_l = 665 mV$, that is the distribution of waiting times, referred to as laminar lengths l, between the fixed-point ϕ_o and the end point ϕ_l, as well as the fitted function $f(l) \propto l^{-p_2} e^{-p_3 l}$ with the corresponding exponents $p_2 = 1.49$, $p_3 = 0.000$ with $R^2 = 0.999$. Finally, Fig. 3d shows the obtained plot of the p_2, p_3 exponents vs. ϕ_l. From Fig. 3d it is apparent that the criticality conditions, $p_2 > 1$ and $p_3 \approx 0$, are satisfied for a wide range of end points ϕ_l, revealing the power-law decay feature of the time series that proves that the system is characterized by intermittent dynamics; in other words, the MHz time series excerpt of Fig. 3a is indeed a CW.

<Figure 3 should be placed around here>

After the $M_w = 6.0$ (EQ1), ~ a week later, the second, $M_w = 5.9$ (EQ2), occurred on the same island with a focal area a few km further than the first one. Six days earlier, both the Cephalonia and Zante stations simultaneously recorded MHz EME. Specifically, a stationary time series excerpt, having a total length of 3.3 h (12,000 samples) starting at 28 Jan. 2014 (05:33:20 UT), from Caphalonia station and a stationary time series excerpt, having a total length of 5 h (18,000 samples) starting at 28 Jan. 2014 (03:53:20 UT), from Zante station were analyzed by the MCF method and both of them were identified to be CWs. Note that the Cephalonia CW was emitted within the time frame in which the Zante CW was emitted. Figs 4 & 5 show the results of the corresponding analyses.

<Figure 4 should be placed around here>

<Figure 5 should be placed around here>

In summary, we conclude that, according to the MCF analysis method, both stations recorded MHz signals that simultaneously presented critical state features two days before the first main event and six days before the second main event. In order to verify this finding, we proceeded to the analysis of all the corresponding MHz signals by means of the NT analysis method, according to the way of application proposed in Potirakis et al. (2013). According to the specific procedure for the application of the NT method on the MHz signals, we performed an exhaustive search seeking for at least one amplitude threshold value (applied over the total length of the analyzed signal), for which the corresponding fracto-EME events satisfy the natural time method criticality conditions. The idea is that if the MCF gives valid information, and as a consequence the analyzed time series excerpt is indeed in critical condition, then there should be at least one threshold value for which the NT criticality conditions (cf. Sec. 2.2) are satisfied. Indeed, as apparent from Fig. 6, all four signals satisfy the criticality conditions according to the NT method for at least one of the considered threshold values, therefore the results obtained by the MCF method are successfully verified.

<Figure 6 should be placed around here>

On 2 February 2014, i.e., one day before the occurrence of EQ2, MHz EME presenting tricritical characteristics was recorded by the Cephalonia station. This signal emerged five days after the CWs that were identified in the simultaneously recorded, by the Cephalonia and Zante stations, MHz EME. The specific MHz time series excerpt from Cephalonia station, having a total length of 7.5 h (27,000 samples) starting at 2 Feb. 2014 (07:46:40 UT), was analyzed by means of the MCF method yielding the results shown in Fig. 7. As apparent from the results, this signal satisfies the tricriticality conditions $p_2 < 1, p_3 \approx 0$ (cf. Sec. 2.1) for a wide range of end points ϕ_l, revealing the intermediate "mixing state" between the second order phase transition to the first order phase transition. Unfortunately, during the time that the Cephalonia station recorded trictitical MHz signal, the Zante station was out of order; actually, it was out of order for several hours during the specific day.

<Figure 7 should be placed around here>

It has been recently found (Contoyiannis et al., 2015) that such a behavior is identified in the kHz EME which usually emerge near the end of the MHz EME when the environment in which the EQ preparation process evolves changes from heterogeneous to less heterogeneous, and before the emergence of the strong avalanche-like kHz EME which have been attributed to the fracture of the asperities sustaining the fault. Actually, this has been proposed as the second stage of the four-stage model for the preparation of an EQ by means of its observable EM activity (Eftaxias and Potirakis, 2013, and references therein; Contoyiannis et al., 2015, and references therein; Donner et al., 2015). The identification of tricritical behavior in MHz EME is a quite important finding, indicating that the tricritical behavior, attributed to the second stage of the aforementioned four-stage model, can be identified either in kHz or in MHz EME, leading thus to a revision the specific four-stage model in order to include this case too.

As a conclusion, after the first stage of the EQ preparation process where MHz EME with critical features are emitted, a second stage follows where MHz or kHz or both MHz and kHz EME with trictitical features are emitted. As already mentioned (cf. Sec. 2.1), in terms of statistical physics the trictitical behavior is an intermediate dynamical state which is developed in region of the phase diagram of a system around the trictitical point, which can be approached either from the edge of the first order phase transition (characterizing the strong avalanche-like kHz EME attributed to the third stage of the four-stage model) or from the edge of the second order phase transition (characterizing the critical MHz EME attributed to the first stage of the four-stage model). Therefore, although it is expected that the trictitical behavior will be rarely observed, as it has already been discussed in (Contoyiannis et al., 2015), it can be found either in MHz time series, following the emission of a critical MHz EME, or in kHz time series preceding the emission of avalanche-like kHz EME.

4. Foreshock Seismic Activity Analysis Results

As already mentioned in Potirakis et al. (2013, 2015): "seismicity and pre-fracture EMEs should be two sides of the same coin concerning the EQ generation process. If the MHz EMEs and the corresponding foreshock seismic sequence are observable manifestations of the same complex system at critical state, both should be possible to be described as a critical phenomenon by means of the natural time method." Therefore, we also proceeded to the examination of the corresponding foreshock seismic activity around Cephalonia before each one of the significant EQs of interest in order to verify this suggestion. However, we did not apply the NT method on concentric circles around the epicenter of each EQ, as in Potirakis et al. (2013, 2015), but instead we decided to study seismicity within areas determined according to seismotectonic and earthquake hazard criteria.

Following the detailed study presented in Vamvakaris et al. (~~2013~~2016), we incorporated the seismic zones proposed there for our area of study. Thus, as it is presented in Fig. 8, we defined five separate seismic zones, based on the criteria explored in Vamvakaris et al. (~~2013~~2016) and the seismic zonation proposed by them. Since the study area, comprises the most seismically active zone in Greece, assigned also the highest value on the Earthquake Building Code for the country, a large number of source, stress and strain studies have been used in their study to establish such definition of zoning. Hence, it was found well justified to follow their zone definition. In Fig. 8, from east to west and north to south, one can identify the zones of Akarnania (area no. 1), Lefkada island (area no. 2), east Cephalonia island (area no. 3), west Cephalonia island (area no. 4), and Zante island (area no. 5), respectively, covering the area of the Ionian Sea near Cephalonia island.

<Figure 8 should be placed around here>

Before we proceed to the NT analysis of seismicity, the seismic activity prior to EQ1, as well as between EQ1 and EQ2 is briefly discussed in relation to the above mentioned seismic zones. Earthquake parametric data have been retrieved from the National Observatory of Athens on-line catalogue (http://www.gein.noa.gr/en/seismicity/earthquake-catalogs), while for all the presented maps and calculations the local magnitude (M_L), as provided by the specific earthquake catalog, is used. The foreshock seismic activity before EQ1 for the whole investigated area of the Ionian Sea region from 13 December 2013 up to the time of occurrence of the main event is shown in the map of Fig. 9a. As it can be easily observed from this map, there was a high seismic activity mainly focused on two specific zones: west Cephalonia and Zante. Notably, an EQ of $M_L = 4.7$ occurred in Zante on 11/01/2014 04:12:58, indicated by the black arrow in Fig. 9a. No EQs were recorded in Akarnania, while very few events were recorded in Lefkada and east Cephalonia. The events which occurred in west Cephalonia are also shown in a separate map in Fig. 9b for later reference.

<Figure 9 should be placed around here>

Applying the natural time analysis on seismic data (cf. Sec. 2.2), the evolution of the time series (χ_k, Q_k) was studied for the foreshock seismicity prior to EQ1, where Q_k is in this case the seismic energy released during the k^{th} event. The seismic moment, M_0, as proportional to the seismic energy, is usually considered (Varotsos et al., 2005; Uyeda et al., 2009b; Potirakis et al., 2013,2015). Our calculations were based on the seismic moment M_0 (in dyn.cm) resulting from the corresponding M_L as (Varotsos et al., 2005; Potirakis et al., 2013, 2015), $M_0 = 10^{0.99 M_L + 11.8}$. First, we performed an NT analysis on the seismicity activity of the whole investigated Ionian Sea region during the period from 13/12/2013 00:00:00 to 26/01/2014 13:55:44 UT, i.e., just after the occurrence of EQ1, for different magnitude thresholds, M_{thres}, for which all earthquakes having $M_L > M_{thres}$ were included in the analysis. Note that, only $M_{thres} \geq 2$ was considered in order to assure data completeness (Chouliaras et al., 2013a, 2013b).

For all the considered threshold values, the result was the same: no indication of criticality was identified (see for example Fig. 10a). Since, as we have already mentioned, the whole investigated area was mainly dominated by the seismic activity in west Cephalonia and the seismic activity in Zante, while an EQ of $M_L = 4.7$ occurred in Zante, we decided to start the NT analysis after the occurrence of the specific Zante EQ, in order to exclude from our analysis possible foreshock activity related to the specific event. As a result, we performed

NT analysis for the time period 11/01/2014 04:13:00 (just after the $M_L = 4.7$ Zante EQ) to 26/01/2014 13:55:44 UT, for different magnitude thresholds in three successively enclosed areas: namely, the whole investigated area of Ionian Islands region, both Cephalonia (east and west) zones combined, and the zone of west Cephalonia. Representative examples of these analyses are depicted in Fig. 10b – Fig. 10d. The analysis over the whole investigated area of the Ionian Islands region indicates that seismicity reaches criticality on 19 and 20 of January, while the two other progressively narrower areas indicate that the criticality conditions according to NT method are satisfied on 19 and 22 of January. These results imply that seismicity was also in critical condition a few days prior to the occurrence of the first studied significant Cephalonia EQ (EQ1). Actually, in the specific case, the critical condition of seismicity was reached before, but quite close, to the emission of the corresponding MHz signals for which critical behavior was identified (cf. Sec. 3). Note that a very recent analysis on the foreshock seismic activity before EQ1, in terms of a combination of multiresolution wavelets and NT analysis, which was performed on concentric areas of 50 km and 30 km radii around the epicenter of EQ1, also found that NT analysis criticality requirements are met a few days before EQ1 (at approximately 20 January) (Vallianatos et al., 2015).

<Figure 10 should be placed around here>

Before the application of the NT method to the seismic activity prior to EQ2, one should first study the time evolution of the activity between the two significant events of interest, in order to minimize if possible the influence of the first EQ aftershock sequence on the NT analysis. Our first observation about the EQs which occurred during the specific time period was that, all but one had epicenters in west Cephalonia. Only one $M_L = 2.3$ EQ occurred in Zante, at (37.79° N, 21.00° E) on 28 January 2014 02:08:27 UT.

Fig. 11a shows all the events that were recorded in the whole investigated area of the Ionian Islands region vs. time from just after EQ1 ($M_w = 6.0$) up to the time of EQ2 ($M_w = 5.9$), including EQ2. As it can be seen, if one considers that both significant EQs of interest were main events, it is quite difficult to separate the seismic activity of the specific time period into aftershocks of the first EQ and foreshocks of the second one. However, we observe that up to a specific time point, there is a rapid decrease of the running mean magnitude of the recorded EQs, while after that the long range (75 events) running mean value seems to be almost constant over time with the short range (25 events) one varying around it. We arbitrarily set the 29 January 00:00:00 UT as the time point after which the recorded seismicity is no longer dominated by the aftershocks of EQ1; this by no means implies that the aftershock sequence of the EQ1 stops after that date. It should also be underlined that changing this, arbitrarily selected, date within reasonable limits, does not significantly changes the results of our corresponding NT analysis which are presented next. On the other hand, a significant shift of this limit towards EQ1, i.e., to earlier dates, results to severe changes indicating the domination of the recorded seismicity by the aftershock sequence of EQ1. Accordingly, the considered as foreshock seismic activity before EQ2, i.e., from 29/01/2014 00:00 UT up to the time of occurrence of EQ2, is presented in the map of Fig. 11b for west Cephalonia and analyzed in the following.

<Figure 11 should be placed around here>

Next, we applied the NT method on the seismicity of west Cephalonia for the time period from 29/01/2014 00:00:00 to 03/02/2014 03:08:47 UT. Note that we also applied the NT method on the whole investigated area of the Ionian Islands region, obtaining practically the same results. As we have already mentioned, only one $M_L = 2.3$ EQ occurred outside the west Cephalonia zone, so, on the one hand for magnitude threshold values $M_{thres} \geq 2.3$ this event was excluded, while, on the other hand, even for lower threshold values ($2 \leq M_{thres} < 2.3$) its inclusion does not change the results significantly. Fig. 12 shows the NT analysis results for some threshold values proving that seismicity reaches criticality on 1 or 2 February 2014, that is one or two days before the occurrence of the second significant EQ of interest ($M_w = 5.9$).Actually, in the specific case, the critical condition of seismicity was reached after, but quite close, to the emission of the corresponding MHz signals for which critical behavior was identified (cf. Sec. 3).

<Figure 12 should be placed around here>

5. Discussion - Conclusions

Based on the methods of critical fluctuations and natural time, we have shown that the fracture-induced MHz EME recorded by two stations in our network prior to two recent significant EQs occurred in Cephalonia present criticality characteristics, implying that they emerge from a system in critical state.

There are two key points that render these observations unique in the up to now research on the pre-EQ EME:

(i) The Cephalonia station is known for being insensitive to EQ preparation processes happening outside of the wider area of Cephalonia island, as well as to EQ preparation processes leading to low magnitude EQs within the area of Cephalonia island. Note that the only signal that has been previously recorded refers to the M=6 EQ that occurred on the specific island in 2007 (Contoyiannis et al., 2010).

(ii) Prior to each one of the studied significant EQs, two MHz EME time series presenting critical characteristics were recorded simultaneously in two different stations very close to the focal areas, while no other station of our network (cf. Fig. 1) recorded such signals prior to the specific EQs. This indicates that the revealed criticality was not associated with a global phenomenon, such as critical variations in the Ionosphere, but was rather local to the area of the Ionian Islands region, enhancing the hypothesis that these EME were associated with the EQ preparation process taking place prior to the two significant EQs. This feature, combined with the above mentioned sensitivity of the Cephalonia station only to significant EQs occurring on the specific island, could have been considered as an indication of the location of the impending EQs.

EME, as a phenomenon rooted in the damage process, should be an indicator of memory effects. Laboratory studies verify that: during cyclic loading, the level of EME increases significantly when the stress exceeds the maximum previously reached stress level (Kaizer effect). The existence of Kaizer effect predicts the EM silence during the aftershock period (Eftaxias et al., 2013; Eftaxias and Potirakis, 2013, and references therein). Thus, the appearance of the second EM anomaly may reveal that the corresponding preparation of fracture process has been organized in a new barrier.

We note that, according to the view that seismicity and pre-EQ EM emissions should be "two sides of the same coin" concerning the earthquake generation process, the corresponding foreshock seismic activity, as another manifestation of the same complex system, should be at critical state as well, before the occurrence of a main event. We have shown that this really happens for both significant EQs we studied. Importantly, the revealed critical process seems to be focused on an area corresponding to the west Cephalonia zone, one of the parts according to the seismotectonic and hazard zone partitioning of the wider area of the Ionian Islands.

To be more detailed, the foreshock seismicity associated with the first ($M_w = 6.0$) EQ reached critical condition a few days before the occurrence of the main event. Specifically, it came to critical condition before, but quite close, to the emission of the corresponding MHz signals for which critical behavior was identified. The seismicity that was considered as foreshock of the second ($M_w = 5.9$) EQ also reached criticality few days before the occurrence of the main event. In contrary to the first EQ case, it came to criticality after, but quite close, to the emission of the corresponding MHz signals for which critical behavior was identified.

One more outcome of our study was the identification of tricritical crossover dynamics in the MHz emissions recorded just before the occurrence of the second significant EQ of interest ($M_w = 5.9$) at the Cephalonia station. ~~U~~Note that, unfortunately, the Zante station was out of order for several hours during the specific day, including the time window during which the tricritical features were identified in the Cephalonia recordings. As a result, we could not cross check whether tricritical signals simultaneously also reached Zante. This is considered a quite important finding, since it verifies a theoretically expected situation, namely the approach of the intermediate dynamical state of tricritical crossover, either from the first or from the second order phase transition state. In terms of pre-EQ EME, this leads to a revision of the four-stage model for the preparation of an EQ by means of its observable EM activity. Namely, after the first stage of the EQ preparation process where MHz EME with critical features are emitted, a second stage follows where MHz or kHz or both MHz and kHz EME with trictitical features are emitted. Specifically, the trictitical crossover dynamics can be identified either in MHz time series, following the emission of a critical MHz EME, or in kHz time series preceding the emission of avalanche-like kHz EME. In summary, the proposed four stages of the last part of EQ preparation process and the associated, appropriately identified, EM observables appear in the following order: 1st stage: valid MHz anomaly; 2nd stage: MHz or kHz or MHz and kHz anomaly exhibiting tri-critical characteristics; 3rd stage: strong avalanche-like kHz anomaly; 4th stage: electromagnetic quiescence. Note that the specific four-stage model is a suggestion that seems to be verified by the up to now available MHz-kHz observation data and corresponding time-series analyzes, while a rebuttal has not yet appeared in the literature. However, the understanding of the physical processes involved in the preparation of an EQ and their relation to various available observables is an open scientific issue. Much effort still remains to be paid before one can claim clear understanding of EQ preparation processes and associated possible precursors.

As it has been repeatedly pointed out in previous works (e.g., Eftaxias et al., 2013; Eftaxias and Potirakis, 2013, and references therein), our view is that such observations and the associated analyses offer valuable information for the comprehension of the Earth system processes that take place prior to the occurrence of a significant EQ. As it is known, a large number of other precursory phenomena are also observed, both by ground and satellite stations, prior to significant EQs. Only a combined evaluation of our observations with other well documented precursory phenomena could possibly render our observations useful for a reliable short-term forecast solution. Unfortunately, in the cases of the Cephalonia EQs under study this requirement was not fulfilled. To the best of our knowledge, only one paper reporting the emergence of VLF seismic-ionospheric disturbances four days before the first Cephalonia EQ (Skeberis et al., 2015) has been published up to now. It is very important that the specific disturbances, which also correspond to a spatially extensive process as happens with the MHz EME, were recorded during the same time window with the here presented MHz critical signals. However, more precursory phenomena could have been investigated if appropriate observation data were available. For example, if ground-based magnetic observatories in the area of Greece had available magnetometer data for the time period of interest, EQ-related ULF magnetic field variations, either of lithospheric or ionospheric origin, which are also a result of spatially extensive processes and in other cases have been shown to present critical characteristics prior to EQ occurrence (Hayakawa et al., 2015), could also be investigated.

Acknowledgements

The authors S. M. P., Y. C., N. S. M., J. K., G. A., C. N. and K. E. would like to acknowledge that this research was co-funded by the EU (European Social Fund) and national funds, action “Archimedes III—Funding of research groups in T.E.I.”, under the Operational Programme “Education and Lifelong Learning 2007-2013”. The authors G. B. and C. K. would like to acknowledge support from the European Union Seventh Framework Programme (FP7-REGPOT-2012-2013-1) under grant agreement no. 316210 (BEYOND – Building Capacity for a Centre of Excellence for EO-based monitoring of Natural Disasters).

REFERENCES

Abe, S., Sarlis, N. V., Skordas, E. S., Tanaka, H. K., Varotsos, P. A.: Origin of the usefulness of the natural-time representation of complex time series, Phys. Rev. Lett., 94, doi: 10.1103/PhysRevLett.94.170601, 2005.

Bowman, D., Ouillon, G., Sammis, C., Sornette, A., Sornette, D.: An observational test of the critical earthquake concept, J. Geophys. Res., 103, 24359-24372, doi: 10.1029/98JB00792, 1998.

Chelidze, T.: Percolation and fracture, Phys. Earth Planet. In., 28, 93-101, 1982.

Chelidze, T., Kolesnikov, Yu. M.: Percolation modell des bruchprozesses, Gerlands Beitr. Geophysik. Leipzig, 91, 35-44, 1982.

Chelidze, T., Kolesnikov, Yu., Matcharashvili, T.: Seismological criticality concept and percolation model of fracture, Geophys. J. Int., 164, 125-136, 2006.

Chouliaras, G., Melis, N. S., Drakatos, G., Makropoulos, K.: Operational network improvements and increased reporting in the NOA (Greece) seismicity catalog, Geophysical Research Abstracts, 15, EGU2013-12634-6., 2013a.

Chouliaras, G., Melis, N. S., Drakatos, G., Makropoulos, K.: Operational network improvements and increased reporting in the NOA (Greece) seismicity catalog, Adv. Geosci., 36, 7-9, doi: 10.5194/adgeo-36-7-2013, 2013b.

Cicerone, R. D., Ebel, J. E., Britton, J.: A systematic compilation of earthquake precursors, Tectonophysics, 476, 371-396, doi: 10.1016/j.tecto.2009.06.008, 2009.

Contoyiannis, Y., Diakonos, F.: Criticality and intermittency in the order parameter space, Phys. Lett. A, 268, 286 -292, doi: 10.1016/S0375-9601(00)00180-8, 2000.

Contoyiannis, Y., Diakonos, F., Malakis, A.: Intermittent dynamics of critical fluctuations, Phys. Rev. Lett., 89, 035701, doi: 10.1103/PhysRevLett.89.035701, 2002.

Contoyiannis, Y. F, Diakonos, F. K., Kapiris, P. G., Peratzakis, A. S., Eftaxias, K. A.: Intermittent dynamics of critical pre-seismic electromagnetic fluctuations, Phys. Chem. Earth, 29, 397-408, doi: 10.1016/j.pce.2003.11.012, 2004a.

Contoyiannis, Y. F., Diakonos, F. K., Papaefthimiou, C., Theophilidis, G.: Criticality in the relaxation phase of a spontaneously contracting atria isolated from a Frog's Heart, Phys. Rev. Lett., 93, 098101, doi: 10.1103/PhysRevLett.93.098101, 2004b.

Contoyiannis, Y. F., Kapiris, P. G., Eftaxias, K. A.: A Monitoring of a pre-seismic phase from its electromagnetic precursors, Phys. Rev. E, 71, 066123, 066123/1–14, doi: 10.1103/PhysRevE.71.066123, 2005.

Contoyiannis, Y. F., Diakonos, F. K.: Unimodal maps and order parameter fluctuations in the critical region, Phys. Rev. E, 76, 031138, 2007.

Contoyiannis, Y. F., Eftaxias, K.: Tsallis and Levy statistics in the preparation of an earthquake, Nonlin. Processes Geophys., 15, 379-388, doi:10.5194/npg-15-379-2008, 2008.

Contoyiannis, Y. F., Nomicos, C., Kopanas, J., Antonopoulos, G., Contoyianni, L., Eftaxias, K.: Critical features in electromagnetic anomalies detected prior to the L'Aquila earthquake, Physica A, 389, 499-508, doi: 10.1016/j.physa.2009.09.046, 2010.

Contoyiannis, Y. F., Potirakis, S. M., Eftaxias, K.: The Earth as a living planet: human-type diseases in the earthquake preparation process, Nat. Hazards Earth Syst. Sci., 13, 125–139, doi: 10.5194/nhess-13-125-2013, 2013.

Contoyiannis, Y., Potirakis, S. M., Eftaxias, K., Contoyianni, L.: Tricritical crossover in earthquake preparation by analyzing preseismic electromagnetic emissions, J. Geodynamics, 84, 40-54, doi: 10.1016/j.jog.2014.09.015, 2015.

Donner, R. V., Potirakis, S. M., Balasis, G., Eftaxias, K., Kurths, J.: Temporal correlation patterns in pre-seismic electromagnetic emissions reveal distinct complexity profiles prior to major earthquakes, Phys. Chem. Earth, In Press (on-line available), doi: 10.1016/j.pce.2015.03.008, 2015.

Eftaxias, K., Kapiris, P., Polygiannakis, J., Bogris, N., Kopanas, J., Antonopoulos, G., Peratzakis, A., Hadjicontis, V.: Signatures of pending earthquake from electromagnetic anomalies, Geophys. Res. Let., 28, 3321-3324, doi: 10.1029/2001GL013124, 2001.

Eftaxias, K., Frangos, P., Kapiris, P., Polygiannakis, J., Kopanas, J., Peratzakis, A., Skountzos, P., Jaggard, D.: Review and a model of pre-seismic electromagnetic emissions in terms of fractal electrodynamics, Fractals, 12, 243–273, doi: 10.1142/S0218348X04002501, 2004.

Eftaxias, K., Contoyiannis, Y., Balasis, G., Karamanos, K., Kopanas, J., Antonopoulos, G., Koulouras, G., Nomicos, C.: Evidence of fractional-Brownian-motion-type asperity model for earthquake generation in candidate pre-seismic electromagnetic emissions, Nat. Hazards Earth Syst. Sci., 8, 657–669, doi:10.5194/nhess-8-657-2008, 2008.

Eftaxias, K., Potirakis, S. M., Chelidze, T.: On the puzzling feature of the silence of precursory electromagnetic emissions, Nat. Hazards Earth Syst. Sci., 13, 2381-2397, doi: 10.5194/nhess-13-2381-2013, 2013.

Eftaxias, K., Potirakis, S. M.: Current challenges for pre-earthquake electromagnetic emissions: shedding light from micro-scale plastic flow, granular packings, phase transitions and self-affinity notion of fracture process, Nonlin. Processes Geophys., 20, 771–792, doi:10.5194/npg-20-771-2013, 2013.

Ganas, A., Cannavo, F., Chousianitis, K., Kassaras, I., Drakatos, G.: Displacements recorded on continuous GPS stations following the 2014 M6 Cephalonia (Greece) earthquakes: Dynamic characteristics and kinematic implications, Acta Geodyn. Geomater., 12(1), 5–27, doi: 10.13168/AGG.2015.0005, 2015.

Hayakawa, M. (ed.): *The Frontier of Earthquake Prediction Studies*, Nihon-Senmontosho-Shuppan, Tokyo, 2013a.

Hayakawa, M. (ed.): *Earthquake Prediction Studies: Seismo Electromagnetics*, Terrapub, Tokyo, 2013b.

Hayakawa, M., Schekotov, A, Potirakis, S. and Eftaxias, K.: Criticality features in ULF magnetic fields prior to the 2011 Tohoku earthquake, Proc. Japan Acad., Ser. B, 91, 25-30, doi: 10.2183/pjab.91.25, 2015.

Huang, K.: *Statistical Mechanics*, 2nd Ed. John Wiley and sons, New York, 1987.

Kapiris, P., Eftaxias, K., Chelidze, T.: Electromagnetic signature of prefracture criticality in heterogeneous media, Phys. Rev. Lett., 92(6), 065702/1-4, doi: 10.1103/PhysRevLett.92.065702, 2004.

Karamanos, K., Dakopoulos, D., Aloupis, K., Peratzakis, A., Athanasopoulou, L., Nikolopoulos, S., Kapiris, P., Eftaxias, K.: Study of pre-seismic electromagnetic signals in terms of complexity, Phys. Rev. E, 74, 016104/1-21, doi: 10.1103/PhysRevE.74.016104, 2006.

Karastathis, V. K., Mouzakiotis, E., Ganas, A., Papadopoulos, G. A.: High-precision relocation of seismic sequences above a dipping Moho: The case of the January-February 2014 seismic sequence in Cephalonia Isl. (Greece), Solid Earth Discuss., 6, 2699-2733, doi: 10.5194/sed-6-2699-2014, 2014.

Merryman Boncori, J. P., Papoutsis , I., Pezzo, G., Tolomei , C., Atzori, S., Ganas, A., Karastathis, V., Salvi, S., Kontoes, C., Antonioli, A.: The February 2014 Cephalonia earthquake (Greece): 3D deformation field and source modeling from multiple SAR techniques, Seismol. Res. Lett. 86(1), 1-14, doi: 10.1785/0220140126, 2015.

Minadakis, G., Potirakis, S. M., Nomicos, C., Eftaxias, K.: Linking electromagnetic precursors with earthquake dynamics: an approach based on nonextensive fragment and self-affine asperity models, Physica A, 391, 2232-2244, doi: 10.1016/j.physa.2011.11.049, 2012a.

Minadakis, G., Potirakis, S. M., Stonham, J., Nomicos, C., Eftaxias, K.: The role of propagating stress waves in geophysical scale: Evidence in terms of nonextensivity, Physica A, 391(22), 5648-5657, doi:10.1016/j.physa.2012.04.030, 2012b.

Ozun, A., Contoyiannis, Y. F., Diakonos, F. K., Hanias, M., Magafas, L.: Intermittency in stock market dynamic, J. Trading 9(3), 26-33, 2014.

Papadimitriou, K., Kalimeri, M., Eftaxias, K.: Nonextensivity and universality in the earthquake preparation process, Phys. Rev. E, 77, 036101/1-14, doi: 10.1103/PhysRevE.77.036101, 2008.

Papadopoulos, G. A., Karastathis, V. K., Koukouvelas, I., Sachpazi, M., Baskoutas, I., Chouliaras, G., Agalos, A., Daskalaki, E., Minadakis, G., Moshou, A., Mouzakiotis, A., Orfanogiannaki, K., Papageorgiou, A., Spanos, D., Triantafyllou, I.: The Cephalonia, Ionian Sea (Greece), sequence of strong earthquakes of January-February 2014: a first report, Res. Geoph., 4:5441, 19-30, doi:10.4081/rg.2014.5441, 2014.

Pingel, D., Schmelcher, P., Diakonos, F. K.: Theory and examples of the inverse Frobenius-Perron problem for complete chaotic maps, Chaos, 9, 357-366, doi: 10.1063/1.166413, 1999.

Potirakis, S. M., Minadakis, G., Nomicos, C., Eftaxias, K.: A multidisciplinary analysis for traces of the last state of earthquake generation in preseismic electromagnetic emissions, Nat. Hazards and Earth Syst. Sci., 11, 2859-2879, doi:10.5194/nhess-11-2859-2011, 2011.

Potirakis, S. M., Minadakis, G., Eftaxias, K.: Analysis of electromagnetic pre-seismic emissions using Fisher information and Tsallis entropy, Physica A, 391, 300-306, doi:10.1016/j.physa.2011.08.003, 2012a.

Potirakis, S. M., Minadakis, G., Eftaxias, K.: Sudden drop of fractal dimension of electromagnetic emissions recorded prior to significant earthquake, Nat. Hazards, 64, 641-650, doi:10.1007/s11069-012-0262-x, 2012b.

Potirakis, S. M., Minadakis, G., Eftaxias, K.: Relation between seismicity and pre-earthquake electromagnetic emissions in terms of energy, information and entropy content, Nat. Hazards Earth Syst. Sci., 12, 1179-1183, doi:10.5194/nhess-12-1179-2012, 2012c.

Potirakis, S.M., Karadimitrakis, A. and Eftaxias, K.: Natural time analysis of critical phenomena: the case of pre-fracture electromagnetic emissions, Chaos, 23, 2, 023117. doi:10.1063/1.4807908, 2013.

Potirakis, S. M., Contoyiannis, Y., Eftaxias, K., Koulouras, G., and Nomicos, C.: Recent field observations indicating an earth system in critical condition before the occurrence of a significant earthquake, IEEE Geosc. Remote Sens. Lett., 12(3), 631-635, doi: 10.1109/LGRS.2014.2354374, 2015.

Rundle, J. B., Holliday, J. R., Graves, W. R., Turcotte, D. L., Tiampo. K. F., Klein, W.: Probabilities for large events in driven threshold systems, Phys. Rev. E, 86, 021106, 2012.

Sakkas, V., Lagios, E.: Fault modelling of the early-2014 ~ M6 Earthquakes in Cephalonia Island (W. Greece) based on GPS measurements, Tectonophysics, 644-645, 184-196, doi: 10.1016/j.tecto.2015.01.010, 2015.

Sarlis, N. V., Skordas, E. S., Varotsos, P. A.: Similarity of fluctuations in systems exhibiting self-organized criticality, Europhys. Lett., 96, 2, doi:10.1209/0295-5075/96/28006, 2011.

Sarlis, N. V., Skordas, E. S., Lazaridou, M. S., Varotsos, P. A.: Investigation of seismicity after the initiation of a Seismic Electric Signal activity until the main shock, Proc. Japan Acad., Ser. B., 84, 331-343, 2008.

Schuster, H.: *Deterministic Chaos*, VCH, Weinheim, 1998.

Skeberis, C., Zaharis, Z.D., Xenos, T.D., Spatalas, S., Arabelos, D.N., Contadakis, M.E.: Time–frequency analysis of VLF for seismic-ionospheric precursor detection: Evaluation of Zhao-Atlas-Marks and Hilbert-Huang Transforms, Phys. Chem. Earth, 85-86, 174–184~~In Press (on-line available)~~, doi:10.1016/j.pce.2015.02.006, 2015.

Stanley, H. E.: *Introduction to Phase Transitions and Critical Phenomena*, Oxford University Press, New York, 1987.

Stanley, H. E.: Scaling, universality, and renormalization: Three pillars of modern critical phenomena, Rev. Modern Phys., 71, S358-S366, 1999.

Uyeda, S., Nagao, T., Kamogawa, M.: Short-term EQ prediction: Current status of seismo-electromagnetics, Tectonophysics, 470, 205–213, 2009a.

Uyeda, S., Kamogawa, M., Tanaka, H.: Analysis of electrical activity and seismicity in the natural time domain for the volcanic-seismic swarm activity in 2000 in the Izu Island region, Japan, J. Geophys Res., 114(B2), B02310, doi:10.1029/2007JB005332, 2009b.

Valkaniotis, S., Ganas, A., Papathanassiou, G., Papanikolau, M.: Field observations of geological effects triggered by the January-February 2014 Cephalonia (Ionian Sea, Greece) earthquakes, Tectonophysics, 630, 150-157, doi: 10.1016/j.tecto.2014.05.012, 2014.

Vallianatos, F., Michas, G., Hloupis, G.: Multiresolution wavelets and natural time analysis before the January-February 2014 Cephalonia (Mw6.1 & 6.0) sequence of strong earthquake events, Phys. Chem. Earth, 85-86, 201–209, 2015.

Vamvakaris, D. A., Papazachos, C. B., Papaioannou, Ch. A., Scordilis, E. M., and Karakaisis, G. F.: A detailed seismic zonation model for shallow earthquakes in the broader Aegean area, Nat. Hazards Earth Syst. Sci., 16, 55-84, doi:10.5194/nhess-16-55-2016, 2016. ~~Vamvakaris, D. A., Papazachos, C. B., Papaioannou, C., Scordilis, E. M., Karakaisis, G. F.: A detailed seismic zonation model for shallow earthquakes in the broader Aegean area, Nat. Hazards Earth Syst. Sci. Discuss., 1, 6719-6784, doi: 10.5194/nhessd-1-6719-2013, 2013.~~

Varotsos, P. A.: *The Physics of Seismic Electric Signals*,TERRAPUB, Tokyo, 2005.

Varotsos, P. A., Sarlis, N. V., Skordas, E. S.: Spatio-temporal complexity aspects on the interrelation between seismic electric signals and seismicity., Pract. Athens Acad., 76, 294-321, 2001.

Varotsos, P. A., Sarlis, N. V., Skordas, E. S.: Long-range correlations in the electric signals that precede rupture, Phys. Rev. E, 66, 011902.doi:10.1103/ PhysRevE.66.011902, 2002.

Varotsos, P. A., Sarlis, N. V., Tanaka, H. K., Skordas, E. S.: Similarity of fluctuations in correlated systems: The case of seismicity, Phys. Rev. E, 72, 041103. doi: 10.1103/PhysRevE.72.041103, 2005.

Varotsos, P. A., Sarlis, N. V., Skordas, E. S., Tanaka, H. K., Lazaridou, M. S.: Entropy of seismic electric signals: Analysis in the natural time under time reversal, Phys. Rev. E, 73, 031114. doi:10.1103/PhysRevE.73.031114, 2006.

Varotsos, P., Sarlis, N., Skordas, E., Uyeda, S., Kamogawa, M.: Natural time analysis of critical phenomena, Proc. Natl. Acad. Sci. USA, 108, 11361–11364, 2011a.

Varotsos, P., Sarlis, N., Skordas, E. S.: *Natural Time Analysis: The New View of Time*, Springer, Berlin, 2011b.

Wanliss, J., Muñoz, V., Pastén, D., Toledo, B., Valdivia, J. A.: Critical behavior in earthquake energy dissipation, Nonlin. Processes Geophys. Discuss., 2, 619–645, 2015.

Figures

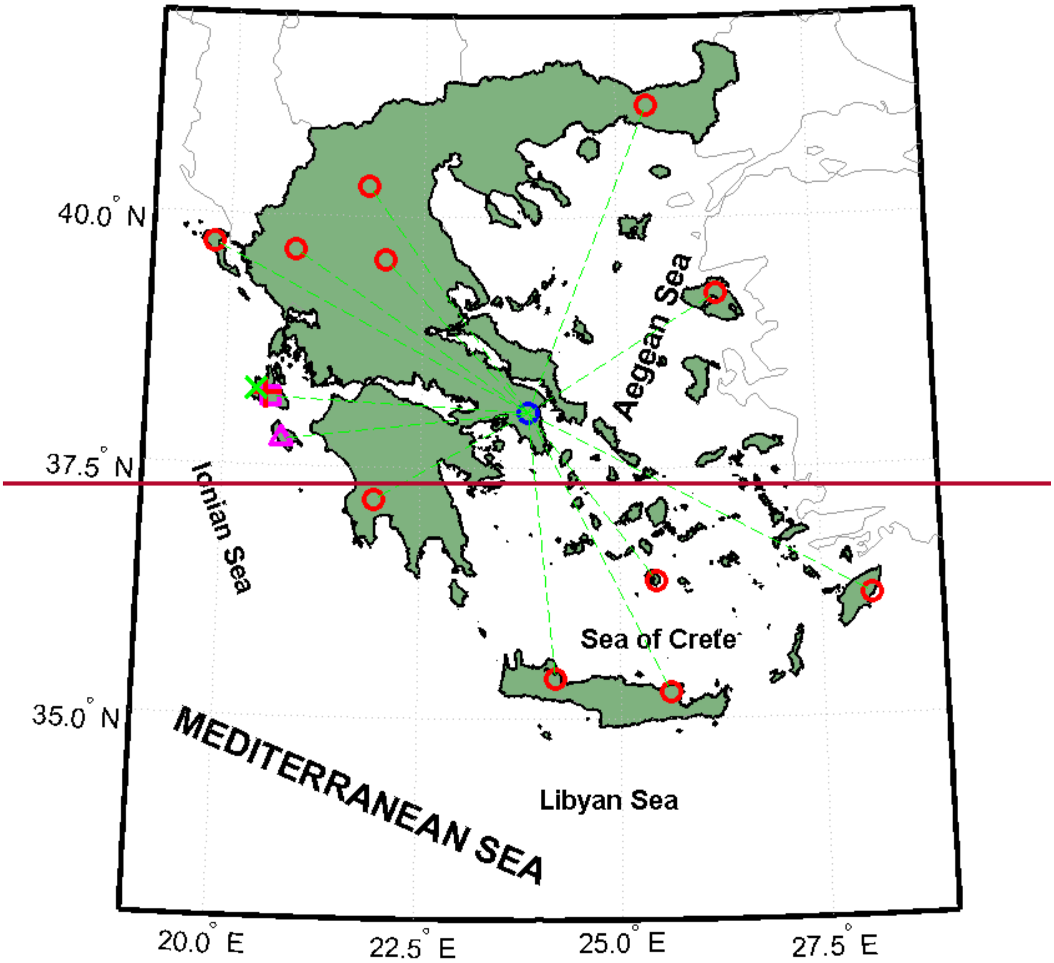
40.0° N
37.5° N
35.0° N
20.0° E
22.5° E
25.0° E
27.5° E
Aegean Sea
Ionian Sea
Sea of Crete
Libyan Sea
MEDITERRANEAN SEA

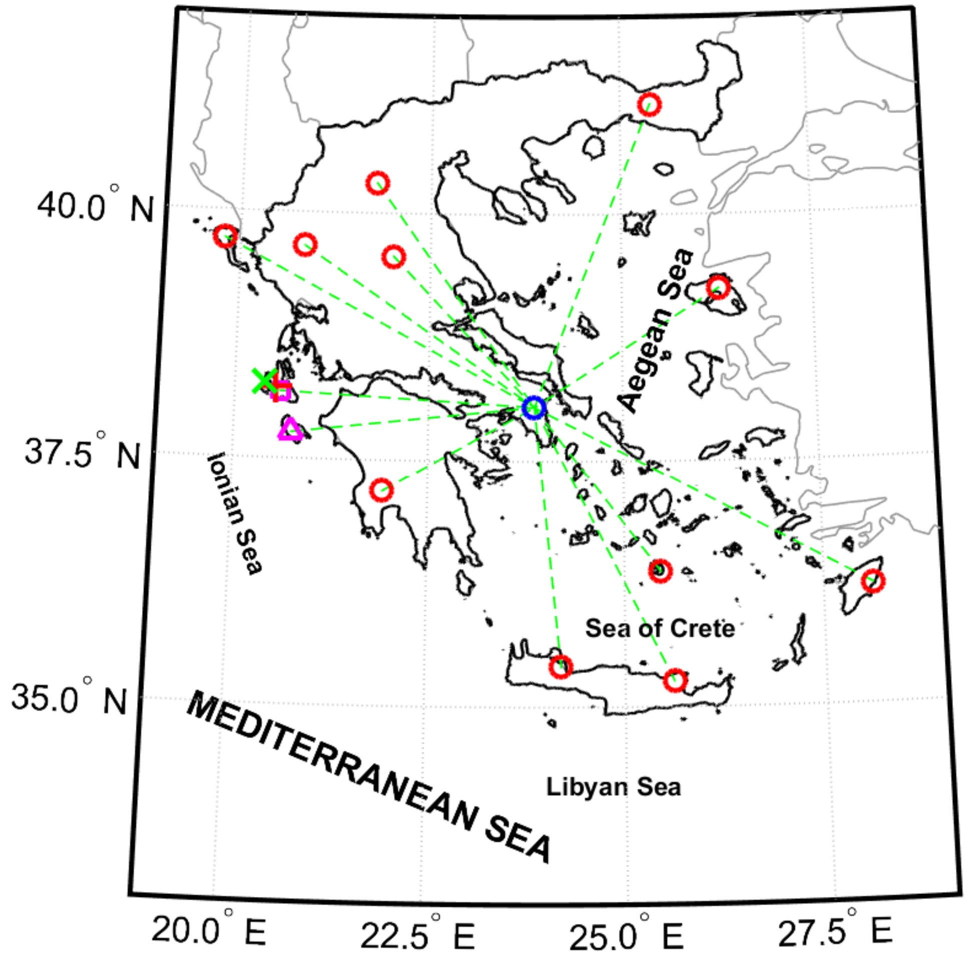

Figure 1. Map with distribution of stations of the telemetric network that monitors electromagnetic variations in the MHz and kHz bands in Greece, which were operating during the time period of interest. The locations of the Cephalonia and Zante stations are marked by the magenta square and triangle, respectively, while the rest of the remote stations are denoted by red circles and the central data recording server by a blue circle. The epicenters of the two significant EQs of interest are also marked, the first (EQ1, $M_w = 6.0$) by a red cross and the second (EQ2, $M_w = 5.9$) by a green X mark. (For interpretation of the references to colors, the reader is referred to the online version of this paper.)

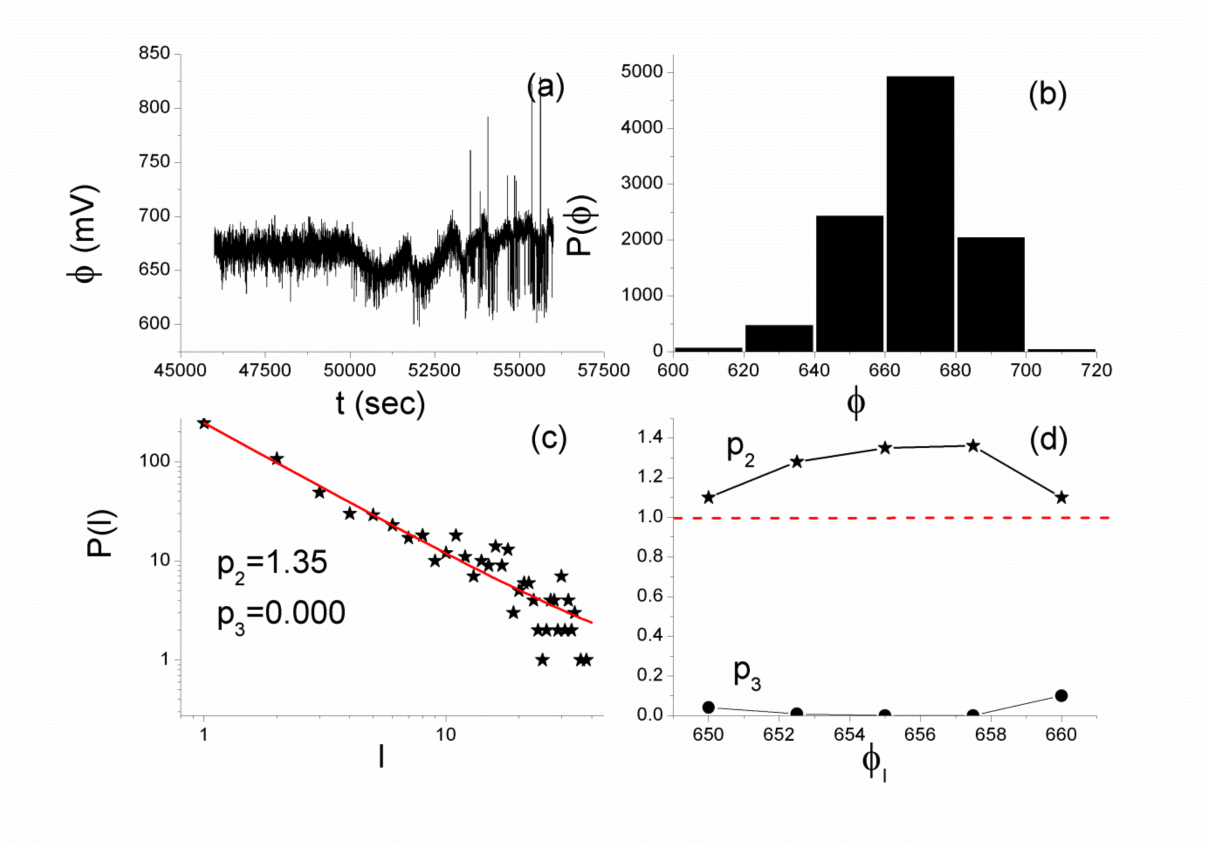

Figure 2. (a) The 10,000 samples long critical window of the MHz EME that was recorded before the Cephalonia $M_w = 6.0$ EQ at the Cephalonia station. (b) Amplitude distribution of the signal of Fig. 2a. (c) ~~Laminar distribution~~Distribution of laminar lengths for the end point $\phi_l = 655mV$, as a representative example of the involved fitting. The solid line corresponds to the fitted function (cf. to text in Sec. 2.1) with the values of the corresponding exponents p_2, p_3 also noted. (d) The obtained exponents p_2, p_3 vs. different values of the end of laminar region ϕ_l. The horizontal dashed line indicates the critical limit ($p_2 = 1$).

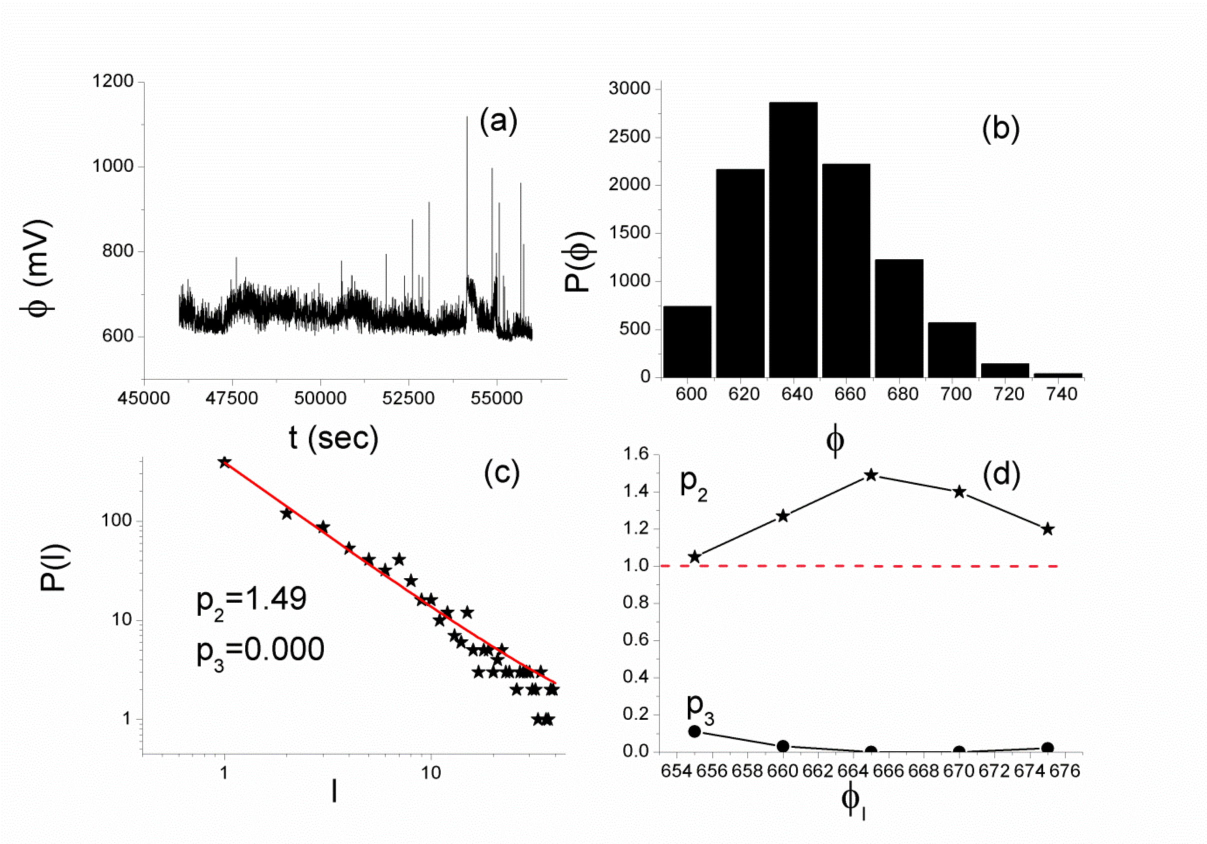

Figure 3. (a) The 10,000 samples long critical window of the MHz EME that was recorded prior to the Cephalonia $M_w = 6.0$ EQ at the Zante station., while (b), (c), and (d) are similar to the corresponding parts of Fig. 2. From 3b, a fixed-point (start of laminar regions), ϕ_o of about 600 mV results, while in Fig. 3c, the d Amplitude distribution of the signal of Fig. 3a. (c) Laminar distributionistribution of laminar lengths is given for the end point $\phi_l = 665mV$, for which the exponents $p_2 = 1.49$, $p_3 = 0.000$ with $R^2 = 0.999$ were obtained.as a representative example of the involved fitting. The solid line corresponds to the fitted function (cf. to text in Sec. 2.1) with the values of the corresponding exponents p_2, p_3 also noted. (d) The obtained exponents p_2, p_3 vs. different values of the end of laminar region ϕ_l. The horizontal dashed line indicates the critical limit ($p_2 = 1$).

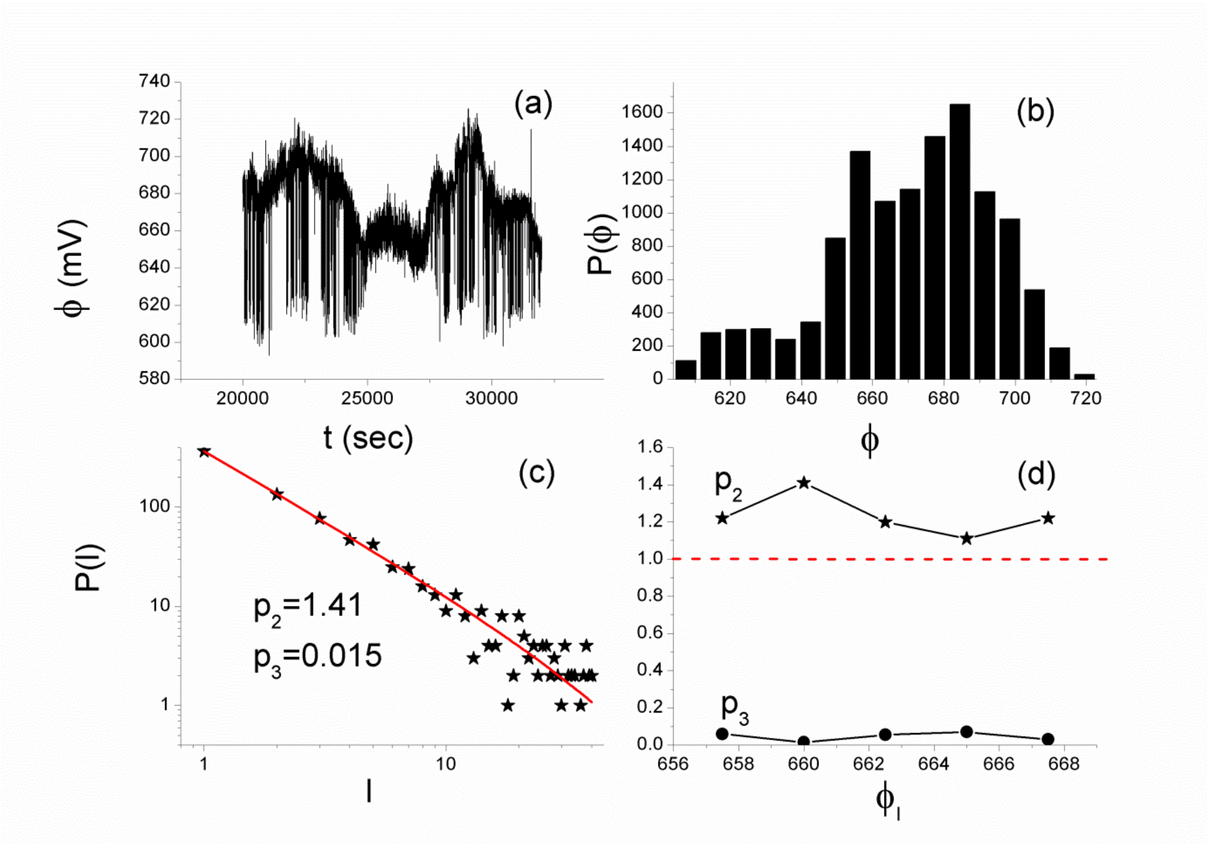

Figure 4. (a) The 12,000 samples long critical window of the MHz EME that was recorded before the Cephalonia $M_w = 5.9$ EQ at the Cephalonia station, while. (b), (c), and (d) are similar to the corresponding parts of Fig. 2. In Fig. 4c, the d Amplitude distribution of the signal of Fig. 4a. (c) Laminar distributionistribution of laminar lengths is given for the end point $\phi_l = 660mV$, as a representative example of the involved fitting. The solid line corresponds to the fitted function (cf. to text in Sec. 2.1) with the values of the corresponding exponents p_2, p_3 also noted. (d) The obtained exponents p_2, p_3 vs. different values of the end of laminar region ϕ_l. The horizontal dashed line indicates the critical limit ($p_2 = 1$).

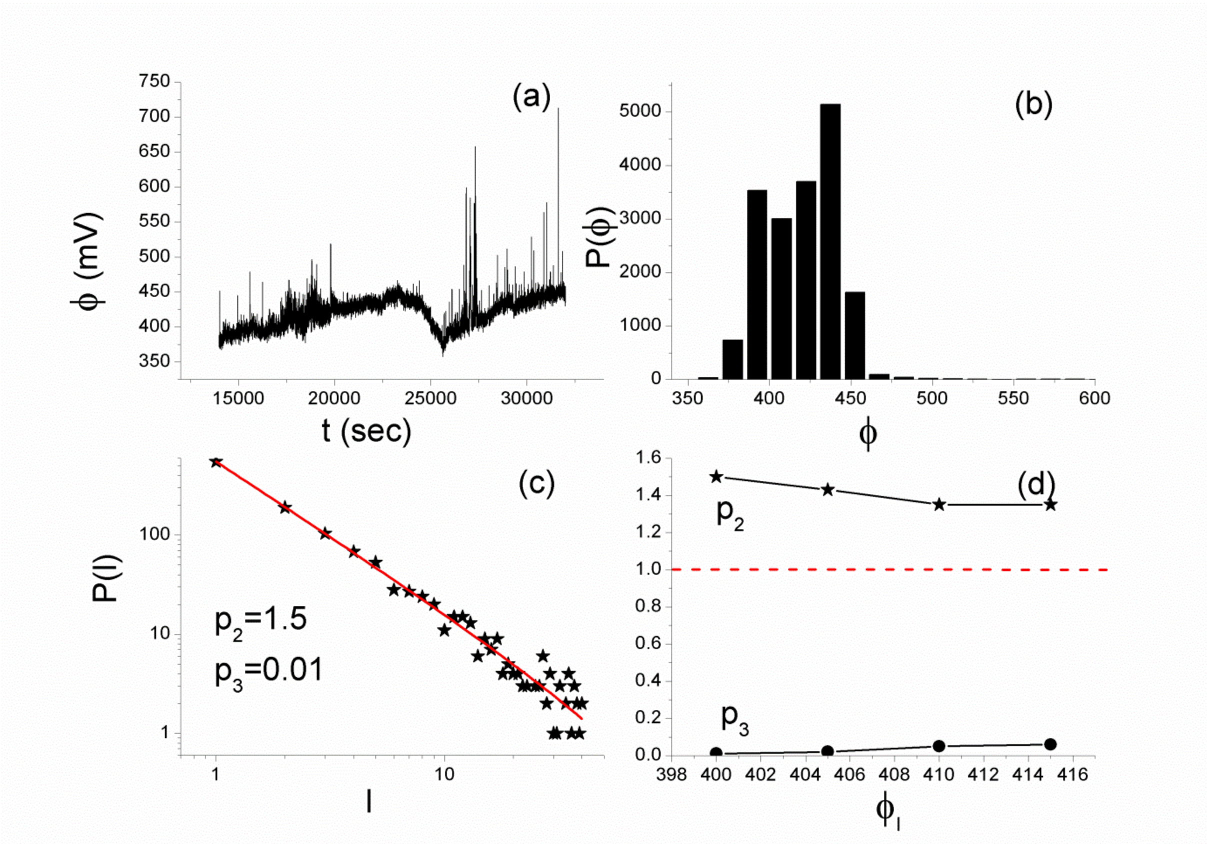

Figure 5. (a) The 18,000 samples long critical window of the MHz EME that was recorded before the Cephalonia $M_w = 5.9$ EQ at the Zante station~~.~~; (b), (c), and (d) are similar to the corresponding parts of Fig. 2. In Fig. 5c, the d~~Amplitude distribution of the signal of Fig. 5a. (c) Laminar distribution~~istribution of laminar lengths ~~for~~ corresponds to the end point $\phi_l = 400mV$ ~~, as a representative example of the involved fitting. The solid line corresponds to the fitted function (cf. to text in Sec. 2.1) with the values of the corresponding exponents p_2, p_3 also noted. (d) The obtained exponents p_2, p_3 vs. different values of the end of laminar region ϕ_l. The horizontal dashed line indicates the critical limit ($p_2 = 1$)~~.

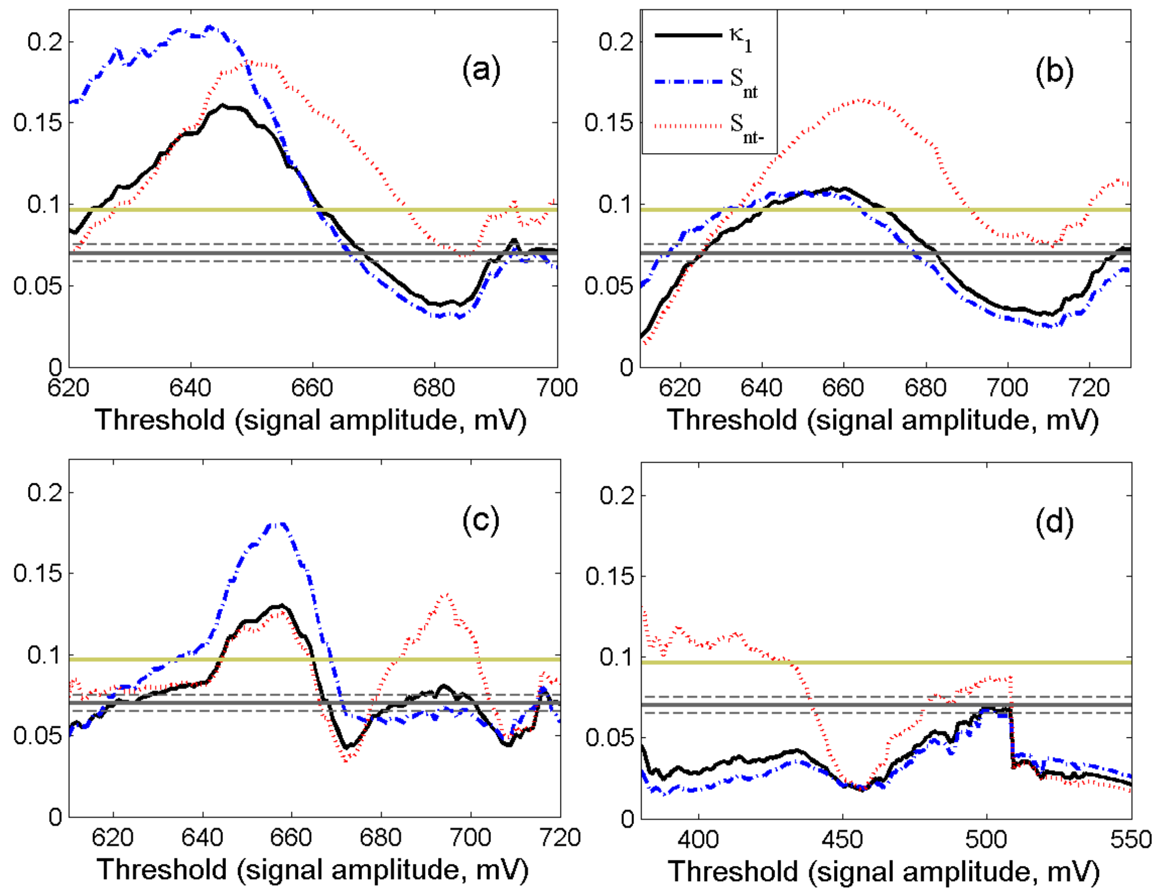

Figure 6. Natural time analysis results obtained for the MHz EME signals shown in: (a) Fig. 2a, recorded at Cephalonia station prior to EQ1, (b) Fig. 3a, recorded at Zante station prior to EQ1, (c) Fig. 4a, recorded at Cephalonia station prior to EQ2, and (d) Fig. 5a, recorded at Zante station prior to EQ2. The quantities κ_1 (solid curve), S_{nt} (dash-dot curve), and S_{nt-} (dot curve) vs. amplitude threshold for each MHz signal are shown. The entropy limit of $S_u\left(\approx 0.0966\right)$, the value 0.070 and a region of ± 0.005 around it are denoted by the horizontal solid light green, solid grey and the grey dashed lines, respectively. (For interpretation of the references to colors, the reader is referred to the online version of this paper.)

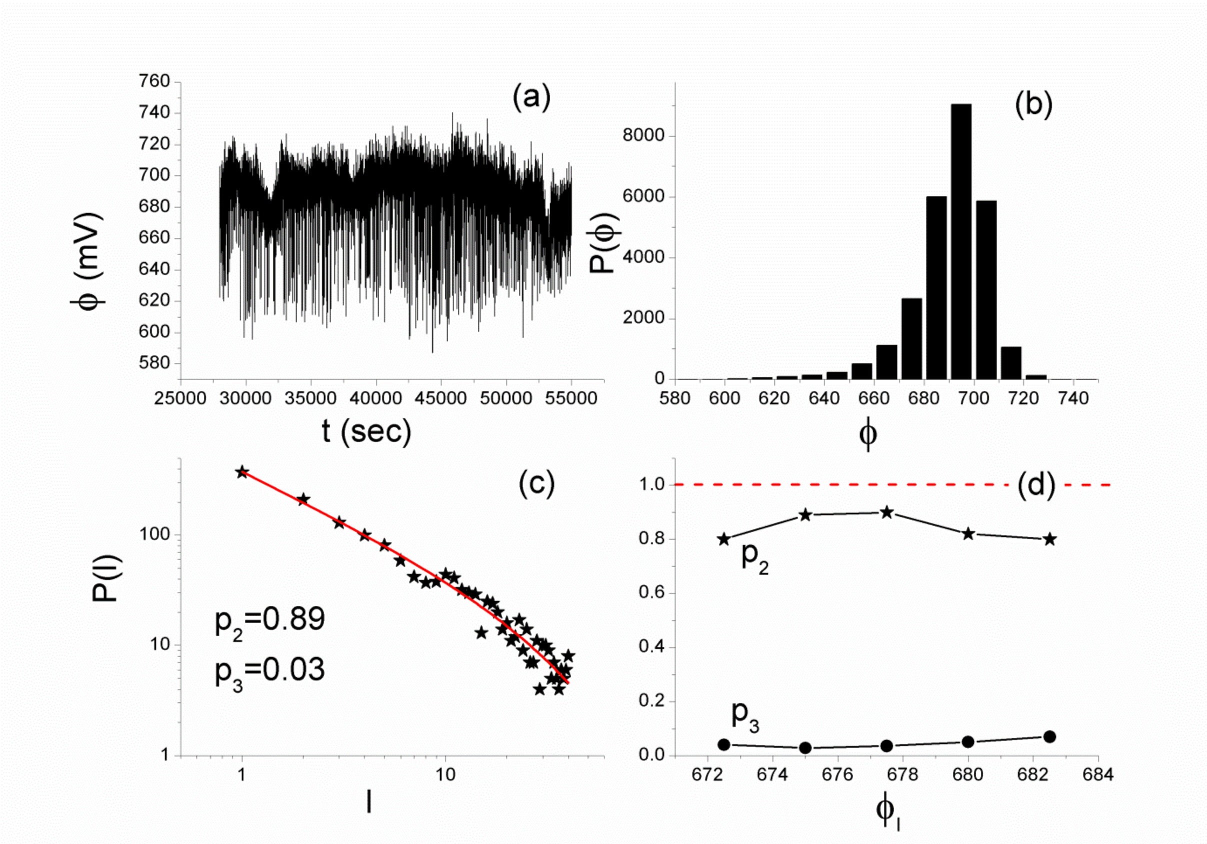

Figure 7. (a) The 27,000 samples long tricritical excerpt of the MHz EME that was recorded before the Cephalonia $M_w = 5.9$ EQ at the Cephalonia station. ; (b), (c), and (d) are similar to the corresponding parts of Fig. 2. In Fig. 7c, the d Amplitude distribution of the signal of Fig. 7a. (c) Laminar distributionistribution of laminar lengths for corresponds to the end point $\phi_l = 675mV$, as a representative example of the involved fitting. The solid line corresponds to the fitted function (cf. to text in Sec. 2.1) with the values of the corresponding exponents p_2, p_3 also noted. (d) The obtained exponents p_2, p_3 vs. different values of the end of laminar region ϕ_l. The horizontal dashed line indicates the critical limit ($p_2 = 1$).

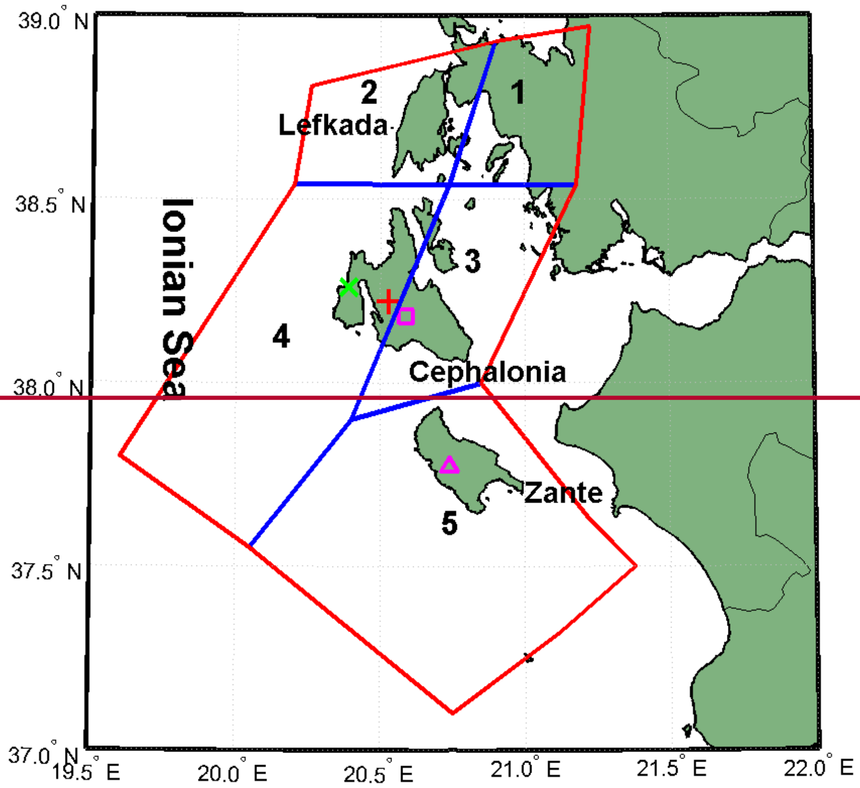
39.0° N
38.5° N
38.0° N
37.5° N
37.0° N
19.5° E
20.0° E
20.5° E
21.0° E
21.5° E
22.0° E
Ionian Sea
Lefkada
Cephalonia
Zante
1
2
3
4
5

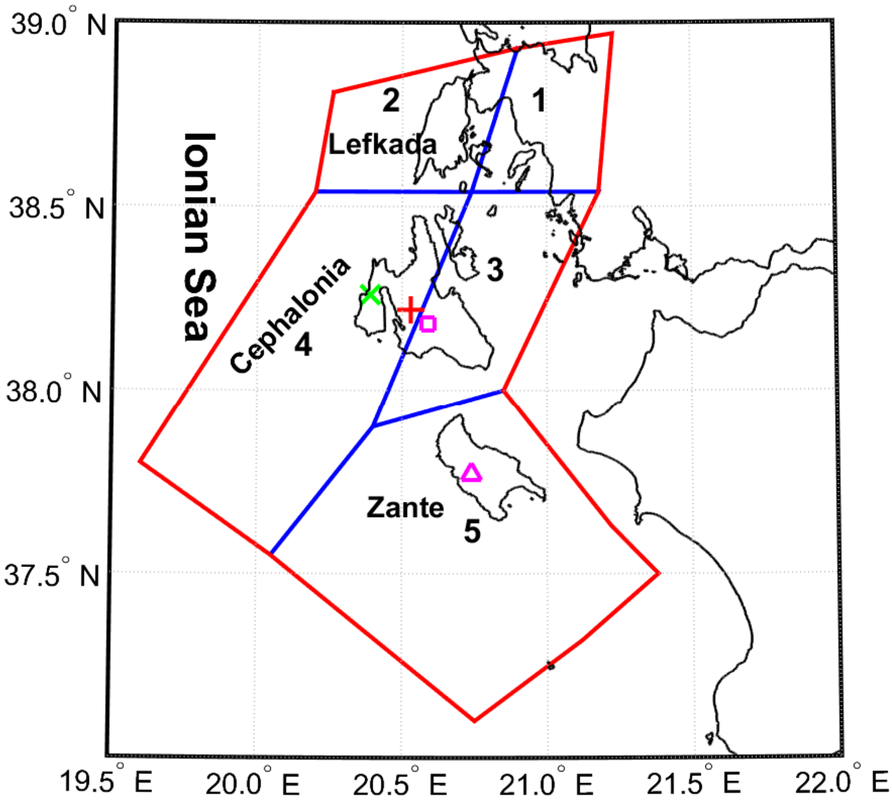

Figure 8. Seismic zonation in the Ionian Islands area. The locations of the Cephalonia and Zante stations, as well as the epicenters of the two significant EQs of interest are marked, using the same signs presented in Fig. 1.

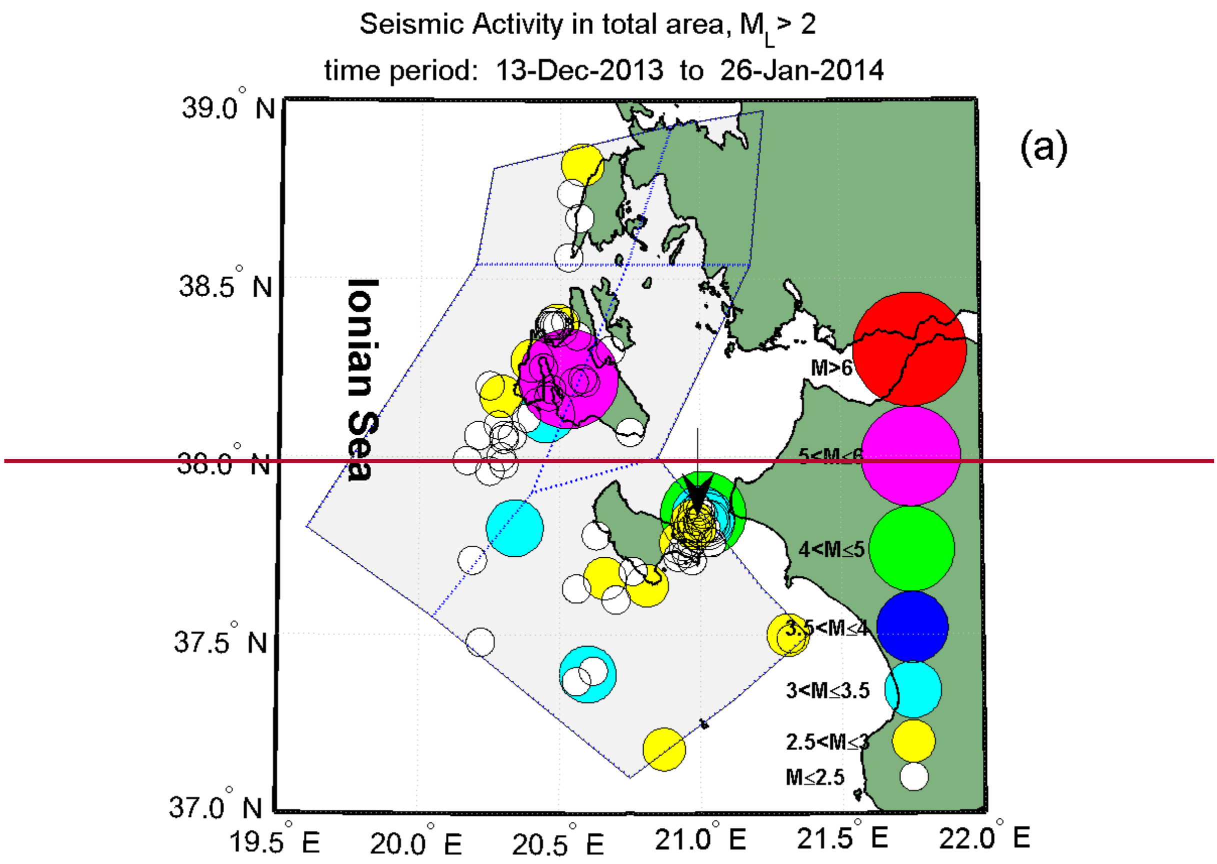

Seismic Activity in total area, M_L > 2
time period: 13-Dec-2013 to 26-Jan-2014
(a)
Ionian Sea
39.0° N
38.5° N
38.0° N
37.5° N
37.0° N
19.5° E
20.0° E
20.5° E
21.0° E
21.5° E
22.0° E
M>6
5<M≤6
4<M≤5
3.5<M≤4
3<M≤3.5
2.5<M≤3
M≤2.5

1

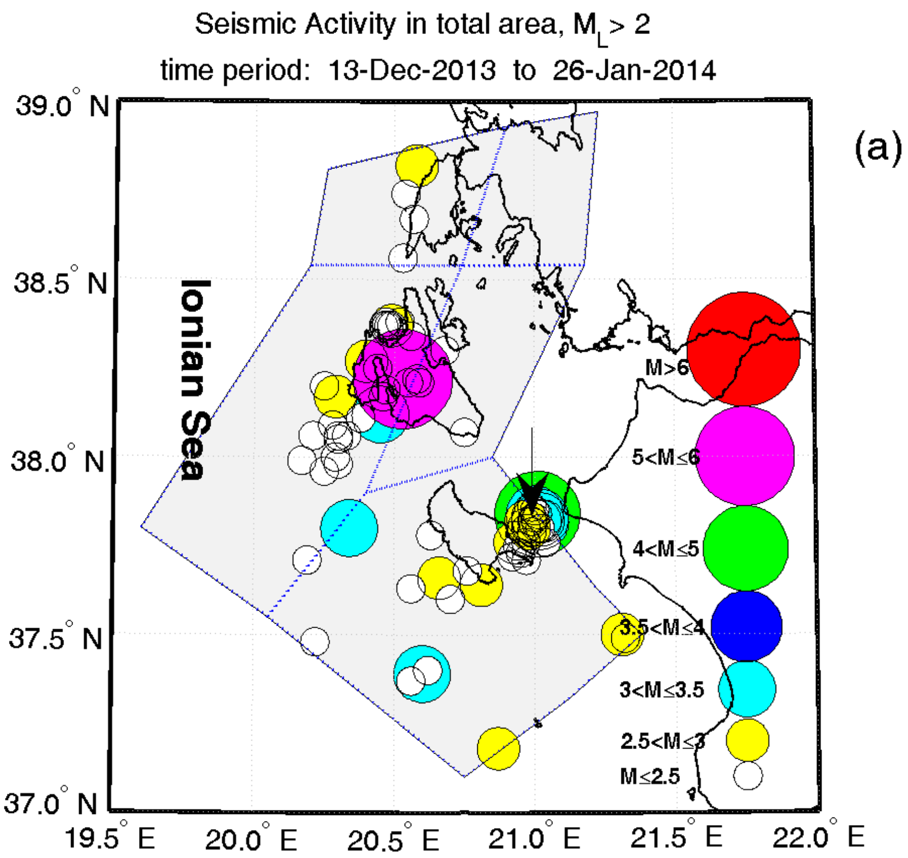
Seismic Activity in total area, $M_L > 2$
time period: 13-Dec-2013 to 26-Jan-2014
(a)
Ionian Sea
39.0° N
38.5° N
38.0° N
37.5° N
37.0° N
19.5° E
20.0° E
20.5° E
21.0° E
21.5° E
22.0° E
M>6
5<M≤6
4<M≤5
3.5<M≤4
3<M≤3.5
2.5<M≤3
M≤2.5

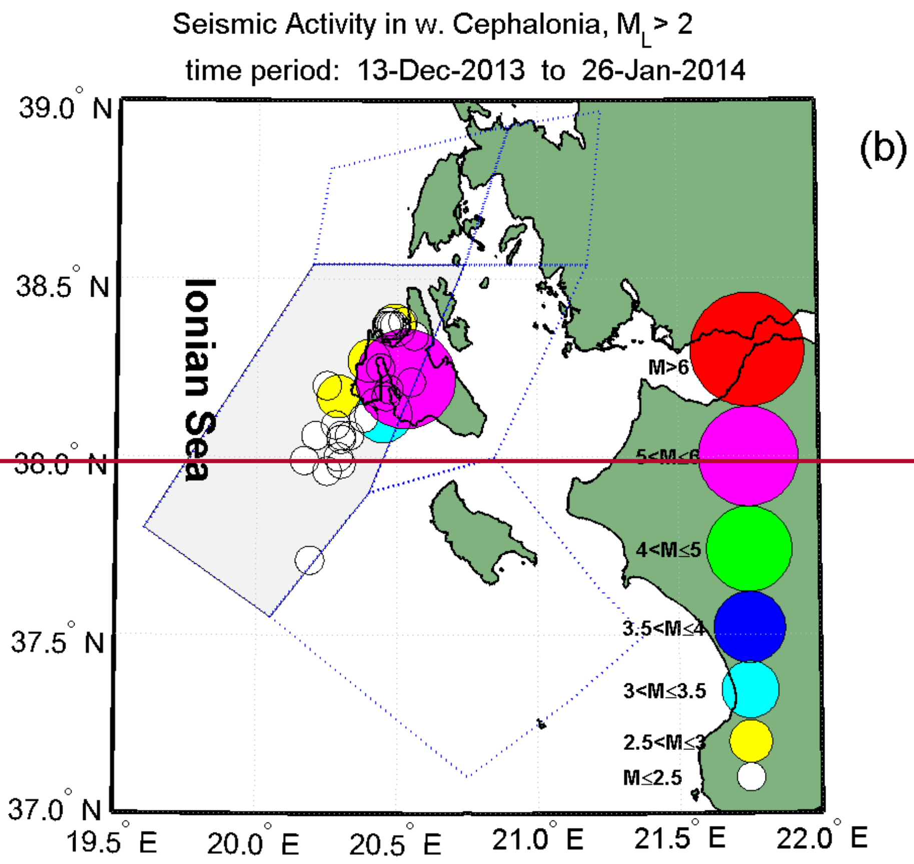
Seismic Activity in w. Cephalonia, $M_L > 2$
time period: 13-Dec-2013 to 26-Jan-2014
(b)
Ionian Sea
39.0° N
38.5° N
38.0° N
37.5° N
37.0° N
19.5° E
20.0° E
20.5° E
21.0° E
21.5° E
22.0° E
M>6
5<M≤6
4<M≤5
3.5<M≤4
3<M≤3.5
2.5<M≤3
M≤2.5

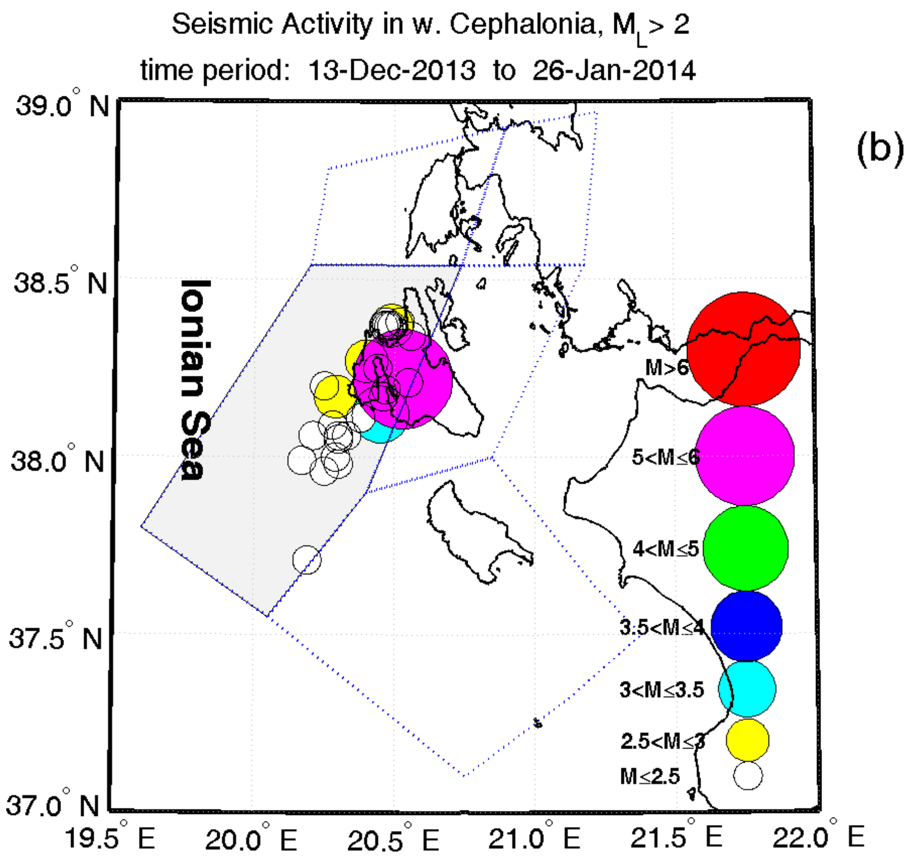

Figure 9. Foreshock seismic activity (M_L) before EQ1: (a) for the whole investigated area of the Ionian Sea region; (b) for west Cephalonia. (For interpretation of the references to colors, the reader is referred to the online version of this paper.)

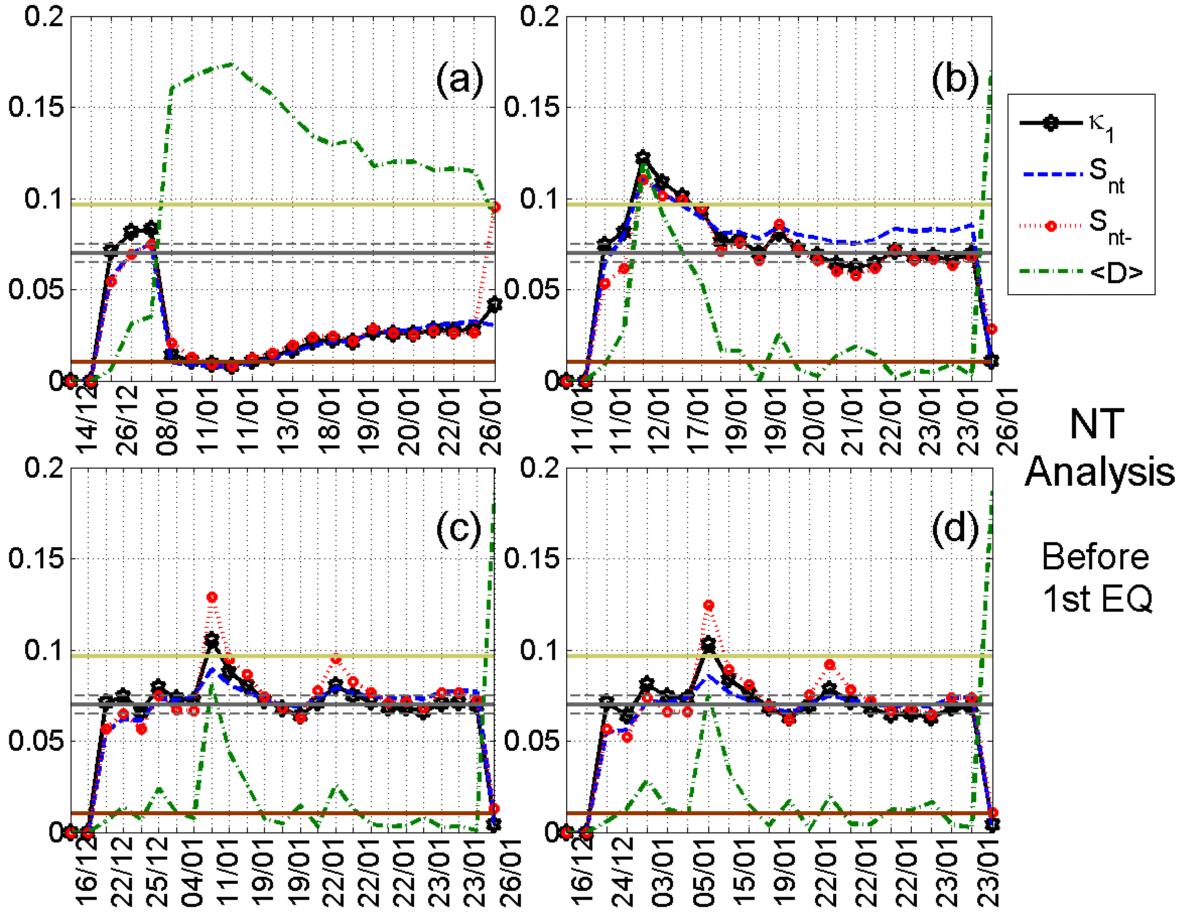

Figure 10. Temporal evolutions of the four natural time (NT) analysis parameters (κ_1, S_{nt}, S_{nt-}, and $\langle D \rangle$) for the foreshock seismic activity recorded prior to EQ1: (a) for the activity of the whole investigated area of the Ionian Sea for M_L threshold 2.5, during the period from 13/12/2013 00:00:00 to 26/01/2014 13:55:44 UT (just after the occurrence of EQ1); (b) for the activity of the whole investigated area of the Ionian Sea for M_L threshold 2.3, during the period from 11/01/2014 04:13:00 (just after the $M_L = 4.7$ occurred in Zante) to 26/01/2014 13:55:44 UT; (c) for the activity of both Cephalonia (east and west) zones combined for M_L threshold 2.1, during the period from 13/12/2013 00:00:00 to 26/01/2014 13:55:44 UT;. (d) for the activity of the west Cephaloniafor M_L threshold 2.1, during the period from 13/12/2013 00:00:00 to 26/01/2014 13:55:44 UT. Note that the events employed depend on the considered threshold. Moreover, the time (x-) axis is not linear in terms of the conventional date of occurrence of the events, since the employed events appear equally spaced relative to x-axis, as the natural time representation demands, although they are not

equally spaced in conventional time. The horizontal solid light green, solid grey and the grey dashed lines, denote the same quantities as in Fig. 6, while the horizontal solid brown line denotes the 10^{-2} limit for $\langle D \rangle$. (For interpretation of the references to colors, the reader is referred to the online version of this paper.)

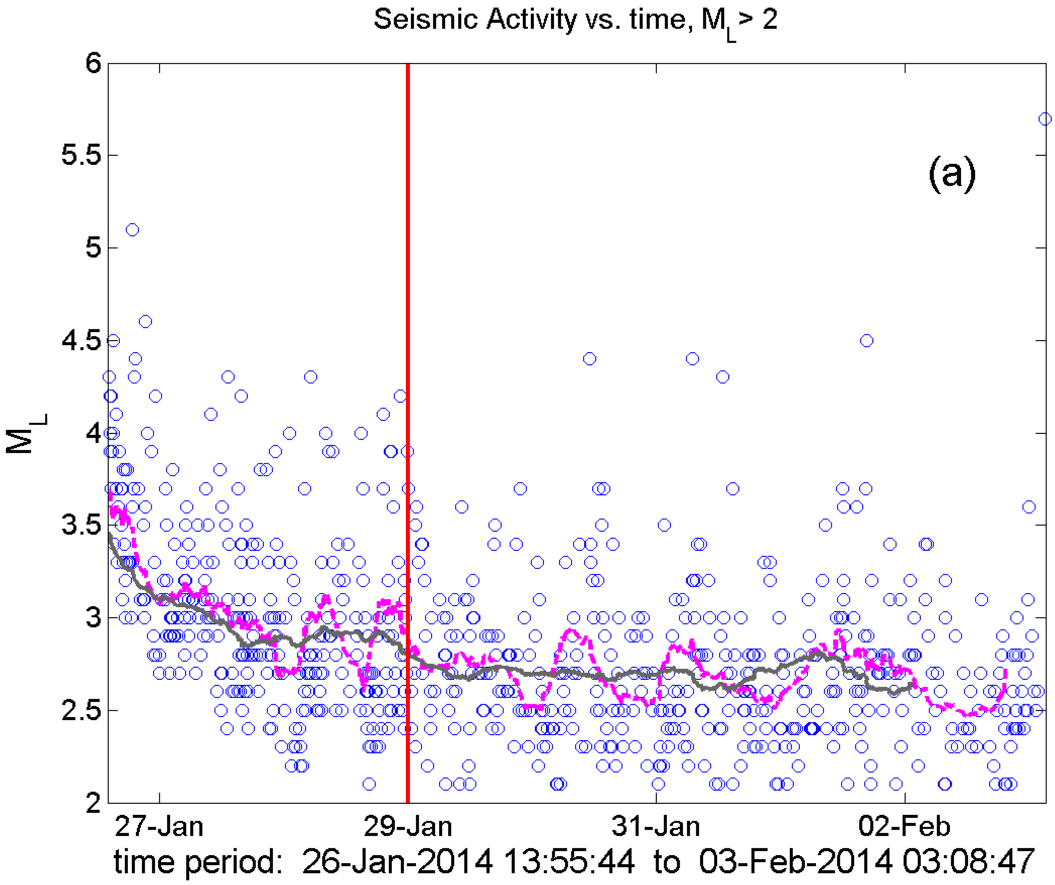
Seismic Activity vs. time, $M_L > 2$
(a)
M_L
6
5.5
5
4.5
4
3.5
3
2.5
2
27-Jan
29-Jan
31-Jan
02-Feb
time period: 26-Jan-2014 13:55:44 to 03-Feb-2014 03:08:47

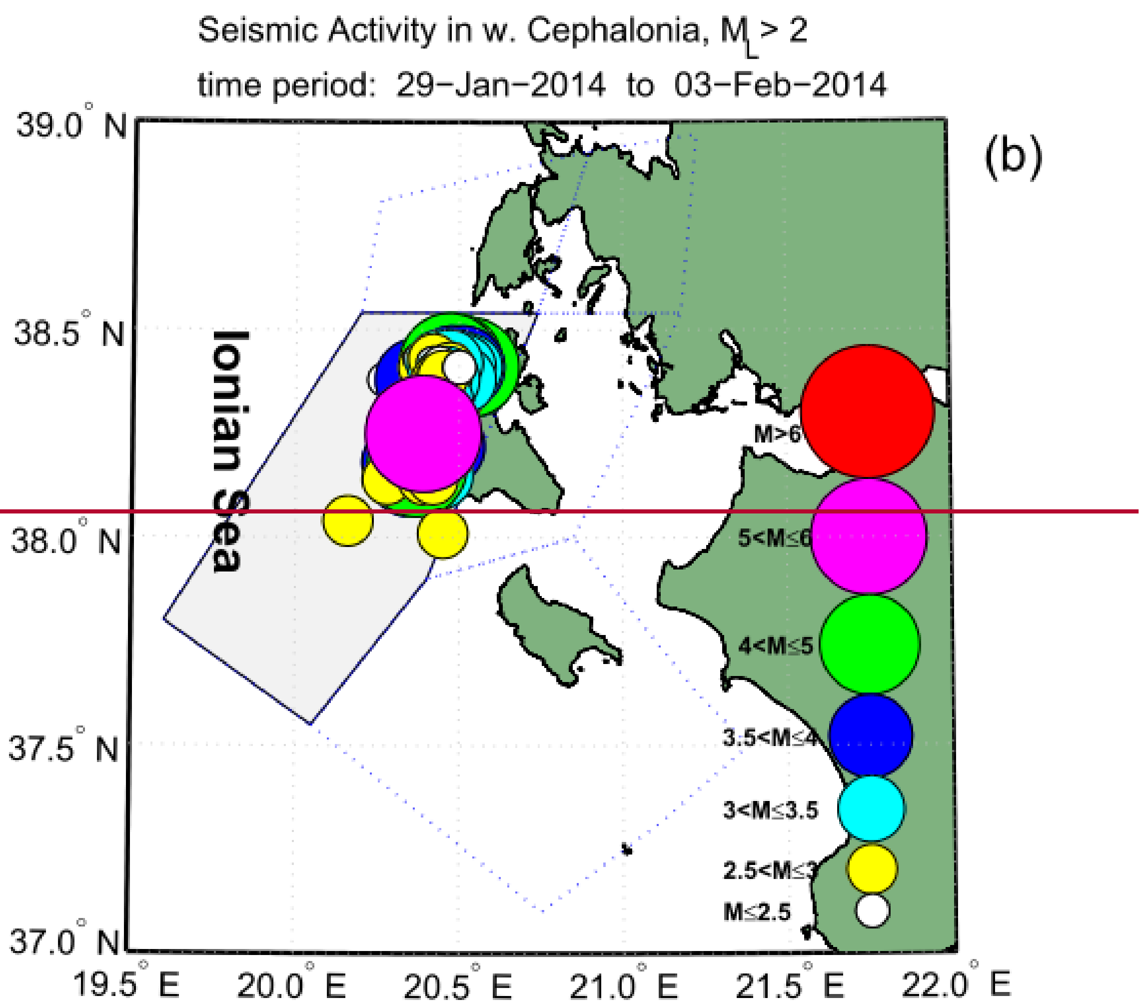
Seismic Activity in w. Cephalonia, $M_L > 2$
time period: 29−Jan−2014 to 03−Feb−2014
(b)
39.0° N
38.5° N
38.0° N
37.5° N
37.0° N
19.5° E
20.0° E
20.5° E
21.0° E
21.5° E
22.0° E
Ionian Sea
M>6
5<M≤6
4<M≤5
3.5<M≤4
3<M≤3.5
2.5<M≤3
M≤2.5

1

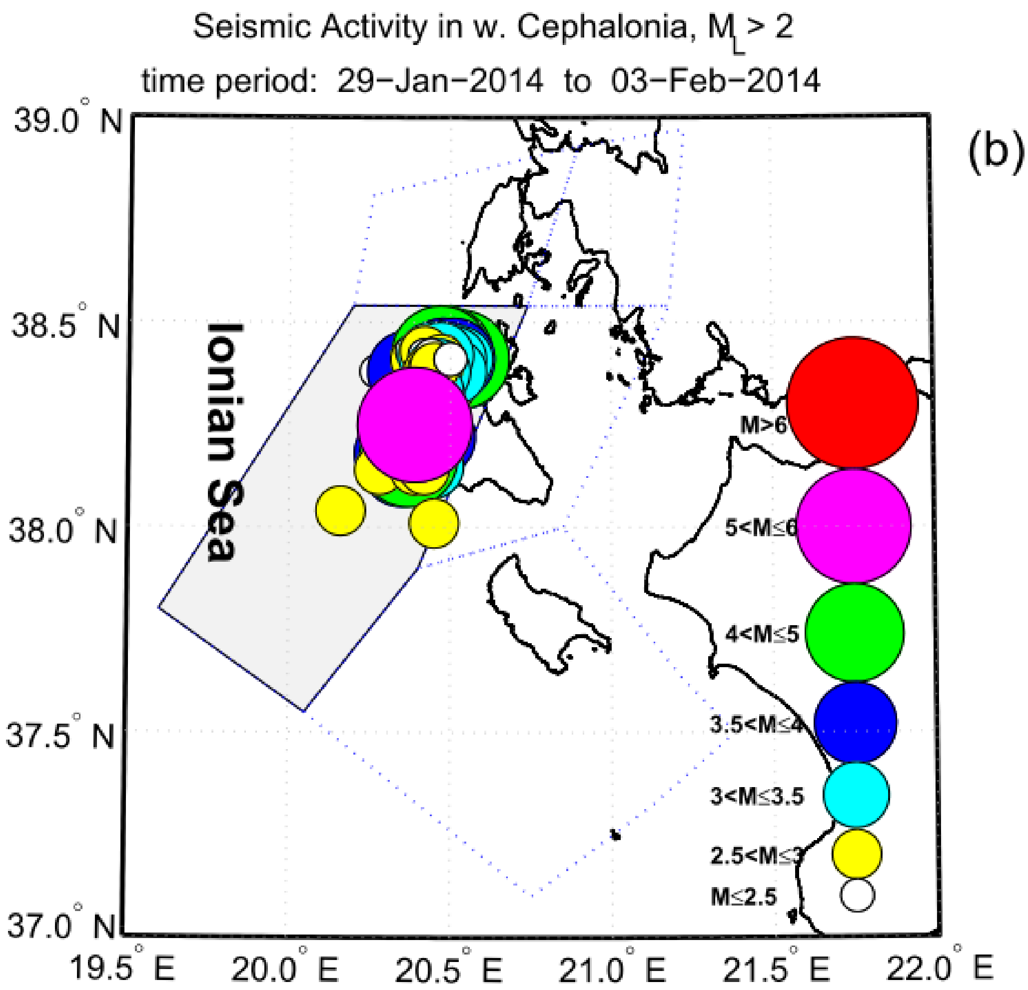

Figure 11. (a) Seismic activity from the time immediately after EQ1 ($M_w = 6.0$) up to the time of EQ2 ($M_w = 5.9$) for the whole investigated area of the Ionian Sea. The moving averages of the recorded earthquake local magnitudes vs. time for calculation windows of 25 and 75 successive events are shown by the dashed magenta and solid grey curve, respectively. The vertical solid red line denotes the time point 29 January 00:00:00 UT. (b) The considered as foreshock seismic activity before EQ2 (from 29/01/2014 00:00 UT up to the time of occurrence of EQ2) for west Cephalonia. All presented magnitudes are local magnitudes (M_L).(For interpretation of the references to colors, the reader is referred to the online version of this paper.)

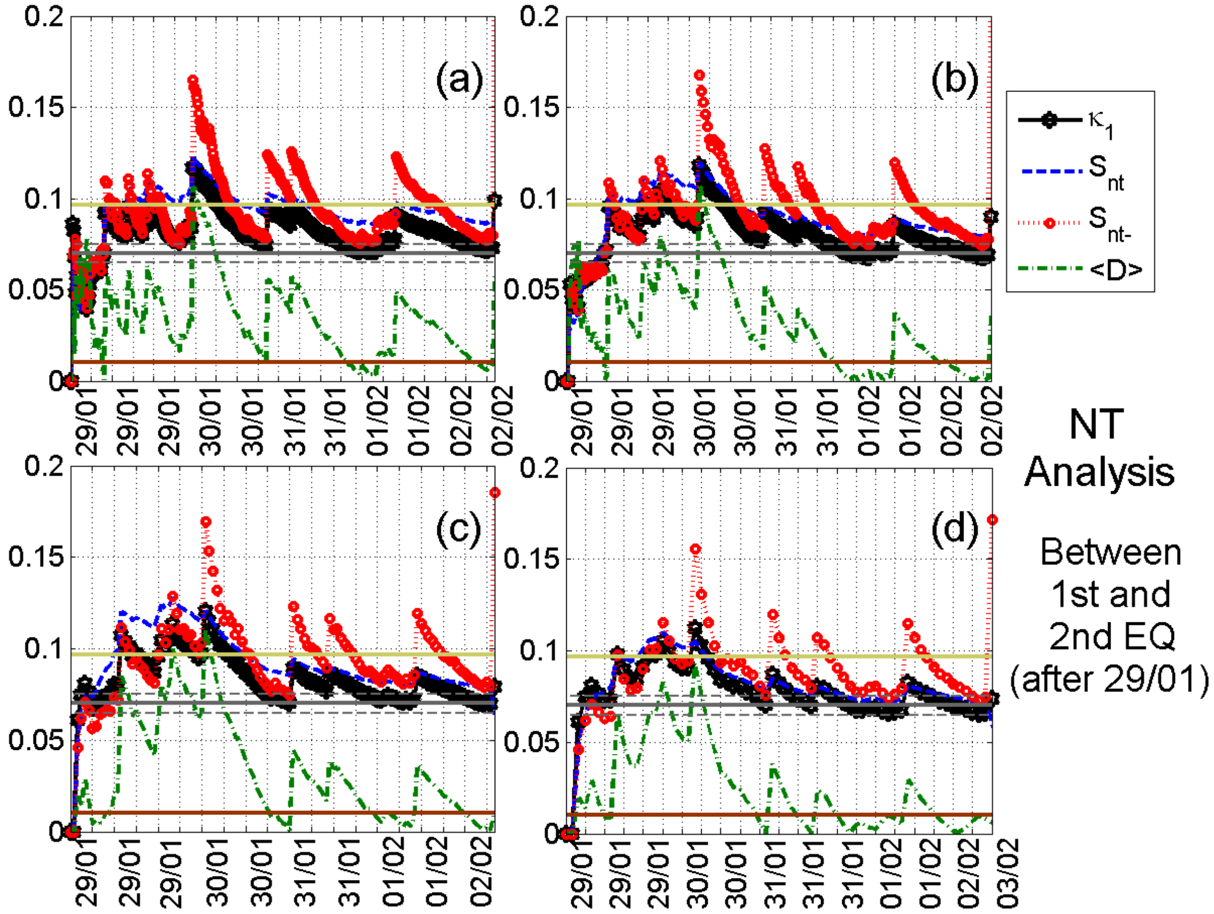

Figure 12. Natural time (NT) analysis results for the seismicity in the partition of west Cephalonia during the time period from 29/01/2014 00:00:00 to 03/02/2014 03:08:47 UT (between EQ1, $M_w = 6.0$, and EQ2, $M_w = 5.9$): (a)-(d) Temporal evolutions of the four natural time analysis parameters (κ_1, S_{nt}, S_{nt-}, and $\langle D \rangle$) for the different M_L thresholds 2.2, 2.6, 2.8, and 3.0, respectively. Note that the events employed depend on the considered threshold. Moreover, the time (x-) axis is not linear in terms of the conventional date of occurrence of the events, since the employed events appear equally spaced relative to x-axis, as the natural time representation demands, although they are not equally spaced in conventional time. The horizontal solid light green, solid grey and the grey dashed lines, denote the same quantities as in Fig. 6, while the horizontal solid brown line denotes the 10^{-2} limit for $\langle D \rangle$. (For interpretation of the references to colors, the reader is referred to the online version of this paper.)

Recent seismic activity at Cephalonia island (Greece): A study through candidate electromagnetic precursors in terms of nonlinear dynamics.

S. M. Potirakis [1], Y. Contoyiannis [2], N. S. Melis [3], J. Kopanas [4], G. Antonopoulos [4], G. Balasis [5], C. Kontoes [5], C. Nomicos [6], K. Eftaxias [2]

[1] {Department of Electronics Engineering, Piraeus University of Applied Sciences (TEI of Piraeus), 250 Thivon and P. Ralli, Aigalao, Athens, GR-12244, Greece, spoti@teipir.gr }.

[2] {Department of Physics, Section of Solid State Physics, University of Athens, Panepistimiopolis, GR-15784, Zografos, Athens, Greece,(Y. C: yconto@yahoo.gr ; K. E.: ceftax@phys.uoa.gr)}

[3] {Institute of Geodynamics, National Observatory of Athens, Lofos Nimfon, Thissio, Athens, GR-11810, Greece, nmelis@noa.gr}

[4] {Department of Environmental Technologists, Technological Education Institute (TEI) of the Ionian islands, Zakynthos, GR-29100, Greece, (J. K.: jkopan@otenet.gr ; G. A.: sv8rx@teiion.gr)}

[5] {Institute for Astronomy, Astrophysics, Space Applications and Remote Sensing, National Observatory of Athens, Metaxa and Vasileos Pavlou, Penteli, Athens, GR-15236, Greece, (G. B.:gbalasis@noa.gr ; C. K.: kontoes@noa.gr)}

[6] {Department of Electronics Engineering, Technological Education Institute (TEI) of Athens, Ag. Spyridonos, Aigaleo, Athens, GR-12210, Greece, cnomicos@teiath.gr}

Correspondence to: G. Balasis (*gbalasis@noa.gr*)

Abstract

The preparation process of two recent earthquakes (EQs) occurred in Cephalonia (Kefalonia) island, Greece, [(38.22^{o} N, 20.53^{o} E), 26 January 2014, $M_w = 6.0$, depth = 21 km], and [(38.25^{o} N, 20.39^{o} E), 3 February 2014, $M_w = 5.9$, depth = 10 km], respectively, is studied in terms of the critical dynamics revealed in observables of the involved non-linear processes. Specifically, we show, by means of the method of critical fluctuations (MCF), that signatures of critical, as well as tricritical, dynamics were embedded in the fracture-induced electromagnetic emissions (EME) recorded by two stations in locations near the epicenters of these two EQs. It is worth noting that both, the MHz EME recorded by the telemetric stations on the island of Cephalonia and the neighboring island of Zante (Zakynthos), reached simultaneously critical condition a few days before the occurrence of each earthquake. The critical characteristics embedded in the EME signals were further verified using the natural time (NT) method. Moreover, we show, in terms of the NT method, that the foreshock seismic activity also presented critical characteristics before each one of these events. Importantly, the revealed critical process seems to be focused on the area corresponding to the west Cephalonia zone, following the seismotectonic and hazard zoning of the Ionian Islands area near Cephalonia.

Keywords: Fracture-induced electromagnetic emissions; Earthquake dynamics; Criticality - Tricriticality; Method of Critical Fluctuations; Natural Time Analysis; Seismotectonic Zone Partitioning.

1. Introduction

The possible connection of the electromagnetic (EM) activity that is observed prior to significant earthquakes (EQs) with the corresponding EQ preparation processes, often referred to as seismo-electromagnetics, has been intensively investigated during the last years. Several possible EQ precursors have been suggested in the literature (Uyeda et al., 2009a; Cicerone et al., 2009; Hayakawa, 2013a, 2013b; Varotsos 2005; Varotsos et al., 2011b). The possible relation of the field observed fracture-induced electromagnetic emissions (EME) in the frequency bands of MHz and kHz, associated with shallow EQs with magnitude 6 or larger that occurred in land or near coast, has been examined in a series of publications in order to contribute to a better understanding of the underlying processes (e.g., Eftaxias et al., 2001, 2004, 2008, 2013; Kapiris et al., 2004; Karamanos et al., 2006; Papadimitriou et al., 2008; Contoyiannis et al., 2005, 2013, 2015; Eftaxias and Potirakis, 2013; Potirakis et al., 2011, 2012a, 2012b, 2012c, 2013, 2015; Minadakis et al., 2012a, 2012b), while a four-stage model for the preparation of an EQ by means of its observable EM activity has been recently put forward (Eftaxias and Potirakis, 2013, and references therein; Contoyiannis et al., 2015, and references therein). In summary, the proposed four stages of the last part of EQ preparation process and the associated, appropriately identified, EM observables, specifically EM time series excerpts for which specific features have been identified using appropriate time series analysis methods, appear in the following order (Donner et al., 2015, and references therein): 1st stage: valid MHz anomaly; 2nd stage: kHz anomaly exhibiting tri-critical characteristics; 3rd stage: strong avalanche-like kHz anomaly; 4th stage: electromagnetic quiescence. It is noted that, according to the aforementioned four-stage model, the pre-EQ MHz EME is considered to be emitted during the fracture of the part of the Earth's crust that is characterized by high heterogeneity. During this phase the fracture is non-directional and spans over a large area that surrounds the family of large high-strength entities distributed along the fault sustaining the system. Note that for an EQ of magnitude ~6 the corresponding fracture process extends to a radius of ~120km (Bowman et al., 1998).

Διαγράφηκε: Note that the specific four-stage model is a suggestion that seems to be supported by the up to now available MHz-kHz observation data and corresponding time-series analyzes, while a rebuttal has not yet appeared in the literature.

Διαγράφηκε: emission

Two strong shallow EQs occurred recently in western Greece (see Fig. 1). On 26 January 2014 (13:55:43 UT) an $M_w = 6.0$ EQ, hereafter also referred to as "EQ1", occurred on the island of Cephalonia (Kefalonia), with epicenter at (38.22^{o} N, 20.53^{o} E) and depth of ~16km. The second significant EQ, $M_w = 5.9$, hereafter also referred to as "EQ2", occurred on the same island on 3 February 2014 (03:08:45 UT), with epicenter at (38.25^{o} N, 20.40^{o} E) and depth of ~11km. Various studies of the two earthquakes have already been published indicating their seismotectonic importance (Karastathis et al., 2014; Valkaniotis et al., 2014; Papadopoulos et al., 2014; Ganas et al., 2015; Sakkas and Lagios, 2015; Merryman Boncori et al., 2015) as they were located on two different active faults that belong to the same seismic source zone.

Two pairs of MHz EM signals were recorded, with a sampling rate of 1 sample/s, prior to each one of the above mentioned significant shallow EQs; one pair of simultaneous signals was recorded by two different stations prior to each one of them. On 24 January 2014, two days before the $M_w = 6.0$ Cephalonia EQ (EQ1), two telemetric stations of our EM signal monitoring network (see Fig. 1), the station of Cephalonia, located on the same island (38.18^o N, 20.59^o E), and the station of Zante (Zakynthos), located on a neighboring island belonging to the same (Ionian) island complex (37.77^o N, 20.74^o E), simultaneously recorded the first pair of aforementioned signals. The same picture was repeated for the second significant Cephalonia EQ, $M_w = 5.9$ (EQ2). Specifically, both the Cephalonia and the Zante stations simultaneously recorded the second pair of aforementioned signals on 28 January 2014, six days prior to the specific EQ. Note that it has been repeatedly made clear that all the pre-EQ EME signals, which have been observed by our monitoring network, have been recorded only prior to strong shallow EQs, that have taken place on land (or near the coast-line); this fact, in combination to the recently proposed fractal geo-antenna model (Eftaxias et al., 2004; Eftaxias and Potirakis, 2013), explains why they succeed to be transmitted on air. This model gives a good reason for the increased possibility of detection of such EM radiation, since a fractal geo-antenna emits significantly increased power, compared to the power that would be radiated by the same source, if a dipole antenna model was considered. It should also be noted that, none of the recordings of the other monitoring stations of our network (except from the ones of Cephalonia and Zante) presented critical characteristics before these two specific EQs.

<Figure 1 should be placed around here>

The analysis of the specific EM time series, using the method of critical fluctuations (MCF) (Contoyiannis and Diakonos, 2000; Contoyiannis et al., 2002, 2013), revealed critical features, implying that the possibly related underlying geophysical process was at critical state before the occurrence of each one of the EQs of interest. The critical characteristics embedded in the specific time series were further verified by means of the natural time (NT) method (Varotsos et al., 2011a, 2011b, Potirakis et al., 2013, 2015). The presence of the "critical point" during which any two active parts of the system are highly correlated, theoretically even at arbitrarily long distances, in other words when "everything depends on everything else", is consistent with the view that the EQ preparation process during the period that the MHz EME are emitted is a spatially extensive process. Note that this process corresponds to the first stage of the aforementioned four-stage model.

Moreover, we analyzed the foreshock seismic activity using the NT method; the obtained results indicate that seismicity also presented critical characteristics before each one of the two important events. This result implies that the observed EM anomaly and the associated foreshock seismic activity might be considered as “two sides of the same coin”. Last but not least, one day before the occurrence of EQ2, and five days after the corresponding critical EME signal, tricritical characteristics were revealed in the EME recorded by the Cephalonia station.

Διαγράφηκε: Importantly, the revealed critical process seems to be focused on an area corresponding to the west Cephalonia zone, one of the parts according to the seismotectonic and hazard zone partitioning of the wider area of the Ionian Islands.¶

Διαγράφηκε: This finding is also quite important, indicating that the tricritical behavior attributed to the second stage of the aforementioned four-stage model can be identified either in kHz or in MHz EME, leading thus to a revision of the specific four-stage model. Unfortunately, the Zante station was out of order for several hours during the specific day, including the time window during which the tricritical features were identified in the Cephalonia recordings. As a result, we could not cross check whether tricritical signals simultaneously also reached Zante.

The remainder of this manuscript is organized as follows: A brief introduction to the MCF and the NT analysis methods is provided in Section 2. The analysis of the EME recordings according to these two methods is presented in Section 3. Section 4 presents the results obtained by the analysis of the foreshock seismic activity using the NT method, while Section 5 concludes the manuscript by summarizing and discussing the findings.

2. Critical Dynamics Analysis Methods

Criticality has early been suggested as an EQ precursory sign (Chelidze, 1982; Chelidze and Kolesnikov, 1982; Chelidze et al., 2006; Rundle et al., 2012; Wanliss et al., 2015). Critical phenomena have been proposed as the likely framework to study the origins of EQ related EM fluctuations, suggesting that the theory of phase transitions and critical phenomena may be useful in gaining insight to the mechanism of their complex dynamics (Bowman et al., 1998; Contoyiannis et al., 2004a, 2005, 2015; Varotsos et al., 2011a, 2011b). One possible reason for the appropriateness of this model may be the way in which correlations spread thought a disordered medium/ system comprised of subunits. From a qualitative / intuitive perspective, according to the specific approach, initially single isolated activated parts emerge in the system which, then, progressively grow and proliferate, leading to cooperative effects. Local interactions evolve to long-range correlations, eventually extending along the entire system. A key point in the study of dynamical systems that develop critical phenomena is the identification of the “critical epoch” during which the “short-range” correlations evolve into “long-range” ones. Therefore, the theory of phase transitions and critical phenomena seem to

Διαγράφηκε: model

Διαγράφηκε: multiply

be appropriate for the study of dynamical complex systems in which local interactions evolve to long-range correlations, such as the disordered Earth's crust during the preparation of an EQ. Note that for an EQ of magnitude ~6 the corresponding fracture process extends to a radius of ~120km (Bowman et al., 1998).

It is worth noting that key characteristics of a critical point in a phase transition of the second order are the existence of highly correlated fluctuations and scale invariance in the statistical properties. By means of experiments on systems presenting this kind of criticality as well as by appropriately designed numerical experiments, it has been confirmed that right at the "critical point" the subunits are highly correlated even at arbitrarily large "distance". At the critical state self-similar structures appear both in time and space. This fact is quantitatively manifested by power law expressions describing the distributions of spatial or temporal quantities associated with the aforementioned self-similar structures (Stanley, 1987, 1999).

The time series analysis methods employed in this paper for the evaluation of the MHz EME recordings and the seismicity around the Cephalonia island in terms of critical dynamics are briefly presented in the following. Specifically, the method of critical fluctuations (MCF) is described in Sub-Section 2.1, while the natural time (NT) method is described in Sub-Section 2.2.

2.1 Method of critical fluctuations (MCF)

In the direction of comprehending the dynamics of a system undergoing a continuous phase transition at critical state, the method of critical fluctuations (MCF) has been proposed for the analysis of critical fluctuations in the systems' observables (Contoyiannis and Diakonos, 2000; Contoyiannis et al., 2002). The dynamics of various dynamical systems have been successfully analyzed by MCF; these include thermal (e.g., 3D Ising) (Contoyiannis et al., 2002), geophysical (Contoyiannis and Eftaxias 2008; Contoyiannis et al., 2004a, 2010, 2015), biological (electro-cardiac signals) (Contoyiannis et al., 2004b; Contoyiannis et al., 2013) and economic systems (Ozun et al., 2014).

It has been shown (Contoyiannis and Diakonos, 2000) that the dynamics of the order parameter fluctuations ϕ at the critical state for a second-order phase transition can be theoretically formulated by the non-linear intermittent map:

$$\phi_{n+1} = \phi_n + u\phi_n^{\ z}, \tag{1}$$

where ϕ_n is the scaled order parameter value at the time interval n; u denotes an effective positive coupling parameter describing the non-linear self-interaction of the order parameter; z stands for a characteristic exponent associated with the isothermal exponent δ for critical systems at thermal equilibrium ($z = \delta + 1$). The marginal fixed-point of the above map is the zero point, as expected from critical phenomena theory.

However, it has been shown that in order to quantitatively study a real (or numerical) dynamical system one has to add an unavoidable "noise" term, ε_n, to Eq. (1), which is produced by all stochastic processes (Contoyiannis and Diakonos, 2007). Note that, from the intermittency mathematical framework point of view, the "noise" term denotes ergodicity in the available phase space. In this respect, the map of Eq. (1), for positive values of the order parameter, becomes:

$$\phi_{n+1} = \left| \ \phi_n + u\phi_n^{\ z} + \varepsilon_n \ \right|. \tag{2}$$

Based on the map of Eq. (2), MCF has been introduced as a method capable of identifying whether a system is in critical state of intermittent type by analyzing time-series corresponding to an observable of the specific system. In a few words, MCF is based on the property of maps of intermittent-type, like the ones of Eqs. (1) and (2), that the distribution of properly defined laminar lengths (waiting times) l follow a power-law $P(l) \sim l^{-p_l}$ (Schuster, 1998), where the exponent p_l is $p_l = 1 + \frac{1}{\delta}$ (Contoyiannis et al., 2002). However, the distribution of waiting times for a real data time series which is not characterized by critical dynamics follows an exponential decay, rather than a power-law one (Contoyiannis et al., 2004a), due to stochastic noise and finite size effects. Therefore, the dynamics of a real time series can be estimated by fitting the distribution of waiting times (laminar lengths) to a function $\rho(l)$ combining both power-law and exponential decay (Contoyiannis and Diakonos, 2007):

Διαγράφηκε: forming
Διαγράφηκε: the distribution of laminar lengths and
Διαγράφηκε: it

$$\rho(l) \sim l^{-p_2} e^{-lp_3}. \tag{3}$$

The values of the two exponents p_2 and p_3, which result after fitting laminar lengths distribution in a log-log scale diagram, reveal the underlying dynamics. Exact critical state calls for $p_3 = 0$; in such a case it is $p_2 = p_l > 1$. As a result, in order for a real system to be considered to be at critical state, *both criticality conditions* $p_2 > 1$ *and* $p_3 \approx 0$ *have to be satisfied*.

Note that the choice of the function $\rho(l)$ of Eq. (3), which combines both power-law and exponential decay, to model the distribution of waiting times was deliberately made in order to include both these fundamentally different behaviors, i.e., the critical dynamics (Contoyiannis et al., 2002) and the complete absence of specific dynamics (stochastic processes) (Contoyiannis et al., 2004b), respectively. Of course, the specific function also models intermediate behaviors (Contoyiannis and Diakonos, 2007).

In applying the MCF the corresponding factors of $\rho(l)$ appear to be competitive: any increase of the p_2 exponent value corresponds to a p_3 exponent value reduction and vice versa. However, this is expected because, for example, any increase of the value of p_3 exponent signifies the departure from critical dynamics and thus the reduction of p_2 exponent value. What is interesting to us is to apply MCF analysis to observe this competition in the case of pre-earthquake EME time-series and see whether the obtained exponent values are consistent with those of MCF analyzes performed on other time-series with large statistics which are considered as references for the application of our method. This competition can be observed even within the critical windows as shown in Figs. 2d and 3d.

Moreover, a special dynamics case is the one known as “tricritical crossover dynamics”. In statistical physics, a tricritical point is a point in the phase diagram of a system at which the two basic kinds of phase transition, that is the first order transition and the second order transition, meet (Huang, 1987). A characteristic property of the area around this point is the co-existence of three phases, specifically, the high symmetry phase, the low symmetry phase, and an intermediate “mixing state”. A passage through this area, around the tricritical point, from the second order phase transition to the first order phase transition through the intermediate mixing state constitutes a tricritical crossover (Huang, 1987).

The specific dynamics is proved to be expressed by the map (Contoyiannis et al., 2015):

$$m_{n+1} = \left| m_n - u m_n^{-z} + \varepsilon_n \right|, \quad (4)$$

where m stands for the order parameter. This map differs from the critical map of Eq. (2) in the sigh of the parameter u and exponent z. Note that for reasons of unified formulation we use for these parameters the same notation as in the critical map of Eq. (2). At the level of MCF analysis this dynamics is expressed by the estimated values for the two characteristic exponents p_2, p_3 values, that satisfy *the tricriticality condition* $p_2 < 1, p_3 \approx 0$. These values have been characterized in (Contoyiannis and Diakonos, 2007) as a signature of tricritical behavior.

Note that in order for a time-series to be possible to be analyzed by the MCF, it should at least present cumulative stationarity. Therefore, a cumulative stationarity test is always performed before applying the MCF method; examples can be found in already published articles (e.g., Contoyiannis et al., 2004a, 2005, 2010; Contoyiannis and Eftaxias, 2008; Potirakis et al., 2015). More details on the application of MCF can be found in several published articles (e.g., Contoyiannis et al. 2002, 2013, 2015), as well as in Section 3 where its application on the MHz EM variations is presented.

2.2 Natural time method (NT)

The natural time method was originally proposed for the analysis for a point process like DC or ultra-low frequency (≤1 Hz) SES (Varotsos et al., 2002; Varotsos, 2005), and has been shown to be optimal for enhancing the signals in the time-frequency space (Abe et al., 2005). The transformation of a time-series of "events" from the conventional time domain to natural time domain is performed by ignoring the time-stamp of each event and retaining only their normalized order (index) of occurrence. Explicitly, in a time series of N successive events, the natural time, χ_k, of the k^{th} event is the index of occurrence of this event normalized, by dividing by the total number of the considered events, $\chi_k = k/N$. On the other hand, the "energy", Q_k, of each, k^{th}, event is preserved. We note that the quantity Q_k represents different physical quantities for various time series: for EQ time series it has been assigned to a seismic energy released (e.g., seismic moment) (Varotsos et al., 2005; Uyeda et al., 2009b), and for SES signals that are of dichotomous nature it corresponds to SES pulse duration (Varotsos, 2005), while for MHz electromagnetic emission signals that are of non-dichotomous nature, it has been attributed to the energy of fracto-electromagnetic emission

Διαγράφηκε: to extract the maximum information possible from a given time series events as defined in Potirakis et al. (2013). The transformed time series (χ_k, Q_k) is then studied through the normalized power spectrum $\Pi(\varpi) = \left|\sum_{k=1}^{N} p_k \exp(j\varpi\chi_k)\right|^2$, where ϖ is the natural angular frequency, $\varpi = 2\pi\varphi$, with φ standing for the frequency in natural time, termed "natural frequency", and $p_k = Q_k \big/ \sum_{n=1}^{N} Q_n$ corresponds to the k^{th} event's normalized energy. Note that, the term "natural frequency" should not be confused with the rate at which a system oscillates when it is not driven by an external force; it defines an analysis domain dual to the natural time domain, in the framework of Fourier–Stieltjes transform (Varotsos et al., 2011b).

Διαγράφηκε: the

The study of $\Pi(\varpi)$ at ϖ close to zero reveals the dynamic evolution of the time series under analysis. This is because all the moments of the distribution of p_k can be estimated from $\Pi(\varpi)$ at $\varpi \to 0$ (Varotsos et al., 2011a). Aiming to that, by the Taylor expansion $\Pi(\varpi) = 1 - \kappa_1\varpi^2 + \kappa_2\varpi^4 + \ldots$, the quantity κ_1 is defined, where $\kappa_1 = \sum_{k=1}^{N} p_k\chi_k^2 - \left(\sum_{k=1}^{N} p_k\chi_k\right)^2$, i.e., the variance of χ_k weighted for p_k characterizing the dispersion of the most significant events within the "rescaled" interval $(0,1]$. Moreover, the entropy in natural time, S_{nt}, is defined (Varotsos et al., 2006) as $S_{nt} = \sum_{k=1}^{N} p_k\chi_k \ln \chi_k - \left(\sum_{k=1}^{N} p_k\chi_k\right)\ln\left(\sum_{k=1}^{N} p_k\chi_k\right)$ and corresponds (Varotsos et al., 2006, 2011b) to the value at $q=1$ of the derivative of the fluctuation function $F(q) = \langle\chi^q\rangle - \langle\chi\rangle^q$ with respect to q (while κ_1 corresponds to $F(q)$ for $q=2$). It is a dynamic entropy depending on the sequential order of events (Varotsos et al., 2006). The entropy, S_{nt-}, obtained upon considering (Varotsos et al., 2006) the time reversal T, i.e., $Tp_m = p_{N-m+1}$, is also considered.

A system is considered to approach criticality when the parameter κ_1 converges to the value $\kappa_1 = 0.070$ and at the same time both the entropy in natural time and the entropy under time reversal satisfy the condition $S_{nt}, S_{nt-} < S_u = (\ln 2/2) - 1/4$ (Sarlis et al., 2011), where S_u stands for the entropy of a "uniform" distribution in natural time (Varotsos et al., 2006).

In the special case of natural time analysis of foreshock seismicity (Varotsos et al., 2001, 2005,2006; Sarlis et al., 2008), the seismicity is considered to be in a true critical state, a "true coincidence" is achieved, when three additional conditions are satisfied: (i) The "average" distance $\langle D \rangle$ between the curves of normalized power spectra $\Pi(\varpi)$ of the evolving seismicity and the theoretical estimation of $\Pi(\varpi)$, $\Pi_{critical}(\varpi) = (18/5\varpi^2) - (6\cos\varpi/5\varpi^2) - (12\sin\varpi/5\varpi^3)$, $\Pi_{critical}(\varpi) \approx 1 - \kappa_1\varpi^2$, for $\kappa_1 = 0.070$ should be smaller than 10^{-2}, i.e., $\langle D \rangle = \langle |\Pi(\varpi) - \Pi_{critical}(\varpi)| \rangle < 10^{-2}$; (ii) the parameter κ_1 should approach the value $\kappa_1 = 0.070$ "by descending from above" (Varotsos et al., 2001); (iii) Since the underlying process is expected to be self-similar, the time of the true coincidence should not vary upon changing (within reasonable limits) either the magnitude threshold, M_{thres}, or the area, used in the calculation.

Διαγράφηκε:

It should be finally clarified that in the case of seismicity analysis, the temporal evolution of the parameters κ_1, S_{nt}, S_{nt-}, and $\langle D \rangle$ is studied as new events that exceed the magnitude threshold M_{thres} are progressively included in the analysis. Specifically, as soon as one more event is included, first the time series (χ_k, Q_k) is rescaled in the natural time domain, since each time the k^{th} event corresponds to a natural time $\chi_k = k/N$, where N is the progressively increasing (by each new event inclusion) total number of the considered successive events; then all the parameters involved in the natural time analysis are calculated for this new time series; this process continues until the time of occurrence of the main event.

More details on the application of NT on MHz EME as well as on foreshock seismicity can be found in already published articles (Potirakis et al. 2013, 2015), as well as in Sections 3 and 4, where its application on the MHz EM variations and foreshock seismicity is presented, respectively.

Note that in the case of NT analysis of foreshock seismicity, the introduction of magnitude threshold, M_{thres}, excludes some of the weaker EQ events (with magnitude below this threshold) from the NT analysis. On one hand, this is necessary in order to exclude events for which the recorded magnitude is not considered reliable; depending on the installed seismographic network characteristics, a specific magnitude threshold is usually defined to assure data completeness. On the other hand, the use of various magnitude thresholds, M_{thres}, offers a means of more accurate determination of the time when criticality is reached. In some cases, it happens that more than one time-points may satisfy the rest of NT critical state conditions, however the time of the true coincidence is finally selected by the last condition that "true coincidence should not vary upon changing (within reasonable limits) either the magnitude threshold, M_{thres}, or the area, used in the calculation."

3. Electromagnetic Emissions Analysis Results

Part of the MHz recordings of the Cephalonia station associated with the $M_w = 6.0$ EQ (EQ1) is shown in Fig. 2a. This was recorded in day of year 24, that is ~2 days before the occurrence of EQ1. This stationary time series excerpt, having a total length of 2.8 h (10,000 samples) starting at 24 Jan. 2014 (12:46:40 UT), was analyzed by the MCF method and was identified to be a "critical window" (CW). CWs are time intervals of the MHz EME signals presenting features analogous to the critical point of a second order phase transition (Contoyiannis et al., 2005).

The main steps of the MCF analysis (e.g., Contoyiannis et al., 2013, 2015) on the specific time series are shown in Fig. 2b- Fig. 2d. First, a distribution of the amplitude values of the analyzed signal was obtained from which, using the method of turning points (Pingel et al., 1999), a fixed-point, that is the start of laminar regions, ϕ_o of about 700 mV was determined. Fig. 2c portrays the obtained distribution of laminar lengths for the end point $\phi_l = 655mV$, that is the distribution of waiting times, referred to as laminar lengths l, between the fixed-point ϕ_o and the end point ϕ_l, as well as the fitted function $f(l) \propto l^{-p_2} e^{-p_3 l}$ with the corresponding exponents $p_2 = 1.35$, $p_3 = 0.000$ with $R^2 = 0.999$. Note that the distribution of laminar lengths is directly fitted to the specific model using the Levenberg-Marquardt algorithm, while the fitting criterion is the chi-square minimization. The fitting is not done in log-log space; the axes of Fig. 2c are logarithmic for the easier depiction of the distribution of laminar lengths. Finally, Fig. 2d shows the obtained plot of the p_2, p_3 exponents vs. ϕ_l. From Fig. 2d it is apparent that the criticality conditions, $p_2 > 1$ and $p_3 \approx 0$, are satisfied for a wide range of end points ϕ_l, revealing the power-law decay feature of the time series that proves

Διαγράφηκε: laminar distribution

that the system is characterized by intermittent dynamics; in other words, the MHz time series excerpt of Fig. 2a is indeed a CW.

<Figure 2 should be placed around here>

Part of the MHz recordings of the Zante station associated with EQ1 is shown in Fig. 3a. This was also recorded in day of year 24, that is ~2 days before the occurrence of Cephalonia EQ1. This stationary time series excerpt, having a total length of 2.8 h (10,000 samples) starting at 24 Jan. 2014 (12:46:40 UT), was also analyzed by the MCF method and was identified to be a "critical window" (CW).

The application of the MCF analysis on the specific time series (cf. Fig. 3), revealed that the criticality conditions, $p_2 > 1$ and $p_3 \approx 0$, are satisfied for a wide range of end points ϕ_l, for this signal too. In other words, this signal has also embedded the power-law decay feature that indicates intermittent dynamics, rendering it a CW.

<Figure 3 should be placed around here>

After the $M_w = 6.0$ (EQ1), ~ a week later, the second, $M_w = 5.9$ (EQ2), occurred on the same island with a focal area a few km further than the first one. Six days earlier, both the Cephalonia and Zante stations simultaneously recorded MHz EME. Specifically, a stationary time series excerpt, having a total length of 3.3 h (12,000 samples) starting at 28 Jan. 2014 (05:33:20 UT), from Caphalonia station and a stationary time series excerpt, having a total length of 5 h (18,000 samples) starting at 28 Jan. 2014 (03:53:20 UT), from Zante station were analyzed by the MCF method and both of them were identified to be CWs. Note that the Cephalonia CW was emitted within the time frame in which the Zante CW was emitted. Figs 4 & 5 show the results of the corresponding analyses.

<Figure 4 should be placed around here>

Διαγράφηκε: main steps

Διαγράφηκε: (e.g., Contoyiannis et al., 2013, 2015)

Διαγράφηκε: are shown in Fig. 3b- Fig. 3d

Διαγράφηκε: First, a distribution of the amplitude values of the analyzed signal was obtained from which, using the method of turning points (Pingel et al., 1999), a fixed-point, that is the start of laminar regions, ϕ_o of about 600 mV was determined. Fig. 3c portrays the obtained laminar distribution for the end point $\phi_l = 665mV$, that is the distribution of waiting times, referred to as laminar lengths l, between the fixed-point ϕ_o and the end point ϕ_l, as well as the fitted function $f(l) \propto l^{-p_2} e^{-p_3 l}$ with the corresponding exponents $p_2 = 1.49$, $p_3 = 0.000$ with $R^2 = 0.999$. Finally, Fig. 3d shows the obtained plot of the p_2, p_3 exponents vs. ϕ_l. From Fig. 3d it is apparent that the criticality conditions, $p_2 > 1$ and $p_3 \approx 0$, are satisfied for a wide range of end points ϕ_l, revealing the power-law decay feature of the time series that proves that the system is characterized by intermittent dynamics; in other words, the MHz time series excerpt of Fig. 3a is indeed a CW.¶

<Figure 5 should be placed around here>

In summary, we conclude that, according to the MCF analysis method, both stations recorded MHz signals that simultaneously presented critical state features two days before the first main event and six days before the second main event. In order to verify this finding, we proceeded to the analysis of all the corresponding MHz signals by means of the NT analysis method, according to the way of application proposed in Potirakis et al. (2013). According to the specific procedure for the application of the NT method on the MHz signals, we performed an exhaustive search seeking for at least one amplitude threshold value (applied over the total length of the analyzed signal), for which the corresponding fracto-EME events satisfy the natural time method criticality conditions. The idea is that if the MCF gives valid information, and as a consequence the analyzed time series excerpt is indeed in critical condition, then there should be at least one threshold value for which the NT criticality conditions (cf. Sec. 2.2) are satisfied. Indeed, as apparent from Fig. 6, all four signals satisfy the criticality conditions according to the NT method for at least one of the considered threshold values, therefore the results obtained by the MCF method are successfully verified.

<Figure 6 should be placed around here>

On 2 February 2014, i.e., one day before the occurrence of EQ2, MHz EME presenting tricritical characteristics was recorded by the Cephalonia station. This signal emerged five days after the CWs that were identified in the simultaneously recorded, by the Cephalonia and Zante stations, MHz EME. The specific MHz time series excerpt from Cephalonia station, having a total length of 7.5 h (27,000 samples) starting at 2 Feb. 2014 (07:46:40 UT), was analyzed by means of the MCF method yielding the results shown in Fig. 7. As apparent from the results, this signal satisfies the tricriticality conditions $p_2 < 1, p_3 \approx 0$ (cf. Sec. 2.1) for a wide range of end points ϕ_l, revealing the intermediate "mixing state" between the second order phase transition to the first order phase transition. Unfortunately, during the time that the Cephalonia station recorded trictitical MHz signal, the Zante station was out of order; actually, it was out of order for several hours during the specific day.

<Figure 7 should be placed around here>

It has been recently found (Contoyiannis et al., 2015) that such a behavior is identified in the kHz EME which usually emerge near the end of the MHz EME when the environment in which the EQ preparation process evolves changes from heterogeneous to less heterogeneous, and before the emergence of the strong avalanche-like kHz EME which have been attributed to the fracture of the asperities sustaining the fault. Actually, this has been proposed as the second stage of the four-stage model for the preparation of an EQ by means of its observable EM activity (Eftaxias and Potirakis, 2013, and references therein; Contoyiannis et al., 2015, and references therein; Donner et al., 2015). The identification of tricritical behavior in MHz EME is a quite important finding, indicating that the tricritical behavior, attributed to the second stage of the aforementioned four-stage model, can be identified either in kHz or in MHz EME, leading thus to a revision the specific four-stage model in order to include this case too.

As a conclusion, after the first stage of the EQ preparation process where MHz EME with critical features are emitted, a second stage follows where MHz or kHz or both MHz and kHz EME with trictitical features are emitted. As already mentioned (cf. Sec. 2.1), in terms of statistical physics the trictitical behavior is an intermediate dynamical state which is developed in region of the phase diagram of a system around the trictitical point, which can be approached either from the edge of the first order phase transition (characterizing the strong avalanche-like kHz EME attributed to the third stage of the four-stage model) or from the edge of the second order phase transition (characterizing the critical MHz EME attributed to the first stage of the four-stage model). Therefore, although it is expected that the trictitical behavior will be rarely observed, as it has already been discussed in (Contoyiannis et al., 2015), it can be found either in MHz time series, following the emission of a critical MHz EME, or in kHz time series preceding the emission of avalanche-like kHz EME.

4. Foreshock Seismic Activity Analysis Results

As already mentioned in Potirakis et al. (2013, 2015): “seismicity and pre-fracture EMEs should be two sides of the same coin concerning the EQ generation process. If the MHz EMEs and the corresponding foreshock seismic sequence are observable manifestations of the same complex system at critical state, both should be possible to be described as a critical phenomenon by means of the natural time method.” Therefore, we also proceeded to the examination of the corresponding foreshock seismic activity around Cephalonia before each one of the significant EQs of interest in order to verify this suggestion. However, we did not apply the NT method on concentric circles around the epicenter of each EQ, as in Potirakis et al. (2013, 2015), but instead we decided to study seismicity within areas determined according to seismotectonic and earthquake hazard criteria.

Following the detailed study presented in Vamvakaris et al. (2016), we incorporated the seismic zones proposed there for our area of study. Thus, as it is presented in Fig. 8, we defined five separate seismic zones, based on the criteria explored in Vamvakaris et al. (2016) and the seismic zonation proposed by them. Since the study area, comprises the most seismically active zone in Greece, assigned also the highest value on the Earthquake Building Code for the country, a large number of source, stress and strain studies have been used in their study to establish such definition of zoning. Hence, it was found well justified to follow their zone definition. In Fig. 8, from east to west and north to south, one can identify the zones of Akarnania (area no. 1), Lefkada island (area no. 2), east Cephalonia island (area no. 3), west Cephalonia island (area no. 4), and Zante island (area no. 5), respectively, covering the area of the Ionian Sea near Cephalonia island.

Διαγράφηκε: 2013

Διαγράφηκε: 2013

<Figure 8 should be placed around here>

Before we proceed to the NT analysis of seismicity, the seismic activity prior to EQ1, as well as between EQ1 and EQ2 is briefly discussed in relation to the above mentioned seismic zones. Earthquake parametric data have been retrieved from the National Observatory of Athens on-line catalogue (http://www.gein.noa.gr/en/seismicity/earthquake-catalogs), while for all the presented maps and calculations the local magnitude (M_L), as provided by the specific earthquake catalog, is used. The foreshock seismic activity before EQ1 for the whole investigated area of the Ionian Sea region from 13 December 2013 up to the time of occurrence of the main event is shown in the map of Fig. 9a. As it can be easily observed from this map, there was a high seismic activity mainly focused on two specific zones: west Cephalonia and Zante. Notably, an EQ of $M_L = 4.7$ occurred in Zante on 11/01/2014 04:12:58, indicated by the black arrow in Fig. 9a. No EQs were recorded in Akarnania, while very few events were recorded in Lefkada and east Cephalonia. The events which occurred in west Cephalonia are also shown in a separate map in Fig. 9b for later reference.

<Figure 9 should be placed around here>

Applying the natural time analysis on seismic data (cf. Sec. 2.2), the evolution of the time series (χ_k, Q_k) was studied for the foreshock seismicity prior to EQ1, where Q_k is in this case the seismic energy released during the k^{th} event. The seismic moment, M_0, as proportional to the seismic energy, is usually considered (Varotsos et al., 2005; Uyeda et al., 2009b; Potirakis et al., 2013,2015). Our calculations were based on the seismic moment M_0 (in dyn.cm) resulting from the corresponding M_L as (Varotsos et al., 2005; Potirakis et al., 2013, 2015), $M_0 = 10^{0.99 M_L + 11.8}$. First, we performed an NT analysis on the seismicity activity of the whole investigated Ionian Sea region during the period from 13/12/2013 00:00:00 to 26/01/2014 13:55:44 UT, i.e., just after the occurrence of EQ1, for different magnitude thresholds, M_{thres}, for which all earthquakes having $M_L > M_{thres}$ were included in the analysis. Note that, only $M_{thres} \geq 2$ was considered in order to assure data completeness (Chouliaras et al., 2013a, 2013b).

For all the considered threshold values, the result was the same: no indication of criticality was identified (see for example Fig. 10a). Since, as we have already mentioned, the whole investigated area was mainly dominated by the seismic activity in west Cephalonia and the seismic activity in Zante, while an EQ of $M_L = 4.7$ occurred in Zante, we decided to start the NT analysis after the occurrence of the specific Zante EQ, in order to exclude from our analysis possible foreshock activity related to the specific event. As a result, we performed

NT analysis for the time period 11/01/2014 04:13:00 (just after the $M_L = 4.7$ Zante EQ) to 26/01/2014 13:55:44 UT, for different magnitude thresholds in three successively enclosed areas: namely, the whole investigated area of Ionian Islands region, both Cephalonia (east and west) zones combined, and the zone of west Cephalonia. Representative examples of these analyses are depicted in Fig. 10b – Fig. 10d. The analysis over the whole investigated area of the Ionian Islands region indicates that seismicity reaches criticality on 19 and 20 of January, while the two other progressively narrower areas indicate that the criticality conditions according to NT method are satisfied on 19 and 22 of January. These results imply that seismicity was also in critical condition a few days prior to the occurrence of the first studied significant Cephalonia EQ (EQ1). Actually, in the specific case, the critical condition of seismicity was reached before, but quite close, to the emission of the corresponding MHz signals for which critical behavior was identified (cf. Sec. 3). Note that a very recent analysis on the foreshock seismic activity before EQ1, in terms of a combination of multiresolution wavelets and NT analysis, which was performed on concentric areas of 50 km and 30 km radii around the epicenter of EQ1, also found that NT analysis criticality requirements are met a few days before EQ1 (at approximately 20 January) (Vallianatos et al., 2015).

<Figure 10 should be placed around here>

Before the application of the NT method to the seismic activity prior to EQ2, one should first study the time evolution of the activity between the two significant events of interest, in order to minimize if possible the influence of the first EQ aftershock sequence on the NT analysis. Our first observation about the EQs which occurred during the specific time period was that, all but one had epicenters in west Cephalonia. Only one $M_L = 2.3$ EQ occurred in Zante, at (37.79^o N, 21.00^o E) on 28 January 2014 02:08:27 UT.

Fig. 11a shows all the events that were recorded in the whole investigated area of the Ionian Islands region vs. time from just after EQ1 ($M_w = 6.0$) up to the time of EQ2 ($M_w = 5.9$), including EQ2. As it can be seen, if one considers that both significant EQs of interest were main events, it is quite difficult to separate the seismic activity of the specific time period into aftershocks of the first EQ and foreshocks of the second one. However, we observe that up to a specific time point, there is a rapid decrease of the running mean magnitude of the recorded EQs, while after that the long range (75 events) running mean value seems to be almost constant over time with the short range (25 events) one varying around it. We arbitrarily set the 29 January 00:00:00 UT as the time point after which the recorded seismicity is no longer dominated by the aftershocks of EQ1; this by no means implies that the aftershock sequence of the EQ1 stops after that date. It should also be underlined that changing this, arbitrarily selected, date within reasonable limits, does not significantly changes the results of our corresponding NT analysis which are presented next. On the other hand, a significant shift of this limit towards EQ1, i.e., to earlier dates, results to severe changes indicating the domination of the recorded seismicity by the aftershock sequence of EQ1. Accordingly, the considered as foreshock seismic activity before EQ2, i.e., from 29/01/2014 00:00 UT up to the time of occurrence of EQ2, is presented in the map of Fig. 11b for west Cephalonia and analyzed in the following.

<Figure 11 should be placed around here>

Next, we applied the NT method on the seismicity of west Cephalonia for the time period from 29/01/2014 00:00:00 to 03/02/2014 03:08:47 UT. Note that we also applied the NT method on the whole investigated area of the Ionian Islands region, obtaining practically the same results. As we have already mentioned, only one $M_L = 2.3$ EQ occurred outside the west Cephalonia zone, so, on the one hand for magnitude threshold values $M_{thres} \geq 2.3$ this event was excluded, while, on the other hand, even for lower threshold values ($2 \leq M_{thres} < 2.3$) its inclusion does not change the results significantly. Fig. 12 shows the NT analysis results for some threshold values proving that seismicity reaches criticality on 1 or 2 February 2014, that is one or two days before the occurrence of the second significant EQ of interest ($M_w = 5.9$).Actually, in the specific case, the critical condition of seismicity was reached after, but quite close, to the emission of the corresponding MHz signals for which critical behavior was identified (cf. Sec. 3).

<Figure 12 should be placed around here>

5. Discussion - Conclusions

Based on the methods of critical fluctuations and natural time, we have shown that the fracture-induced MHz EME recorded by two stations in our network prior to two recent significant EQs occurred in Cephalonia present criticality characteristics, implying that they emerge from a system in critical state.

There are two key points that render these observations unique in the up to now research on the pre-EQ EME:

(i) The Cephalonia station is known for being insensitive to EQ preparation processes happening outside of the wider area of Cephalonia island, as well as to EQ preparation processes leading to low magnitude EQs within the area of Cephalonia island. Note that the only signal that has been previously recorded refers to the M=6 EQ that occurred on the specific island in 2007 (Contoyiannis et al., 2010).

(ii) Prior to each one of the studied significant EQs, two MHz EME time series presenting critical characteristics were recorded simultaneously in two different stations very close to the focal areas, while no other station of our network (cf. Fig. 1) recorded such signals prior to the specific EQs. This indicates that the revealed criticality was not associated with a global phenomenon, such as critical variations in the Ionosphere, but was rather local to the area of the Ionian Islands region, enhancing the hypothesis that these EME were associated with the EQ preparation process taking place prior to the two significant EQs. This feature, combined with the above mentioned sensitivity of the Cephalonia station only to significant EQs occurring on the specific island, could have been considered as an indication of the location of the impending EQs.

EME, as a phenomenon rooted in the damage process, should be an indicator of memory effects. Laboratory studies verify that: during cyclic loading, the level of EME increases significantly when the stress exceeds the maximum previously reached stress level (Kaizer effect). The existence of Kaizer effect predicts the EM silence during the aftershock period (Eftaxias et al., 2013; Eftaxias and Potirakis, 2013, and references therein). Thus, the appearance of the second EM anomaly may reveal that the corresponding preparation of fracture process has been organized in a new barrier.

We note that, according to the view that seismicity and pre-EQ EM emissions should be “two sides of the same coin” concerning the earthquake generation process, the corresponding foreshock seismic activity, as another manifestation of the same complex system, should be at critical state as well, before the occurrence of a main event. We have shown that this really happens for both significant EQs we studied. Importantly, the revealed critical process seems to be focused on an area corresponding to the west Cephalonia zone, one of the parts according to the seismotectonic and hazard zone partitioning of the wider area of the Ionian Islands.

To be more detailed, the foreshock seismicity associated with the first ($M_w = 6.0$) EQ reached critical condition a few days before the occurrence of the main event. Specifically, it came to critical condition before, but quite close, to the emission of the corresponding MHz signals for which critical behavior was identified. The seismicity that was considered as foreshock of the second ($M_w = 5.9$) EQ also reached criticality few days before the occurrence of the main event. In contrary to the first EQ case, it came to criticality after, but quite close, to the emission of the corresponding MHz signals for which critical behavior was identified.

One more outcome of our study was the identification of tricritical crossover dynamics in the MHz emissions recorded just before the occurrence of the second significant EQ of interest ($M_w = 5.9$) at the Cephalonia station. Note that, unfortunately, the Zante station was out of order for several hours during the specific day, including the time window during which the tricritical features were identified in the Cephalonia recordings. As a result, we could not cross check whether tricritical signals simultaneously also reached Zante. This is considered a quite important finding, since it verifies a theoretically expected situation, namely the approach of the intermediate dynamical state of tricritical crossover, either from the first or from the second order phase transition state. In terms of pre-EQ EME, this leads to a revision of the four-stage model for the preparation of an EQ by means of its observable EM activity. Namely, after the first stage of the EQ preparation process where MHz EME with critical features are emitted, a second stage follows where MHz or kHz or both MHz and kHz EME with trictitical features are emitted. Specifically, the trictitical crossover dynamics can be

Διαγράφηκε: U

Διαγράφηκε:

identified either in MHz time series, following the emission of a critical MHz EME, or in kHz time series preceding the emission of avalanche-like kHz EME. In summary, the proposed four stages of the last part of EQ preparation process and the associated, appropriately identified, EM observables appear in the following order: 1st stage: valid MHz anomaly; 2nd stage: MHz or kHz or MHz and kHz anomaly exhibiting tri-critical characteristics; 3rd stage: strong avalanche-like kHz anomaly; 4th stage: electromagnetic quiescence. Note that the specific four-stage model is a suggestion that seems to be verified by the up to now available MHz-kHz observation data and corresponding time-series analyzes, while a rebuttal has not yet appeared in the literature. However, the understanding of the physical processes involved in the preparation of an EQ and their relation to various available observables is an open scientific issue. Much effort still remains to be paid before one can claim clear understanding of EQ preparation processes and associated possible precursors.

As it has been repeatedly pointed out in previous works (e.g., Eftaxias et al., 2013; Eftaxias and Potirakis, 2013, and references therein), our view is that such observations and the associated analyses offer valuable information for the comprehension of the Earth system processes that take place prior to the occurrence of a significant EQ. As it is known, a large number of other precursory phenomena are also observed, both by ground and satellite stations, prior to significant EQs. Only a combined evaluation of our observations with other well documented precursory phenomena could possibly render our observations useful for a reliable short-term forecast solution. Unfortunately, in the cases of the Cephalonia EQs under study this requirement was not fulfilled. To the best of our knowledge, only one paper reporting the emergence of VLF seismic-ionospheric disturbances four days before the first Cephalonia EQ (Skeberis et al., 2015) has been published up to now. It is very important that the specific disturbances, which also correspond to a spatially extensive process as happens with the MHz EME, were recorded during the same time window with the here presented MHz critical signals. However, more precursory phenomena could have been investigated if appropriate observation data were available. For example, if ground-based magnetic observatories in the area of Greece had available magnetometer data for the time period of interest, EQ-related ULF magnetic field variations, either of lithospheric or ionospheric origin, which are also a result of spatially extensive processes and in other cases have been shown to present critical characteristics prior to EQ occurrence (Hayakawa et al., 2015), could also be investigated.

Acknowledgements

The authors S. M. P., Y. C., N. S. M., J. K., G. A., C. N. and K. E. would like to acknowledge that this research was co-funded by the EU (European Social Fund) and national funds, action “Archimedes III—Funding of research groups in T.E.I.”, under the Operational Programme “Education and Lifelong Learning 2007-2013”. The authors G. B. and C. K. would like to acknowledge support from the European Union Seventh Framework Programme (FP7-REGPOT-2012-2013-1) under grant agreement no. 316210 (BEYOND – Building Capacity for a Centre of Excellence for EO-based monitoring of Natural Disasters).

REFERENCES

Abe, S., Sarlis, N. V., Skordas, E. S., Tanaka, H. K., Varotsos, P. A.: Origin of the usefulness of the natural-time representation of complex time series, Phys. Rev. Lett., 94, doi: 10.1103/PhysRevLett.94.170601, 2005.

Bowman, D., Ouillon, G., Sammis, C., Sornette, A., Sornette, D.: An observational test of the critical earthquake concept, J. Geophys. Res., 103, 24359-24372, doi: 10.1029/98JB00792, 1998.

Chelidze, T.: Percolation and fracture, Phys. Earth Planet. In., 28, 93-101, 1982.

Chelidze, T., Kolesnikov, Yu. M.: Percolation modell des bruchprozesses, Gerlands Beitr. Geophysik. Leipzig, 91, 35-44, 1982.

Chelidze, T., Kolesnikov, Yu., Matcharashvili, T.: Seismological criticality concept and percolation model of fracture, Geophys. J. Int., 164, 125-136, 2006.

Chouliaras, G., Melis, N. S., Drakatos, G., Makropoulos, K.: Operational network improvements and increased reporting in the NOA (Greece) seismicity catalog, Geophysical Research Abstracts, 15, EGU2013-12634-6., 2013a.

Chouliaras, G., Melis, N. S., Drakatos, G., Makropoulos, K.: Operational network improvements and increased reporting in the NOA (Greece) seismicity catalog, Adv. Geosci., 36, 7-9, doi: 10.5194/adgeo-36-7-2013, 2013b.

Cicerone, R. D., Ebel, J. E., Britton, J.: A systematic compilation of earthquake precursors, Tectonophysics, 476, 371-396, doi: 10.1016/j.tecto.2009.06.008, 2009.

Contoyiannis, Y., Diakonos, F.: Criticality and intermittency in the order parameter space, Phys. Lett. A, 268, 286 -292, doi: 10.1016/S0375-9601(00)00180-8, 2000.

Contoyiannis, Y., Diakonos, F., Malakis, A.: Intermittent dynamics of critical fluctuations, Phys. Rev. Lett., 89, 035701, doi: 10.1103/PhysRevLett.89.035701, 2002.

Contoyiannis, Y. F, Diakonos, F. K., Kapiris, P. G., Peratzakis, A. S., Eftaxias, K. A.: Intermittent dynamics of critical pre-seismic electromagnetic fluctuations, Phys. Chem. Earth, 29, 397-408, doi: 10.1016/j.pce.2003.11.012, 2004a.

Contoyiannis, Y. F., Diakonos, F. K., Papaefthimiou, C., Theophilidis, G.: Criticality in the relaxation phase of a spontaneously contracting atria isolated from a Frog's Heart, Phys. Rev. Lett., 93, 098101, doi: 10.1103/PhysRevLett.93.098101, 2004b.

Contoyiannis, Y. F., Kapiris, P. G., Eftaxias, K. A.: A Monitoring of a pre-seismic phase from its electromagnetic precursors, Phys. Rev. E, 71, 066123, 066123/1–14, doi: 10.1103/PhysRevE.71.066123, 2005.

Contoyiannis, Y. F., Diakonos, F. K.: Unimodal maps and order parameter fluctuations in the critical region, Phys. Rev. E, 76, 031138, 2007.

Contoyiannis, Y. F., Eftaxias, K.: Tsallis and Levy statistics in the preparation of an earthquake, Nonlin. Processes Geophys., 15, 379-388, doi:10.5194/npg-15-379-2008, 2008.

Contoyiannis, Y. F., Nomicos, C., Kopanas, J., Antonopoulos, G., Contoyianni, L., Eftaxias, K.: Critical features in electromagnetic anomalies detected prior to the L'Aquila earthquake, Physica A, 389, 499-508, doi: 10.1016/j.physa.2009.09.046, 2010.

Contoyiannis, Y. F., Potirakis, S. M., Eftaxias, K.: The Earth as a living planet: human-type diseases in the earthquake preparation process, Nat. Hazards Earth Syst. Sci., 13, 125–139, doi: 10.5194/nhess-13-125-2013, 2013.

Contoyiannis, Y., Potirakis, S. M., Eftaxias, K., Contoyianni, L.: Tricritical crossover in earthquake preparation by analyzing preseismic electromagnetic emissions, J. Geodynamics, 84, 40-54, doi: 10.1016/j.jog.2014.09.015, 2015.

Donner, R. V., Potirakis, S. M., Balasis, G., Eftaxias, K., Kurths, J.: Temporal correlation patterns in pre-seismic electromagnetic emissions reveal distinct complexity profiles prior to major earthquakes, Phys. Chem. Earth, In Press (on-line available), doi: 10.1016/j.pce.2015.03.008, 2015.

Eftaxias, K., Kapiris, P., Polygiannakis, J., Bogris, N., Kopanas, J., Antonopoulos, G., Peratzakis, A., Hadjicontis, V.: Signatures of pending earthquake from electromagnetic anomalies, Geophys. Res. Let., 28, 3321-3324, doi: 10.1029/2001GL013124, 2001.

Eftaxias, K., Frangos, P., Kapiris, P., Polygiannakis, J., Kopanas, J., Peratzakis, A., Skountzos, P., Jaggard, D.: Review and a model of pre-seismic electromagnetic emissions in terms of fractal electrodynamics, Fractals, 12, 243–273, doi: 10.1142/S0218348X04002501, 2004.

Eftaxias, K., Contoyiannis, Y., Balasis, G., Karamanos, K., Kopanas, J., Antonopoulos, G., Koulouras, G., Nomicos, C.: Evidence of fractional-Brownian-motion-type asperity model for earthquake generation in candidate pre-seismic electromagnetic emissions, Nat. Hazards Earth Syst. Sci., 8, 657–669, doi:10.5194/nhess-8-657-2008, 2008.

Eftaxias, K., Potirakis, S. M., Chelidze, T.: On the puzzling feature of the silence of precursory electromagnetic emissions, Nat. Hazards Earth Syst. Sci., 13, 2381-2397, doi: 10.5194/nhess-13-2381-2013, 2013.

Eftaxias, K., Potirakis, S. M.: Current challenges for pre-earthquake electromagnetic emissions: shedding light from micro-scale plastic flow, granular packings, phase transitions and self-affinity notion of fracture process, Nonlin. Processes Geophys., 20, 771–792, doi:10.5194/npg-20-771-2013, 2013.

Ganas, A., Cannavo, F., Chousianitis, K., Kassaras, I., Drakatos, G.: Displacements recorded on continuous GPS stations following the 2014 M6 Cephalonia (Greece) earthquakes: Dynamic characteristics and kinematic implications, Acta Geodyn. Geomater., 12(1), 5–27, doi: 10.13168/AGG.2015.0005, 2015.

Hayakawa, M. (ed.): *The Frontier of Earthquake Prediction Studies*, Nihon-Senmontosho-Shuppan, Tokyo, 2013a.

Hayakawa, M. (ed.): *Earthquake Prediction Studies: Seismo Electromagnetics*, Terrapub, Tokyo, 2013b.

Hayakawa, M., Schekotov, A, Potirakis, S. and Eftaxias, K.: Criticality features in ULF magnetic fields prior to the 2011 Tohoku earthquake, Proc. Japan Acad., Ser. B, 91, 25-30, doi: 10.2183/pjab.91.25, 2015.

Huang, K.: *Statistical Mechanics*, 2nd Ed. John Wiley and sons, New York, 1987.

Kapiris, P., Eftaxias, K., Chelidze, T.: Electromagnetic signature of prefracture criticality in heterogeneous media, Phys. Rev. Lett., 92(6), 065702/1-4, doi: 10.1103/PhysRevLett.92.065702, 2004.

Karamanos, K., Dakopoulos, D., Aloupis, K., Peratzakis, A., Athanasopoulou, L., Nikolopoulos, S., Kapiris, P., Eftaxias, K.: Study of pre-seismic electromagnetic signals in terms of complexity, Phys. Rev. E, 74, 016104/1-21, doi: 10.1103/PhysRevE.74.016104, 2006.

Karastathis, V. K., Mouzakiotis, E., Ganas, A., Papadopoulos, G. A.: High-precision relocation of seismic sequences above a dipping Moho: The case of the January-February 2014 seismic sequence in Cephalonia Isl. (Greece), Solid Earth Discuss., 6, 2699-2733, doi: 10.5194/sed-6-2699-2014, 2014.

Merryman Boncori, J. P., Papoutsis , I., Pezzo, G., Tolomei , C., Atzori, S., Ganas, A., Karastathis, V., Salvi, S., Kontoes, C., Antonioli, A.: The February 2014 Cephalonia earthquake (Greece): 3D deformation field and source modeling from multiple SAR techniques, Seismol. Res. Lett. 86(1), 1-14, doi: 10.1785/0220140126, 2015.

Minadakis, G., Potirakis, S. M., Nomicos, C., Eftaxias, K.: Linking electromagnetic precursors with earthquake dynamics: an approach based on nonextensive fragment and self-affine asperity models, Physica A, 391, 2232-2244, doi: 10.1016/j.physa.2011.11.049, 2012a.

Minadakis, G., Potirakis, S. M., Stonham, J., Nomicos, C., Eftaxias, K.: The role of propagating stress waves in geophysical scale: Evidence in terms of nonextensivity, Physica A, 391(22), 5648-5657, doi:10.1016/j.physa.2012.04.030, 2012b.

Ozun, A., Contoyiannis, Y. F., Diakonos, F. K., Hanias, M., Magafas, L.: Intermittency in stock market dynamic, J. Trading 9(3), 26-33, 2014.

Papadimitriou, K., Kalimeri, M., Eftaxias, K.: Nonextensivity and universality in the earthquake preparation process, Phys. Rev. E, 77, 036101/1-14, doi: 10.1103/PhysRevE.77.036101, 2008.

Papadopoulos, G. A., Karastathis, V. K., Koukouvelas, I., Sachpazi, M., Baskoutas, I., Chouliaras, G., Agalos, A., Daskalaki, E., Minadakis, G., Moshou, A., Mouzakiotis, A., Orfanogiannaki, K., Papageorgiou, A., Spanos, D., Triantafyllou, I.: The Cephalonia, Ionian Sea (Greece), sequence of strong earthquakes of January-February 2014: a first report, Res. Geoph., 4:5441, 19-30, doi:10.4081/rg.2014.5441, 2014.

Pingel, D., Schmelcher, P., Diakonos, F. K.: Theory and examples of the inverse Frobenius-Perron problem for complete chaotic maps, Chaos, 9, 357-366, doi: 10.1063/1.166413, 1999.

Potirakis, S. M., Minadakis, G., Nomicos, C., Eftaxias, K.: A multidisciplinary analysis for traces of the last state of earthquake generation in preseismic electromagnetic emissions, Nat. Hazards and Earth Syst. Sci., 11, 2859-2879, doi:10.5194/nhess-11-2859-2011, 2011.

Potirakis, S. M., Minadakis, G., Eftaxias, K.: Analysis of electromagnetic pre-seismic emissions using Fisher information and Tsallis entropy, Physica A, 391, 300-306, doi:10.1016/j.physa.2011.08.003, 2012a.

Potirakis, S. M., Minadakis, G., Eftaxias, K.: Sudden drop of fractal dimension of electromagnetic emissions recorded prior to significant earthquake, Nat. Hazards, 64, 641-650, doi:10.1007/s11069-012-0262-x, 2012b.

Potirakis, S. M., Minadakis, G., Eftaxias, K.: Relation between seismicity and pre-earthquake electromagnetic emissions in terms of energy, information and entropy content, Nat. Hazards Earth Syst. Sci., 12, 1179-1183, doi:10.5194/nhess-12-1179-2012, 2012c.

Potirakis, S.M., Karadimitrakis, A. and Eftaxias, K.: Natural time analysis of critical phenomena: the case of pre-fracture electromagnetic emissions, Chaos, 23, 2, 023117. doi:10.1063/1.4807908, 2013.

Potirakis, S. M., Contoyiannis, Y., Eftaxias, K., Koulouras, G., and Nomicos, C.: Recent field observations indicating an earth system in critical condition before the occurrence of a significant earthquake, IEEE Geosc. Remote Sens. Lett., 12(3), 631-635, doi: 10.1109/LGRS.2014.2354374, 2015.

Rundle, J. B., Holliday, J. R., Graves, W. R., Turcotte, D. L., Tiampo. K. F., Klein, W.: Probabilities for large events in driven threshold systems, Phys. Rev. E, 86, 021106, 2012.

Sakkas, V., Lagios, E.: Fault modelling of the early-2014 ~ M6 Earthquakes in Cephalonia Island (W. Greece) based on GPS measurements, Tectonophysics, 644-645, 184-196, doi: 10.1016/j.tecto.2015.01.010, 2015.

Sarlis, N. V., Skordas, E. S., Varotsos, P. A.: Similarity of fluctuations in systems exhibiting self-organized criticality, Europhys. Lett., 96, 2, doi:10.1209/0295-5075/96/28006, 2011.

Sarlis, N. V., Skordas, E. S., Lazaridou, M. S., Varotsos, P. A.: Investigation of seismicity after the initiation of a Seismic Electric Signal activity until the main shock, Proc. Japan Acad., Ser. B., 84, 331-343, 2008.

Schuster, H.: *Deterministic Chaos*, VCH, Weinheim, 1998.

Skeberis, C., Zaharis, Z.D., Xenos, T.D., Spatalas, S., Arabelos, D.N., Contadakis, M.E.: Time–frequency analysis of VLF for seismic-ionospheric precursor detection: Evaluation of Zhao-Atlas-Marks and Hilbert-Huang Transforms, Phys. Chem. Earth, 85-86, 174–184, doi:10.1016/j.pce.2015.02.006, 2015.

Stanley, H. E.: *Introduction to Phase Transitions and Critical Phenomena*, Oxford University Press, New York, 1987.

Stanley, H. E.: Scaling, universality, and renormalization: Three pillars of modern critical phenomena, Rev. Modern Phys., 71, S358-S366, 1999.

Uyeda, S., Nagao, T., Kamogawa, M.: Short-term EQ prediction: Current status of seismo-electromagnetics, Tectonophysics, 470, 205–213, 2009a.

Uyeda, S., Kamogawa, M., Tanaka, H.: Analysis of electrical activity and seismicity in the natural time domain for the volcanic-seismic swarm activity in 2000 in the Izu Island region, Japan, J. Geophys Res., 114(B2), B02310, doi:10.1029/2007JB005332, 2009b.

Valkaniotis, S., Ganas, A., Papathanassiou, G., Papanikolau, M.: Field observations of geological effects triggered by the January-February 2014 Cephalonia (Ionian Sea, Greece) earthquakes, Tectonophysics, 630, 150-157, doi: 10.1016/j.tecto.2014.05.012, 2014.

Vallianatos, F., Michas, G., Hloupis, G.: Multiresolution wavelets and natural time analysis before the January-February 2014 Cephalonia (Mw6.1 & 6.0) sequence of strong earthquake events, Phys. Chem. Earth, 85-86, 201–209, 2015.Vamvakaris, D. A., Papazachos, C. B., Papaioannou, Ch. A., Scordilis, E. M., and Karakaisis, G. F.: A detailed seismic zonation model for shallow earthquakes in the broader Aegean area, Nat. Hazards Earth Syst. Sci., 16, 55-84, doi:10.5194/nhess-16-55-2016, 2016.

Varotsos, P. A.: *The Physics of Seismic Electric Signals*,TERRAPUB, Tokyo, 2005.

Varotsos, P. A., Sarlis, N. V., Skordas, E. S.: Spatio-temporal complexity aspects on the interrelation between seismic electric signals and seismicity., Pract. Athens Acad., 76, 294-321, 2001.

Varotsos, P. A., Sarlis, N. V., Skordas, E. S.: Long-range correlations in the electric signals that precede rupture, Phys. Rev. E, 66, 011902.doi:10.1103/ PhysRevE.66.011902, 2002.

Varotsos, P. A., Sarlis, N. V., Tanaka, H. K., Skordas, E. S.: Similarity of fluctuations in correlated systems: The case of seismicity, Phys. Rev. E, 72, 041103. doi: 10.1103/PhysRevE.72.041103, 2005.

Varotsos, P. A., Sarlis, N. V., Skordas, E. S., Tanaka, H. K., Lazaridou, M. S.: Entropy of seismic electric signals: Analysis in the natural time under time reversal, Phys. Rev. E, 73, 031114. doi:10.1103/PhysRevE.73.031114, 2006.

Varotsos, P., Sarlis, N., Skordas, E., Uyeda, S., Kamogawa, M.: Natural time analysis of critical phenomena, Proc. Natl. Acad. Sci. USA, 108, 11361–11364, 2011a.

Varotsos, P., Sarlis, N., Skordas, E. S.: *Natural Time Analysis: The New View of Time*, Springer, Berlin, 2011b.

Διαγράφηκε: In Press (on-line available)

Διαγράφηκε: ¶

Διαγράφηκε: Vamvakaris, D. A., Papazachos, C. B., Papaioannou, C., Scordilis, E. M., Karakaisis, G. F.: A detailed seismic zonation model for shallow earthquakes in the broader Aegean area, Nat. Hazards Earth Syst. Sci. Discuss., 1, 6719–6784, doi: 10.5194/nhessd-1-6719-2013, 2013.¶

Wanliss, J., Muñoz, V., Pastén, D., Toledo, B., Valdivia, J. A.: Critical behavior in earthquake energy dissipation, Nonlin. Processes Geophys. Discuss., 2, 619–645, 2015.

Figures

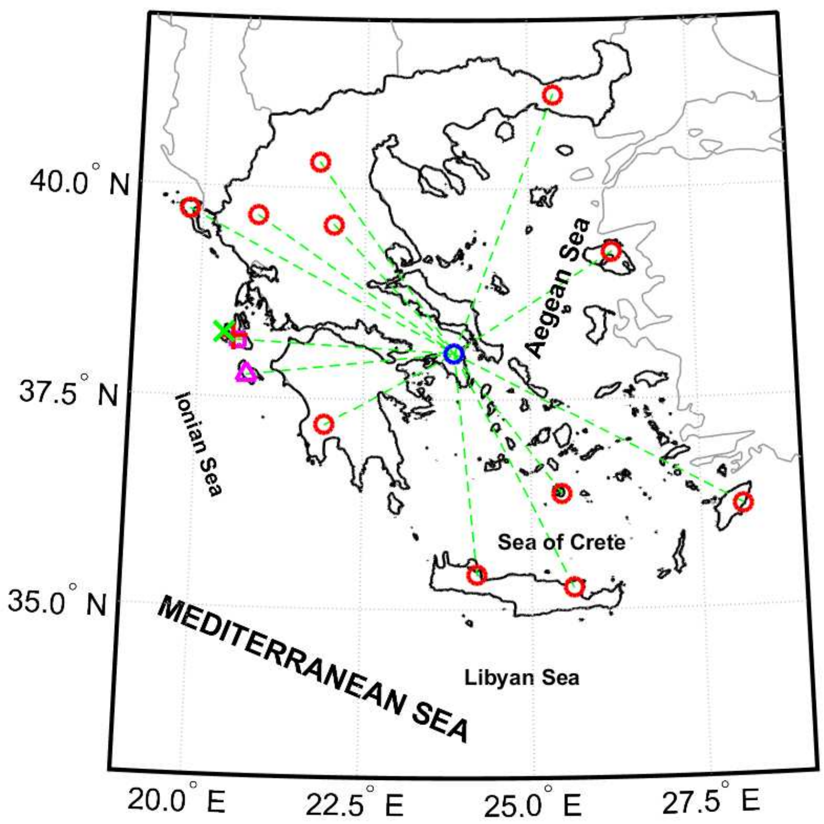

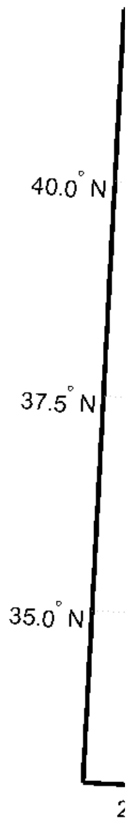

Διαγράφηκε:

Figure 1. Map with distribution of stations of the telemetric network that monitors electromagnetic variations in the MHz and kHz bands in Greece, which were operating during the time period of interest. The locations of the Cephalonia and Zante stations are marked by the magenta square and triangle, respectively, while the rest of the remote stations are denoted by red circles and the central data recording server by a blue circle. The epicenters of the two significant EQs of interest are also marked, the first (EQ1, $M_w = 6.0$) by a red cross and the second (EQ2, $M_w = 5.9$) by a green X mark. (For interpretation of the references to colors, the reader is referred to the online version of this paper.)

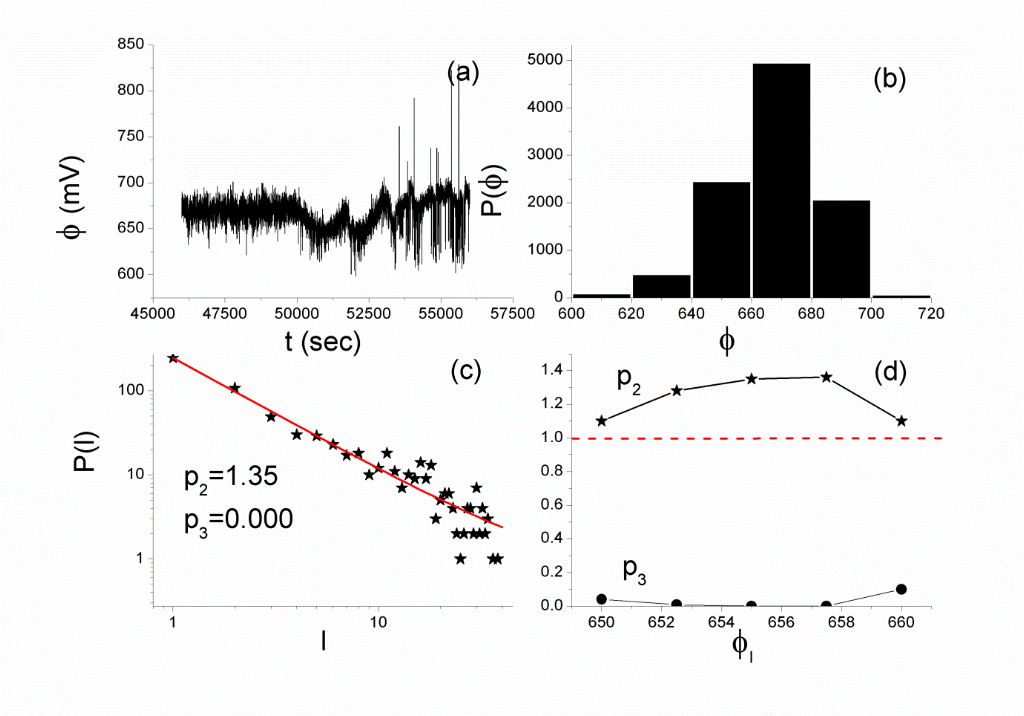

Figure 2. (a) The 10,000 samples long critical window of the MHz EME that was recorded before the Cephalonia $M_w = 6.0$ EQ at the Cephalonia station. (b) Amplitude distribution of the signal of Fig. 2a. (c) Distribution of laminar lengths for the end point $\phi_l = 655 mV$, as a representative example of the involved fitting. The solid line corresponds to the fitted function (cf. to text in Sec. 2.1) with the values of the corresponding exponents p_2, p_3 also noted. (d) The obtained exponents p_2, p_3 vs. different values of the end of laminar region ϕ_l. The horizontal dashed line indicates the critical limit ($p_2 = 1$).

Διαγράφηκε: Laminar distribution

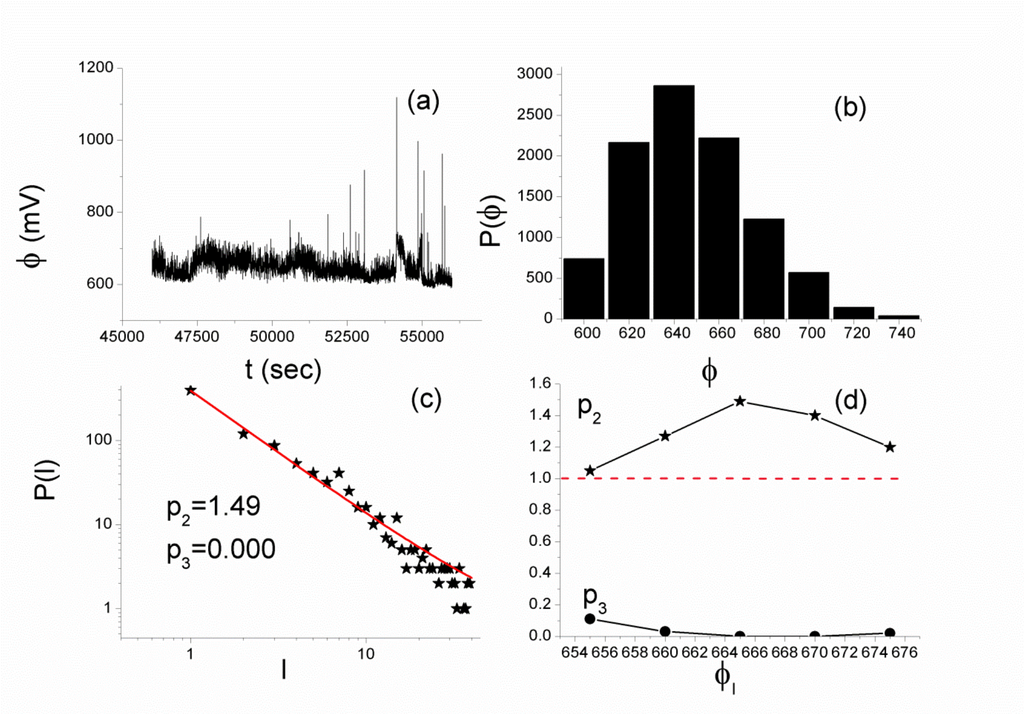

Figure 3. (a) The 10,000 samples long critical window of the MHz EME that was recorded prior to the Cephalonia $M_w = 6.0$ EQ at the Zante station, while (b), (c), and (d) are similar to the corresponding parts of Fig. 2. From 3b, a fixed-point (start of laminar regions), ϕ_o of about 600 mV results, while in Fig. 3c, the distribution of laminar lengths is given for the end point $\phi_l = 665mV$ for which the exponents $p_2 = 1.49$, $p_3 = 0.000$ with $R^2 = 0.999$ were obtained.

Διαγράφηκε: .

Διαγράφηκε: Amplitude distribution of the signal of Fig. 3a. (c) Laminar distribution

Διαγράφηκε: ,

Διαγράφηκε: as a representative example of the involved fitting. The solid line corresponds to the fitted function (cf. to text in Sec. 2.1) with the values of the corresponding exponents p_2, p_3 also noted. (d) The obtained exponents p_2, p_3 vs. different values of the end of laminar region ϕ_l. The horizontal dashed line indicates the critical limit ($p_2 = 1$).

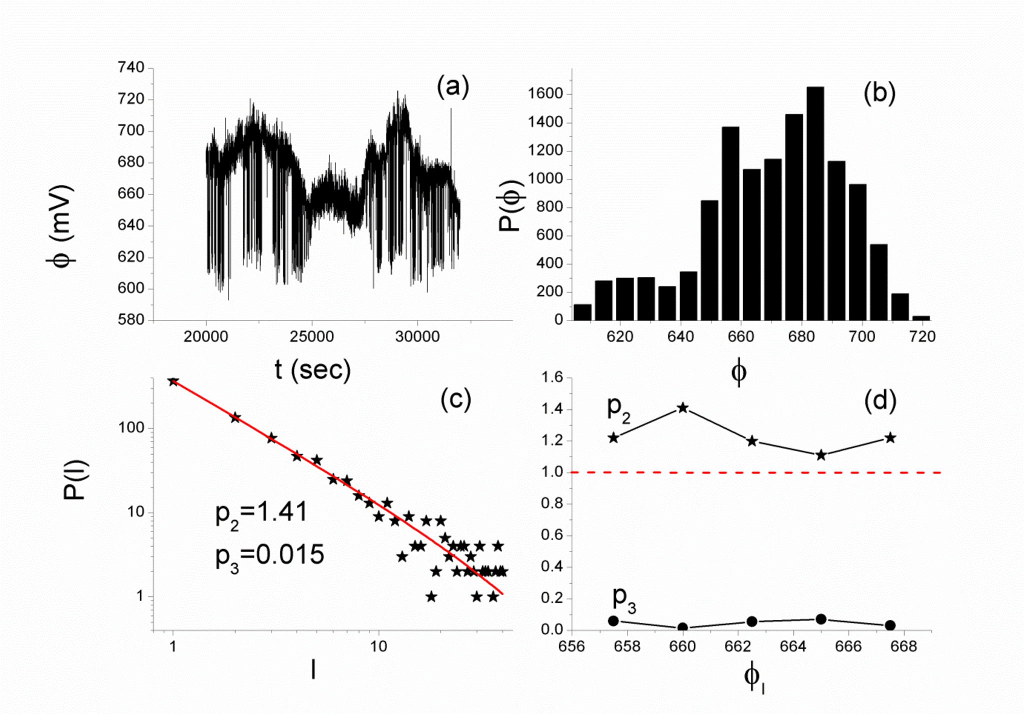

Figure 4. (a) The 12,000 samples long critical window of the MHz EME that was recorded before the Cephalonia $M_w = 5.9$ EQ at the Cephalonia station, while (b), (c), and (d) are similar to the corresponding parts of Fig. 2. In Fig. 4c, the distribution of laminar lengths is given for the end point $\phi_l = 660mV$.

Διαγράφηκε: .

Διαγράφηκε: Amplitude distribution of the signal of Fig. 4a. (c) Laminar distribution

Διαγράφηκε: , as a representative example of the involved fitting. The solid line corresponds to the fitted function (cf. to text in Sec. 2.1) with the values of the corresponding exponents p_2, p_3 also noted. (d) The obtained exponents p_2, p_3 vs. different values of the end of laminar region ϕ_l. The horizontal dashed line indicates the critical limit ($p_2 = 1$)

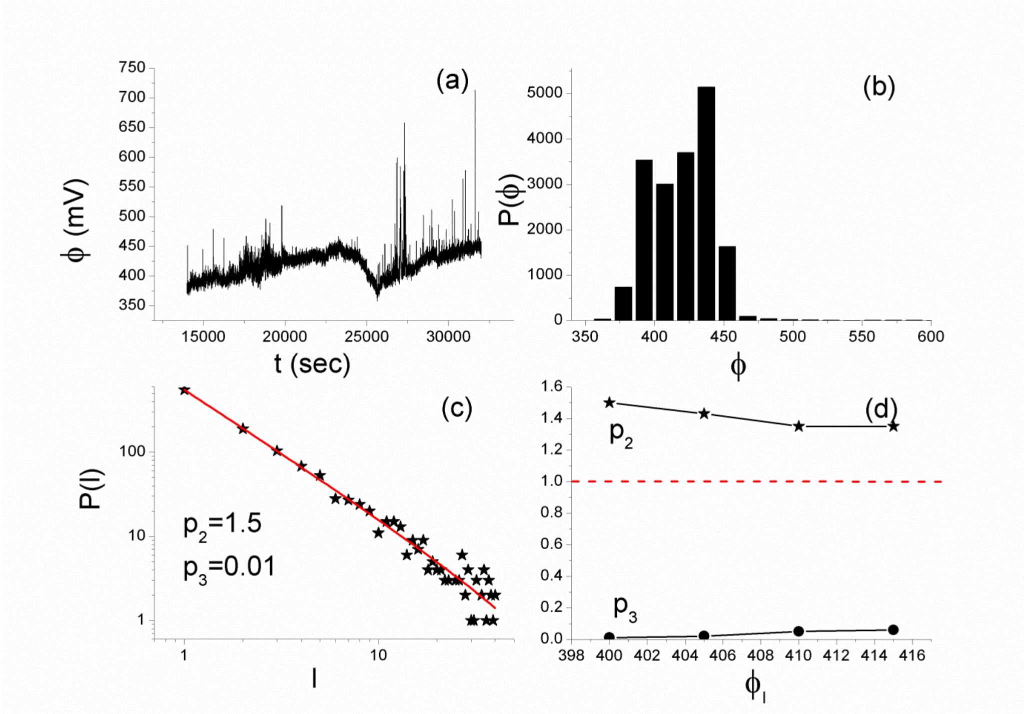

Figure 5. (a) The 18,000 samples long critical window of the MHz EME that was recorded before the Cephalonia $M_w = 5.9$ EQ at the Zante station; (b), (c), and (d) are similar to the corresponding parts of Fig. 2. In Fig. 5c, the distribution of laminar lengths corresponds to the end point $\phi_l = 400mV$.

Διαγράφηκε: .

Διαγράφηκε: Amplitude distribution of the signal of Fig. 5a. (c) Laminar distribution

Διαγράφηκε: for

Διαγράφηκε: , as a representative example of the involved fitting. The solid line corresponds to the fitted function (cf. to text in Sec. 2.1) with the values of the corresponding exponents p_2, p_3 also noted. (d) The obtained exponents p_2, p_3 vs. different values of the end of laminar region ϕ_l. The horizontal dashed line indicates the critical limit ($p_2 = 1$)

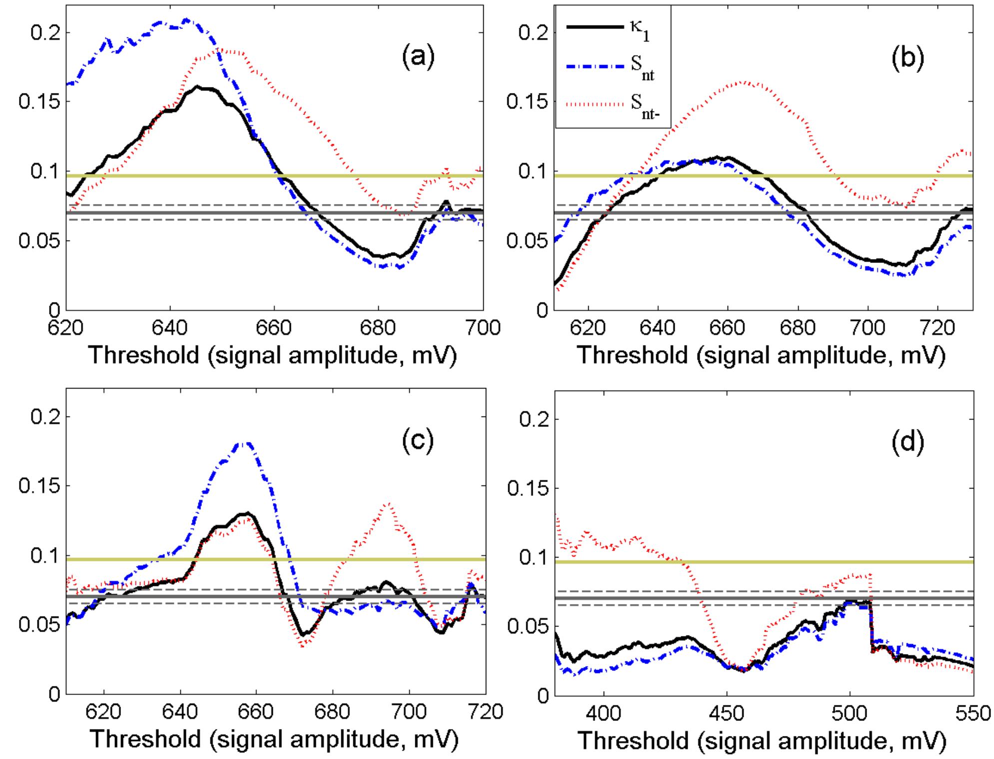

Figure 6. Natural time analysis results obtained for the MHz EME signals shown in: (a) Fig. 2a, recorded at Cephalonia station prior to EQ1, (b) Fig. 3a, recorded at Zante station prior to EQ1, (c) Fig. 4a, recorded at Cephalonia station prior to EQ2, and (d) Fig. 5a, recorded at Zante station prior to EQ2. The quantities κ_1 (solid curve), S_{nt} (dash-dot curve), and S_{nt-} (dot curve) vs. amplitude threshold for each MHz signal are shown. The entropy limit of $S_u\left(\approx 0.0966\right)$, the value 0.070 and a region of ± 0.005 around it are denoted by the horizontal solid light green, solid grey and the grey dashed lines, respectively. (For interpretation of the references to colors, the reader is referred to the online version of this paper.)

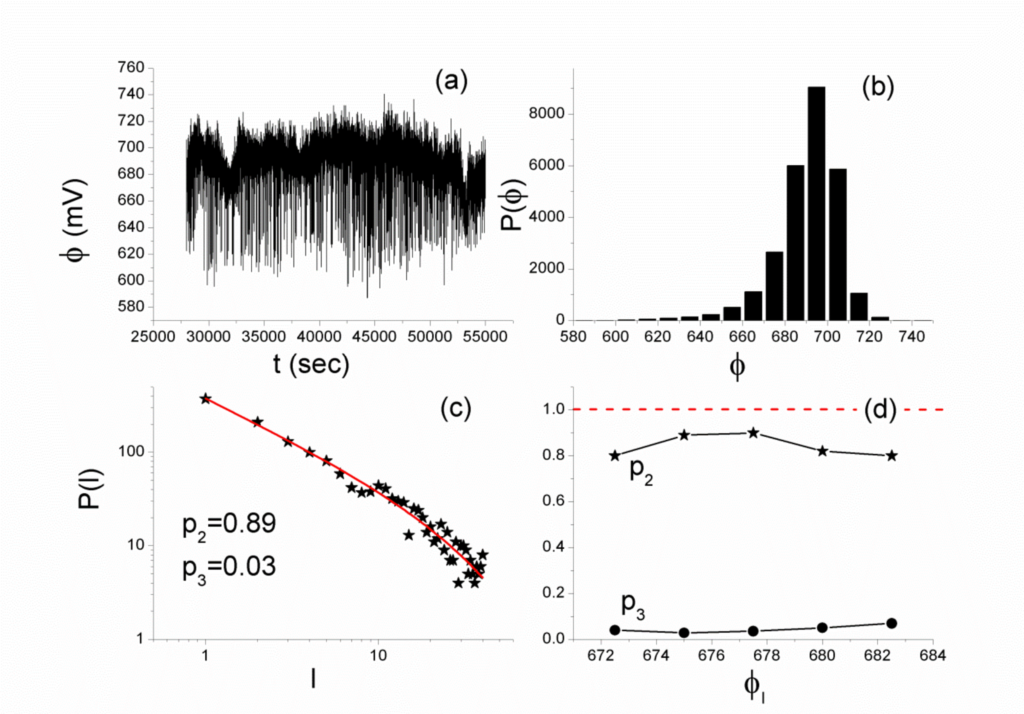

Figure 7. (a) The 27,000 samples long tricritical excerpt of the MHz EME that was recorded before the Cephalonia $M_w = 5.9$ EQ at the Cephalonia station; (b), (c), and (d) are similar to the corresponding parts of Fig. 2. In Fig. 7c, the distribution of laminar lengths corresponds to the end point $\phi_l = 675mV$.

Διαγράφηκε: .

Διαγράφηκε: Amplitude distribution of the signal of Fig. 7a. (c) Laminar distribution

Διαγράφηκε: for

Διαγράφηκε: , as a representative example of the involved fitting. The solid line corresponds to the fitted function (cf. to text in Sec. 2.1) with the values of the corresponding exponents p_2, p_3 also noted. (d) The obtained exponents p_2, p_3 vs. different values of the end of laminar region ϕ_l. The horizontal dashed line indicates the critical limit ($p_2 = 1$)

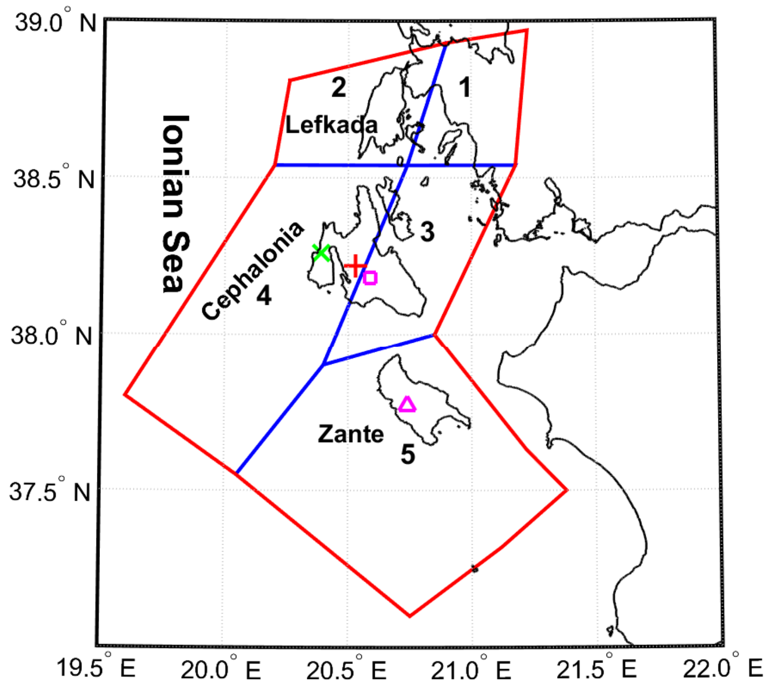

Διαγράφηκε:

Figure 8. Seismic zonation in the Ionian Islands area. The locations of the Cephalonia and Zante stations, as well as the epicenters of the two significant EQs of interest are marked, using the same signs presented in Fig. 1.

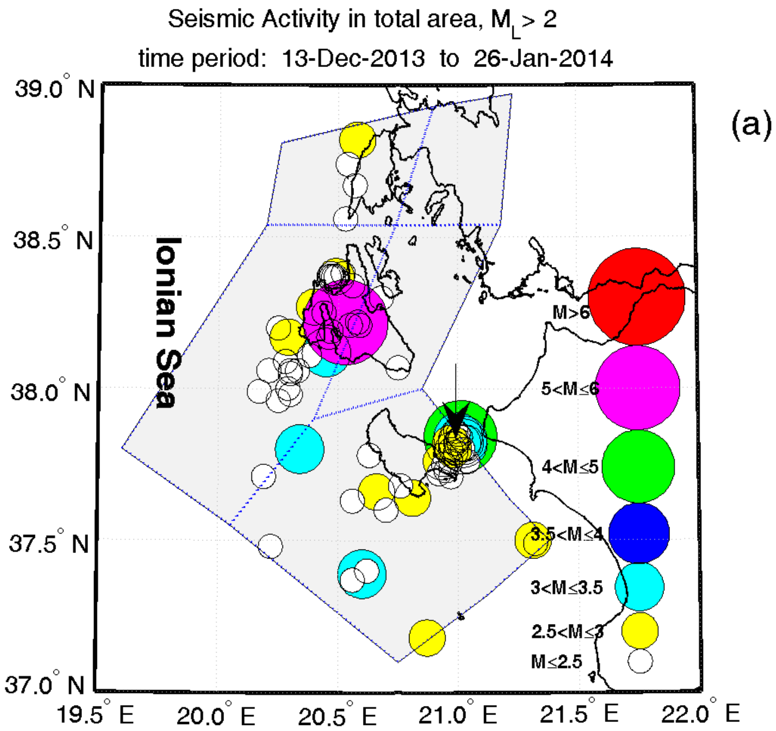
Seismic Activity in total area, M_L > 2
time period: 13-Dec-2013 to 26-Jan-2014
(a)
39.0° N
38.5° N
38.0° N
37.5° N
37.0° N
19.5° E
20.0° E
20.5° E
21.0° E
21.5° E
22.0° E
Ionian Sea
M>6
5<M≤6
4<M≤5
3.5<M≤4
3<M≤3.5
2.5<M≤3
M≤2.5

Διαγράφηκε:

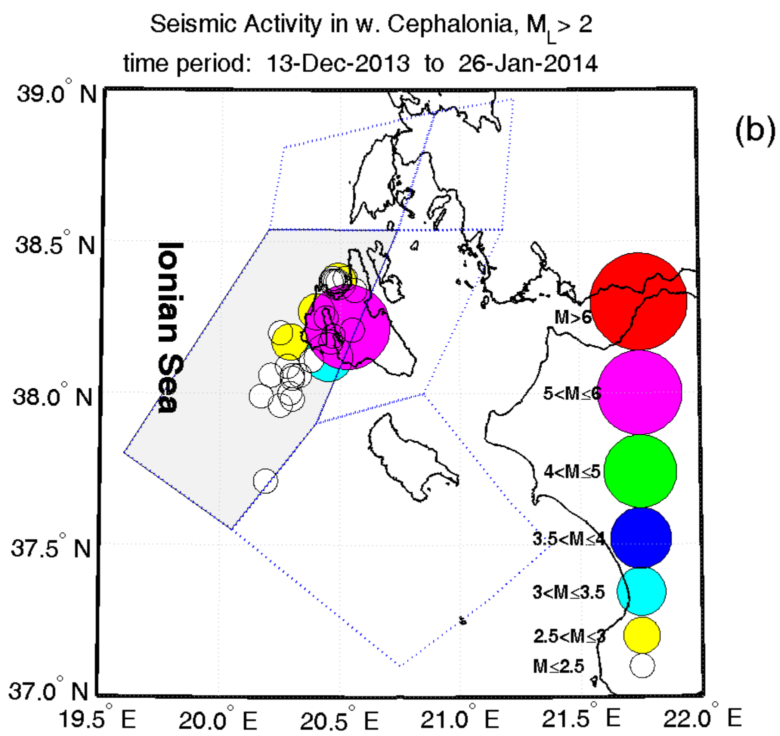

Διαγράφηκε:

Figure 9. Foreshock seismic activity (M_L) before EQ1: (a) for the whole investigated area of the Ionian Sea region; (b) for west Cephalonia. (For interpretation of the references to colors, the reader is referred to the online version of this paper.)

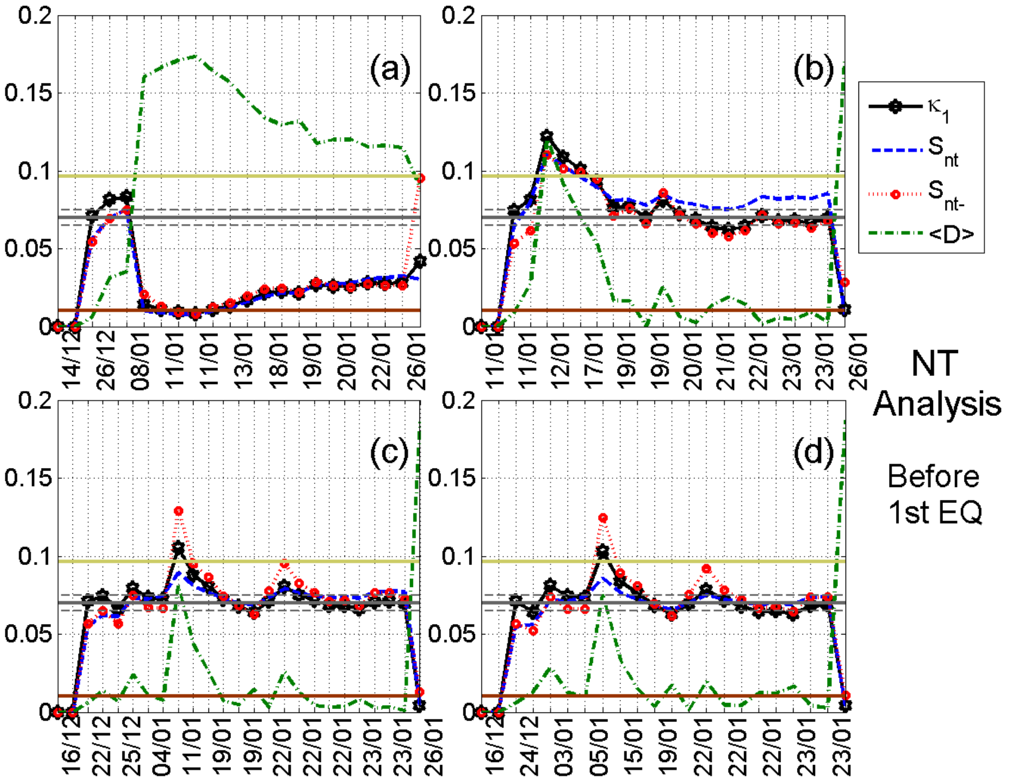

Figure 10. Temporal evolutions of the four natural time (NT) analysis parameters (κ_1, S_{nt}, S_{nt-}, and $\langle D \rangle$) for the foreshock seismic activity recorded prior to EQ1: (a) for the activity of the whole investigated area of the Ionian Sea for M_L threshold 2.5, during the period from 13/12/2013 00:00:00 to 26/01/2014 13:55:44 UT (just after the occurrence of EQ1); (b) for the activity of the whole investigated area of the Ionian Sea for M_L threshold 2.3, during the period from 11/01/2014 04:13:00 (just after the $M_L = 4.7$ occurred in Zante) to 26/01/2014 13:55:44 UT; (c) for the activity of both Cephalonia (east and west) zones combined for M_L threshold 2.1, during the period from 13/12/2013 00:00:00 to 26/01/2014 13:55:44 UT;. (d) for the activity of the west Cephaloniafor M_L threshold 2.1, during the period from 13/12/2013 00:00:00 to 26/01/2014 13:55:44 UT. Note that the events employed depend on the considered threshold. Moreover, the time (x-) axis is not linear in terms of the conventional date of occurrence of the events, since the employed events appear equally spaced relative to x-axis, as the natural time representation demands, although they are not

equally spaced in conventional time. The horizontal solid light green, solid grey and the grey dashed lines, denote the same quantities as in Fig. 6, while the horizontal solid brown line denotes the 10^{-2} limit for $\langle D \rangle$. (For interpretation of the references to colors, the reader is referred to the online version of this paper.)

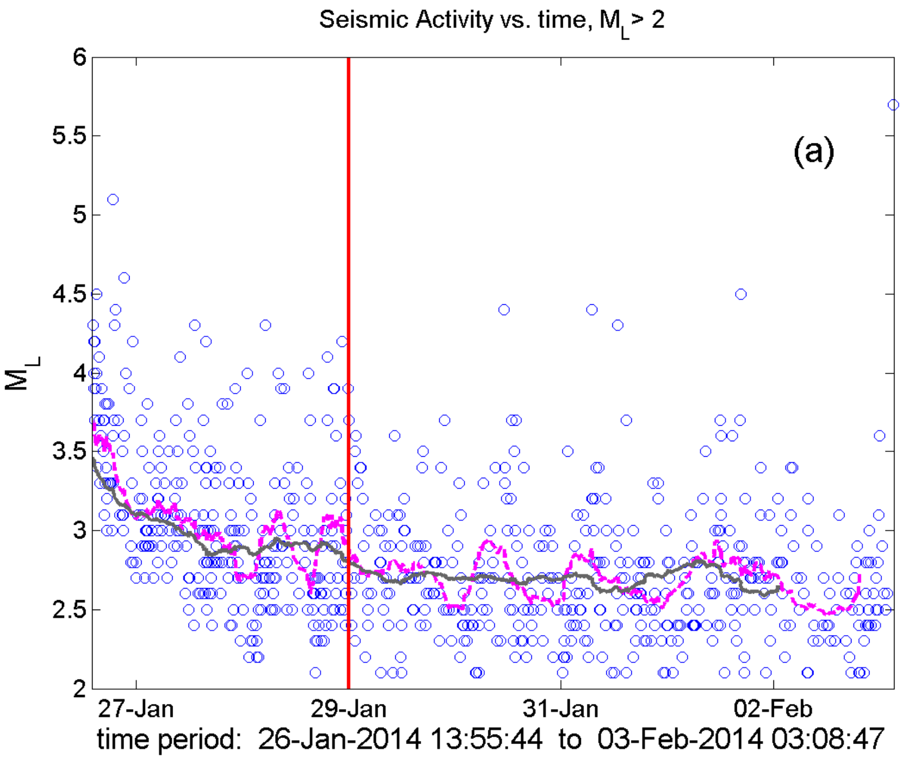
Seismic Activity vs. time, M_L > 2
(a)
M_L
6
5.5
5
4.5
4
3.5
3
2.5
2
27-Jan
29-Jan
31-Jan
02-Feb
time period: 26-Jan-2014 13:55:44 to 03-Feb-2014 03:08:47

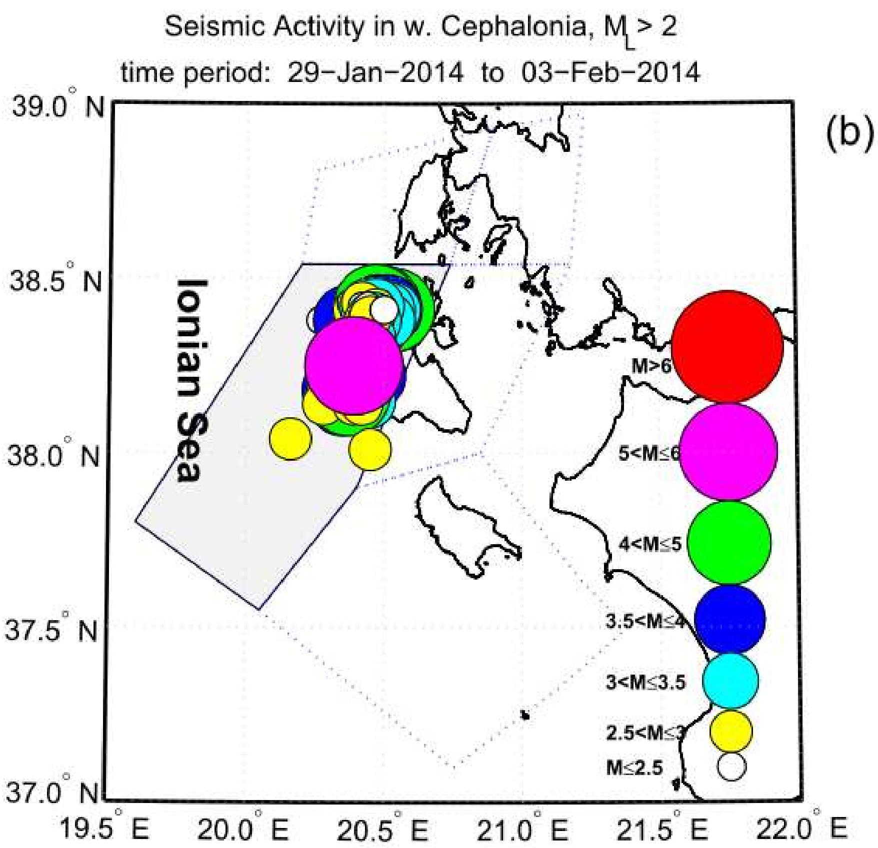

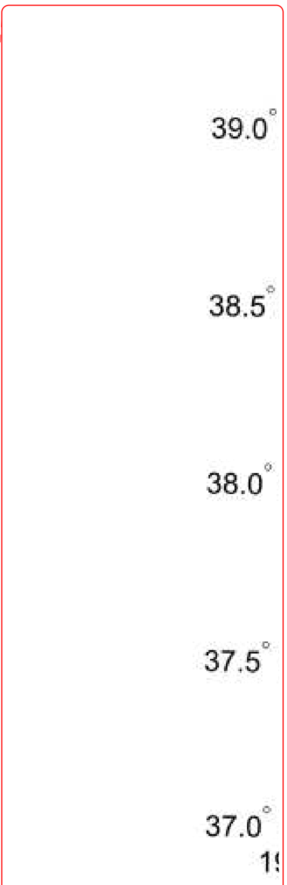

Διαγράφηκε:

Figure 11. (a) Seismic activity from the time immediately after EQ1 ($M_w = 6.0$) up to the time of EQ2 ($M_w = 5.9$) for the whole investigated area of the Ionian Sea. The moving averages of the recorded earthquake local magnitudes vs. time for calculation windows of 25 and 75 successive events are shown by the dashed magenta and solid grey curve, respectively. The vertical solid red line denotes the time point 29 January 00:00:00 UT. (b) The considered as foreshock seismic activity before EQ2 (from 29/01/2014 00:00 UT up to the time of occurrence of EQ2) for west Cephalonia. All presented magnitudes are local magnitudes (M_L).(For interpretation of the references to colors, the reader is referred to the online version of this paper.)

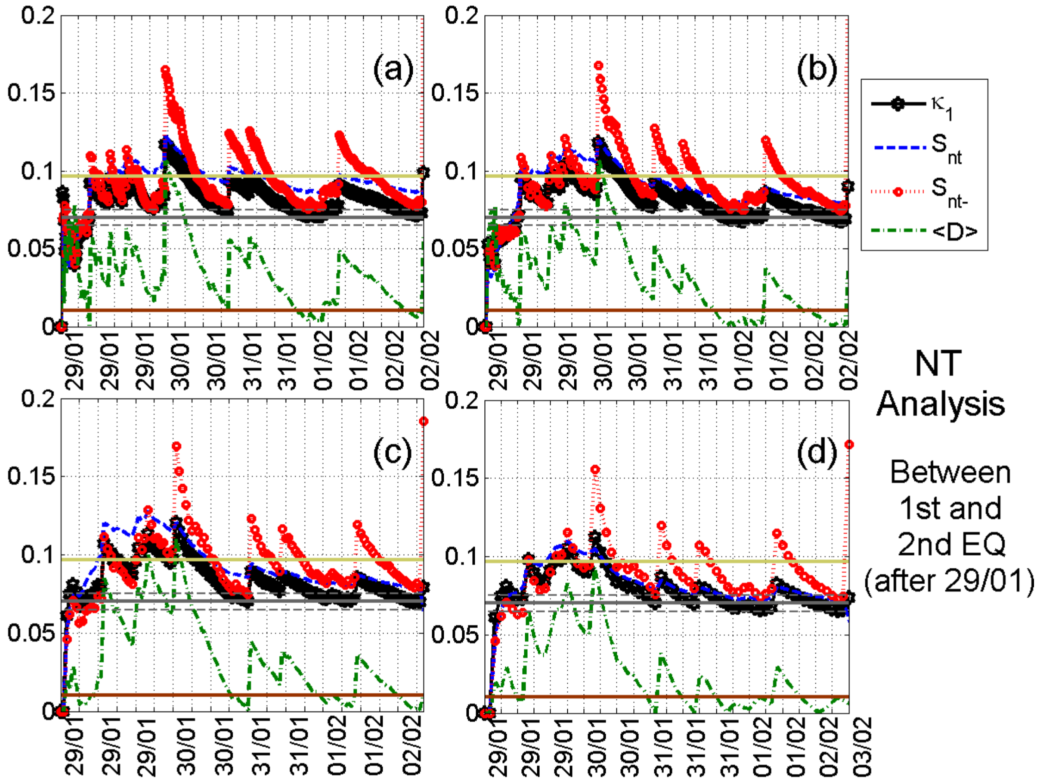

Figure 12. Natural time (NT) analysis results for the seismicity in the partition of west Cephalonia during the time period from 29/01/2014 00:00:00 to 03/02/2014 03:08:47 UT (between EQ1, $M_w = 6.0$, and EQ2, $M_w = 5.9$): (a)-(d) Temporal evolutions of the four natural time analysis parameters (κ_1, S_{nt}, S_{nt-}, and $\langle D \rangle$) for the different M_L thresholds 2.2, 2.6, 2.8, and 3.0, respectively. Note that the events employed depend on the considered threshold. Moreover, the time (x-) axis is not linear in terms of the conventional date of occurrence of the events, since the employed events appear equally spaced relative to x-axis, as the natural time representation demands, although they are not equally spaced in conventional time. The horizontal solid light green, solid grey and the grey dashed lines, denote the same quantities as in Fig. 6, while the horizontal solid brown line denotes the 10^{-2} limit for $\langle D \rangle$. (For interpretation of the references to colors, the reader is referred to the online version of this paper.)